Epigenetic Characterisation of the O6 Methyl-Guanine DNA-Methyltransferase Promoter in New Zealand Melanoma Cell Lines

A thesis presented to Massey University in partial fulfillment of the requirements for the degree of

Master of Science
in
Biochemistry

at Massey University, Palmerston North,
New Zealand

William Ernest Rutherford

2010

Abstract

New Zealand has the second highest incidence of melanoma skin cancer in the world. Chemotherapy is the standard treatment for melanoma derived tumours which have undergone metastasis and current therapies have limited benefit. There is a great need for new therapies and to increase the efficacy of current therapies.

Temozolomide (TMZ) is a chemotherapy agent effective in the treatment of both metastatic melanoma and glioblastoma (brain cancer), although TMZ resistance has been observed in many tumours. The activity of the DNA repair enzyme O^6 methyl-guanine methyltransferase (MGMT) is thought to be largely responsible for TMZ resistance.

MGMT protects the cell from the effects of TMZ by removing cytotoxic lesions placed on the DNA. Mechanisms of regulation of MGMT expression remain unclear in melanoma. DNA methylation at the MGMT promoter has been linked to MGMT silencing in some cancers and has been associated with specific chromatin modifications. The present study was aimed at investigating the promoter methylation status of MGMT in primary melanoma cell lines using a new technique named methyl DNA immuno-precipitation (MeDIP). Next, the chromatin immuno-precipitation (ChIP) method was used to examine post translational modifications on the surrounding chromatin. The data obtained was correlated with both MGMT transcription levels and TMZ sensitivity.

The promoter methylation status of MGMT has been used to predict the clinical responsiveness of glioblastoma patients to TMZ. Establishing the regulatory mechanisms of MGMT expression in melanoma patients would validate a means to predict clinical responsiveness to TMZ. Furthermore, establishing mechanisms of MGMT silencing may provide the basis for future clinical trials of novel therapies for melanoma and glioblastoma.

Acknowledgements

Firstly I would like to thank Associate Professor Kathryn Stowell for her excellent supervision for the duration of my studies. Your support, wisdom and tolerance have allowed me to learn from my mistakes and develop my skills inside and outside the laboratory.

Thank you to everyone in the Twilite Zone lab who kept me interested and made me want to come into the lab every day. I would especially like to thank Robyn Marsten for giving me guidance and for great cooking and gardening tips; Hilbert Grievink for your technical help and comradery; Amanda Gribble for your friendship and conversation; Lili Rhodes for your expert technical advice; Kei Sato for the invaluable Japanese lessons; Natisha Megan for your handy tips in the lab and finally Cornelia Roesl, Britta Majchrzrak and Diana Balasubramanain for making the lab a friendlier place.

I am grateful to Alice Clark for help making figures, also for making my studies much more enjoyable. Thank you Nick Albert, Carlene Starck, Corey Laverty and John Tweedie for many enjoyable and insightful discussions. Thank you Cynthia Cresswell for help with Chemdraw. I would also like to thank Kelly Senior, Miranda Aalderink, Kate Silverwood and Julianne Neubert for their hard work on MGMT in our lab. I am grateful to those who donated the melanoma samples used in this study.

I would like to thank my family and friends for supporting me during my research and writing. Thank you Bev for always believing I could do it. Thank you George for always giving me the right advice when I need it most. Thank you Louise for your encouragement and help. Thank you Sharleen for always listening to my frustration with patience and my excitement with enthusiasm.

Lastly I would like to thank Massey University for helping finance my studies by way of a Masterate scholarship. I would like to thank IMBS for financial support which enabled me to travel to Queenstown to attend the epigenetics satellite meeting at the Queenstown molecular biology conference in 2008.

Table of contents

Abstract i
Acknowledgements ii
Table of contents iii
List of figures vii
List of tables ix
Abbreviations x
1 Introduction 1
1.1 Overview 1
1.2 Melanoma 2
1.2.1 Cancer and the cell 2
1.2.1.1 DNA-based events 3
1.2.1.2 Epigenetic changes in cancer 3
1.3 Anti cancer drugs 5
1.3.1 Temozolomide 6
1.4 O6-methyl-guanine methyltransferase (MGMT) 8
1.4.1 MGMT expression and activity 8
1.5 Transcriptional machinery and MGMT promoter elements 9
1.5.1 5’ cytosine DNA methylation of the MGMT promoter 11
1.6 Chromatin modifications 12
1.6.1 De Novo DNA methylation 14
1.6.2 Mechanisms for Methyl-CpG mediated silencing 15
1.7 Chromatin modifications and binding domains 17
1.7.1 Histone lysine acetylation 17
1.7.2 Histone methylation 18
1.7.2.1 Histone arginine methylation 19
1.7.2.2 Histone lysine methylation 19
1.7.2.3 H3K9 methylation 20
1.7.3 Histone serine phosphorylation 21
1.7.4 Chromatin remodelers and histone variants 21
1.7.5 A role for ncRNA? 22
1.7.6 Epigenetic events involved in MGMT transcription 23
1.8 Hypothesis and aims 24

2 Materials and methods 25
2.1 Materials 25
2.1.1 General chemicals 25
2.1.2 Equipment 25
2.1.3 Cell culture 25
2.1.3.1 Media and supplements 25
2.1.4 Antibodies 25
2.1.5 DNA manipulations 26
2.1.5.1 Restriction endonucleases and DNA modifying enzymes 26
2.1.5.2 PCR reagents 26
2.1.6 Chromatin manipulations 26
2.1.7 Software 26
2.2 Methods 27
2.2.1 Cell culture 27
2.2.1.1 Media preparation 27
2.2.1.2 Starting cells from frozen stock 27
2.2.1.3 Maintenance of cells 27
2.2.1.4 Preparing cells for freezing 28
2.2.2 DNA Manipulations 28
2.2.2.1 Phenol-chloroform extraction and ethanol precipitation 28
2.2.2.2 DNA quantification by absorbance at 260 nm or fluorescence 28
2.2.2.3 Block PCR 28
2.2.2.4 Agarose gel electrophoresis 29
2.2.2.5 Restriction endonuclease digestion 29
2.2.3 Methyl DNA immunoprecipitation 30
2.2.3.1 Genomic DNA extraction 30
2.2.3.2 DNA sonication 30
2.2.3.3 Immunoprecipitation 31
2.2.4 Chromatin immunoprecipitation (ChIP) 31
2.2.4.1 Preparing cells for ChIP 31
2.2.4.2 Formaldehyde cross-linking 32
2.2.4.3 Chromatin sonication 32
2.2.4.4 Chromatin immunoprecipitation 32
3 Real-time quantitative PCR assay development 34

3.1 Introduction 34
3.2 MGMT promoter PCR 34
3.2.1 Amplification of the MGMT101 sequence by block PCR 37
3.2.2 Restriction endonuclease digestion of MGMT101 amplicon 39
3.3 Reference primer design and validation 40
3.3.1 β-actin primer design and Bact114 restriction endonuclease digestion 40
3.3.2 H19 primer design and H19155 restriction endonuclease digestion 42
3.4 Real time quantitative PCR 44
3.4.1 Amplification of target and reference sequences by RT quantitative PCR 46
3.5 PCR amplification efficiency determination 48
3.6 Chapter summary 50
4 Methyl DNA immunoprecipitation 51
4.1 Introduction 51
4.2 MeDIP optimisation 53
4.2.1 Isolation and sonication of genomic DNA 53
4.2.2 PCR-based control for sonication efficiency 54
4.2.2.1 Primer design 54
4.2.2.2 PCR amplification and restriction endonuclease digestion 55
4.2.2.3 Determination of sensitivity of sonication control 56
4.2.2.4 PCR to control for sonication efficiency 57
4.3 MeDIP results 58
4.3.1 Real time quantitative PCR and enrichment for NZM11 (1 of 3 replicates) 58
4.3.2 MeDIP results for seven cell lines 62
Chapter summary 66
5 Chromatin immunoprecipitation 67
5.1 Introduction 67
5.2 Optimisation of the ChIP assay 68
5.2.1 Chromatin isolation, cross-linking and sonication 69
5.3 ChIP results 70
5.3.1 ChIP real time quantitative PCR and enrichment for NZM5 (1 of 3 replicates) 70
5.3.2 ChIP assay results for five cell lines 74
5.4 Chapter summary 77
6 Conclusions and future directions 78

6.1 Overview 78
Conclusions and discussion 79
6.1.1 MeDIP analysis 80
6.1.2 ChIP analysis 81
Summary 85
6.1.3 Possible sources of bias 86
6.1.3.1 Nucleosome reshuffling 86
6.1.3.2 Primer placement 86
6.2 Future directions 87
6.2.1 Future experiments 87
6.2.2 Clinical aspects 89
Bibliography 91
Appendices 101
Appendix I MGMT promoter sequence 101
Appendix II β-actin gene sequence 104
Appendix III H19 gene sequence 106
Appendix IV MeDIP plate setup for relative quantification 107
Appendix V MeDIP plate setup for standard curves 108
Appendix VI ChIP plate setup for absolute quantification 109
Appendix VII MeDIP data 110
Appendix IIX ChIP data 111

List of figures

Figure 1-1 The nucleosome core particle at 2.8 Angstrom resolution (Luger, et al., 1997). 4
Figure 1-2 Cytosine – Guanine base-pair. The additional 5' methyl group is depicted in red. 5
Figure 1-3 Physiological conversion of TMZ (left) to MTIC (right). 6
Figure 1-4 MTIC methyl lesions are depicted in red. 7
Figure 1-5 1157 bp fragment of the human MGMT promoter and potential regulatory elements (adapted from Harris et al., 1991). 9
Figure 1-6 Euchromatic and heterochromatic states and associated modifications. Adapted from (Allis, Jenuwein, & Reinberg, 2007). 13
Figure 1-7 Mechanisms for euchromatic gene silencing. Adapted from (Allis, et al., 2007) 16
Figure 1-8 Lysine and a selection of post-translational modifications 21
Figure 3-1 Schematic representation of restriction endonuclease cutting site and primer binding sites within a 675 bp MGMT promoter fragment of genomic DNA. Accession # NT_008818.16. 36
Figure 3-2 MGMT101 amplification by block PCR. 38
Figure 3-3 MGMT101 amplicon restriction endonuclease digest. 39
Figure 3-4 Schematic representation of restriction endonuclease cutting site and primer binding sites within a 675 bp β-actin gene fragment showing exons 2 and 3. Accession # NC_000007.13. 40
Figure 3-5 Bact114 amplicon restriction endonuclease digest. 41
Figure 3-6 Schematic representation of restriction endonuclease cutting site and primer binding sites within a 675 bp fragment within the H19 gene. Accession # NC_00001.9. 42
Figure 3-7 H19155 amplicon restriction endonuclease digest. 43
Figure 3-8 A) Amplification curves, B) melt curves and C) melt peaks of the MGMT101 amplicon. 45
Figure 3-9 Results of RT-qPCR for H19155, Bact114 and MGMT101 products. 47
Figure 3-10 Standard curve for the Bact114 amplicon for determination of PCR linearity. A) Amplification curves showing dilutions from stock. B) Corresponding melting peaks. 48

Figure 3-11 Standard curves for H19155, Bact114 and MGMT101amplification reactions. 49
Figure 4-1 Genomic DNA isolated from melanoma cell lines and sonicated DNA respectively. 53
Figure 4-2 Schematic representation of restriction endonuclease cutting site and primer binding sites within a 5863 bp fragment upstream of the MGMT gene. Accession NT_008818.16. 54
Figure 4-3 MGMT1966 amplicon restriction endonuclease digestion with *Bam*HI. 55
Figure 4-4 PCR reactions on sonicated DNA spiked with serial dilutions of genomic DNA template. 56
Figure 4-5 Template and PCR reactions using MGMT1966 primers for sonicated DNA prior to MeDIP procedure. 57
Figure 4-6 Amplification curves and enrichment for NZM11 β actin subset (replicate 1 of 3). 59
Figure 4-7 Amplification curves and enrichment for NZM11 H19 subset (replicate 1 of 3). 60
Figure 4-8 MeDIP enrichment values and previously established MGMT expression values. 63
Figure 5-1 DNA purified from sonicated chromatin at 30 - 50 sonications. 69
Figure 5-2 Amplification curves and enrichment for NZM5, MGMT subset (1 of 3). .. 71
Figure 5-3 Amplification curves and enrichment for NZM5, β actin subset (1 of 3). 72
Figure 5-4 A) Relative enrichment of ChIP samples for the MGMT promoter and B) the β actin gene. Error bars shown are standard error. n = 5. 75
Figure 6-1 Possible bias due to nucleosome reshuffling. 86

List of tables

Table 2-1 Block PCR protocol for amplifying MGMT101 product..... 29
Table 3-1 Primers designed to amplify a 101 bp fragment upstream of exon 1. 35
Table 3-2 Block PCR protocol for amplifying MGMT101 product..... 37
Table 3-3 LC480 protocol for amplifying MGMT101, Bact114 and H19155 products 46
Table 6-1 Results summary for MeDIP data..... 80
Table 6-2 Results summary for MGMT ChIP data. 82
Table 6-3 Results summary for β actin ChIP data..... 83
Table 6-4 MGMT expression Cp's (M, Aalderink, personal communication, Nov, 2007) 84

Abbreviations

°C	degrees celsius
ADP	adenosine 5’-diphosphate
AGT	alkylguanine-transferase
AGAT	alkylguanine-alkyltransferase
AP1	activator protein 1
AP2	activator protein 2
ATP	adenosine 5’-triphosphate
ATF	activating transcription factor
α-MEM	alpha-minimal essential medium
bp	base pair
cAMP	cyclic adenosine 5’-monophosphate
CBP	cAMP response element binding protein
CHD	chromodomain helicase DNA-binding chromatin remodelling complex
ChIP	chromatin immunoprecipitation
Cp	crossing point
CpG	cytosine-guanine dinucleotide
CTD	carboxyl terminal domain
dNTP	2’-deoxynucleotide 5’-triphosphate
DMSO	dimethyl sulfoxide
DNA	deoxyribonucleic acid
DNMT	DNA methyl-transferase
ds	double stranded
DSB	double stranded break
EDTA	ethylene-diamine-tetra-acetic acid
EJ	end joining
ES	embryonic stem cell
EtBr	ethidium bromide
FACT	facilitates chromatin transcription
FBS	foetal bovine serum
g	gram
gDNA	genomic DNA
GR	glucocorticoid receptor

GRE	glucocorticoid response element
H3K9	lysine 9 of histone H3
H3K9ac	acetylated lysine 9 of histone H3
H3K9me2	dimethylated lysine 9 of histone H3
H3K9me3	trimethylated lysine 9 of histone H3
HAT	histone acetyl transferase
HCl	hydrochloric acid
HDAC	histone deacetylase
HDACi	histone deacetylase inhibitor
HKMT	histone lysine methyl transferase
HP1	heterochromatin protein 1
HR	homologous recombination
INO80	inositol family chromatin remodelling complex
IP buffer	immunoprecipitation buffer
ISWI	imitation switch family chromatin remodelling complex
ITS	insulin-transferrin selenite
JmjC	jumanji-C domain
kb	kilobase-pairs
L	litre
LC480	lightcycler 480 instrument
LSD	lysine demethylase
M	moles per litre
MAF	masculoaponeurotic fibrosarcoma
MBD	methyl binding domain
MeCP2	methyl CpG binding protein 2
MeDIP	methyl-DNA immunoprecipitation
MGMT	O6 methyl-guanine DNA-methyltransferase
µg	microgram
µL	micolitre
µM	micro moles per litre
mg	milligram
mL	millilitre
MML	mixed lineage leukemia
mM	milli moles per litre

MMR	mismatch repair
M_r	relative molecular mass (g mol^{-1})
mRNA	messenger ribonucleic acid
MTIC	5-(3-methyltriazen-1-yl)imidazole-4-carboxamide
NaOAc	sodium acetate
ncRNA	non-coding RNA
NDR	nucleosome depleted region
Nmol	nanomole
Nt	nucleotide
NZM	New Zealand melanoma
O^6-MG	guanine nucleotide with methylation of the O^6 position
OGAT	O^6-alkylguanine transferase
PBS	phosphate buffered saline
PcG	polycomb group
PCR	polymerase chain reaction
pH	-Log $[H^+]$
PKC	protein kinase C
PRMT	protein arginine methyltransferase
RB	retinoblastoma protein
RISC	RNA-induced silencing complex
RITS	RNA-induced transcriptional silencing
RNA	ribonucleic acid
RNApolII	RNA polymerase II
RNApolIIo	elongation competent RNApolII
RNase	ribonuclease
RNAi	RNA interference
ROS	reactive oxygen species
rpm	revolutions per minute
RT	room temperature
RT-qPCR	real time-quantitative polymerase chain reaction
s	second
SAM	s-adenosyl methionine
SDS	sodium dodecyl sulphate
siRNA	short interfering RNA

SWI/SNF	mating type switching/sucrose non-fermenting family
TAE	tris-HCl, acetic acid, EDTA buffer
TBP	TATA binding protein
TE	tris-HCl, EDTA buffer
TF	transcription factor
TMZ	temozolomide
Tris	tris(hydroxymethyl)aminomethane
TrypleE	express stable trypsin-like enzyme plus phenol red
TSP	transcription start point
UV	ultraviolet light
V	volt (m^2 kg s^{-3} A^{-1})

1 Introduction

1.1 Overview

New Zealand has the second highest incidence of metastatic[1] melanoma in the world (Lens & Dawes, 2004), while the city of Auckland is reported to have the highest incidence in the world (W. O. Jones, Harman, Ng, & Shaw, 1999). Whereas the treatment of primary melanoma consists of a simple surgical excision, chemotherapy is the standard of treatment for metastatic melanoma and current therapies have limited benefit. There is a great need for new therapies and to increase the efficacy of current therapies.

Temozolomide (TMZ) is a chemotherapy agent which is effective in the treatment of both metastatic melanoma and glioblastoma[2], however TMZ resistance is common (Quirt, Verma, Petrella, Bak, & Charette, 2007). The activity of the deoxyribonucleic acid-(DNA) repair enzyme O^6 methyl-guanine methyltransferase (MGMT) has been found to be responsible for TMZ resistance in some types of cancer. In addition, a clear correlation between TMZ sensitivity and a lack of MGMT expression has been demonstrated in a number of cancers (Costello, Futscher, Tano, Graunke, & Pieper, 1994), however this relationship remains unclear regarding melanoma. At the molecular level, TMZ functions by donating cytotoxic[3] methyl lesions to DNA. MGMT removes these lesions and thus protects the cell from apoptosis[4]. 5'-cytosine methylation at the 5' regulatory region of the MGMT gene is associated with transcriptional repression and hence TMZ sensitivity. In 2004, Hegi and colleagues demonstrated that the promoter methylation status of MGMT can be used as a predictor for the clinical response of glioblastoma patients to TMZ. Transcriptional silencing of MGMT is thought to be mediated through a complex relationship between factors including DNA methylation, specific histone lysine de-acetylation and histone lysine methylation events (Danam, Howell, Brent, & Harris, 2005; P. L. Jones et al., 1998).

[1] The ability of a cancer to spread to another part of the body.

[2] A fast growing brain tumour.

[3] Relating to substances which are toxic to cells.

[4] Programmed cell death.

Establishing a pattern of DNA cytosine methylation, specific histone modifications and MGMT expression in melanoma cells may validate a method to predict patient sensitivity to TMZ. Furthermore, establishing the pathway of MGMT silencing may provide the basis for clinical trials of novel epigenetic therapies for melanoma in the future.

1.2 Melanoma

Melanoma is one of the deadliest types of skin cancer (Price & Wilson, 2003). The global incidence of melanoma has been observed to increase over the last two decades (Lens & Dawes, 2004). Even so there has been minimal progress recently in non-surgical treatment for the disease (Bittner et al., 2000). Individuals aged between 20 and 70 show a higher incidence of melanoma, which manifests in a change in the appearance of a pigmented mole or freckle on the skin. Factors which increase the risk of melanoma development include exposure to ultraviolet (UV) radiation and a range of genetic defects. It is now well recognised that inherited mutations in the tumour suppressor gene p16 are directly linked to an increased risk for the development of melanoma (Hussussian et al., 1994). In addition, hereditary skin pigmentation and freckles can predispose certain groups to melanoma (Bliss et al., 1995).

The standard treatment for malignant[5] melanoma is excision of the site and often of the regional lymph node in order to reduce the risk of metastasis. If metastasis is suspected, chemotherapy is the standard treatment used to reduce the risk of additional tumourigenesis[6]. Patients with metastasized tumours can be treated with anti-cancer agents such as TMZ, often in conjunction with radiotherapy or immunotherapy (Miller & Mihm, 2006).

1.2.1 Cancer and the cell

Cancer development and metastasis are gradual processes involving many cellular and epigenetic events. The loss or gain of phenotypic traits can culminate in abnormal cell behaviour, communication and uncontrolled growth. During cancer development many malignant cells will be destroyed by the immune system before they can develop

[5] Dangerous to health; characterised by progressive and uncontrolled growth.

[6] The development of a tumour.

further. Surviving cells, however, will continue to replicate, becoming less like the tissue of origin and eventually becoming dominant over the parent cell type. Over time the tumour mass may invade surrounding tissues, blood or lymph and in some cases may acquire the ability to recruit blood vessels and metastatize to distant sites including the lymph nodes and brain (Furie, Cassileth, Atkins, & Mayer, 2003).

1.2.1.1 DNA-based events

DNA-based cellular events including DNA instability and mutation are well established signatures of cancer. These processes must be controlled in order to preserve the integrity of tumour suppressor genes and prevent changes which may activate proto-oncogenes[7]. DNA instability may arise due to UV radiation, attack by normal metabolic by-products such as reactive oxygen species (ROS) or through spontaneous disintegration of chemical bonds in DNA occurring under physiological conditions. Relevant mechanisms of DNA maintenance in mammals include homologous recombination (HR), end joining (EJ) and mismatch repair (MMR).

When DNA maintenance mechanisms fail to correct genomic infidelity, inherited DNA mutation may result. In melanoma it is common to find mutations in key cell cycle regulators. One well known example is the p53 protein (Lane, 1992). Double stranded DNA breaks (DSB) represent problems for mitosis. DSBs induce chromosomal alterations including an aberrant chromosome number, deletion (loss of heterozygosity), chromosomal translocations and genome fragility. All of these are closely linked to carcinogenesis[8] (Hoeijmakers, 2001). Some anti-cancer agents including TMZ exploit this effect to induce large numbers of DSBs which overload the HR and EJ DNA maintenance systems and lead to activation of apoptosis.

1.2.1.2 Epigenetic changes in cancer

In the eukaryotic cell, genomic DNA is coiled, folded and compacted into a dynamic organised structure consisting of DNA and histone and non-histone proteins, collectively termed chromatin. Epigenetics is the name given to the study of hereditary or dynamic gene expression changes which are influenced by chromatin organisation,

[7] A normal gene that has the potential to become an oncogene.

[8] The development of cancer.

and do not arise as a result of mutation. Factors known to influence chromatin organisation include DNA methylation at the 5' position of the cytosine base within the cytosine-guanine dinucleotide (CpG). Additionally, chromatin post-translational modifications on histone proteins are known to influence gene expression through chromatin structural changes.

In order to understand how epigenetic events such as CpG methylation affect the higher-order structure of DNA and the expression of genes, it is necessary to summarise DNA organisation in terms of its nucleosomal and chromosomal packaging. The higher order organisation of all chromatin begins at the level of the nucleosome, the primary repeating unit of chromatin. Each nucleosome consists of a core octamer of highly evolutionarily conserved basic histone proteins, an H3-H4 tetramer and two H2A-H2B dimers, around which approximately 150 base pairs (bp) of DNA is wound (Figure 1-1), (Luger, Mader, Richmond, Sargent, & Richmond, 1997). The linker histone H1 may be incorporated into more compact/repressive higher order chromatin structures (30 nm).

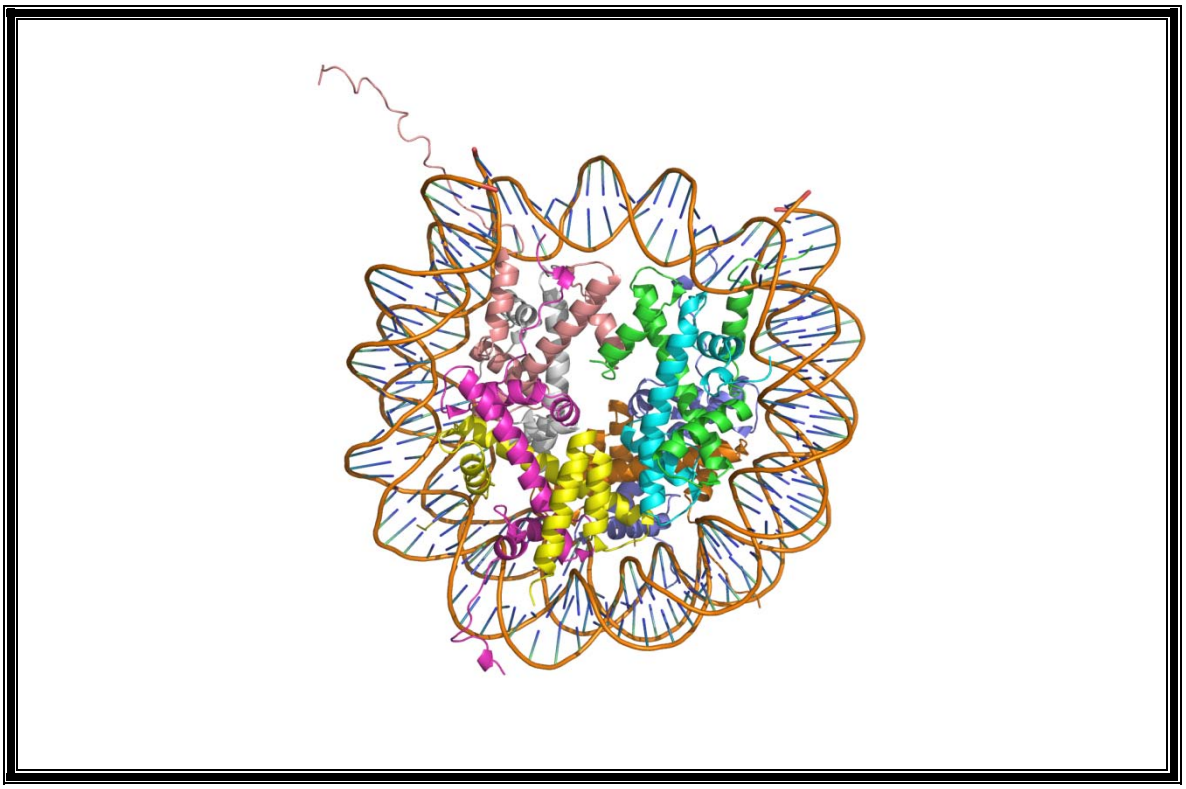

Figure 1-1 The nucleosome core particle at 2.8 Angstrom resolution (Luger, et al., 1997).

Each histone consists of a globular domain and a flexible N-terminal tail domain which acts as the substrate for a variety of post-translational modifications catalysed by histone-modifying enzymes. Nucleosomes are arranged such that efficient packaging of DNA occurs within the nucleus, while still allowing access to DNA polymerase during DNA replication and the transcription machinery at active chromatin.

Aberrant distribution of 5'-cytosine methylation (Figure 1-2) in the genome may play an early role in cancer development. Cancer cells often display a decrease in methylation of non-coding and repeat regions of the genome, which contributes to genome instability through failure to suppress mobile DNA elements. On the other hand specific regions of the genome have been shown to display increased methylation. *De novo* methylation of CpG-rich islands nested within gene promoters is thought to be a common mechanism for the inactivation of tumour suppressor genes in cancer.

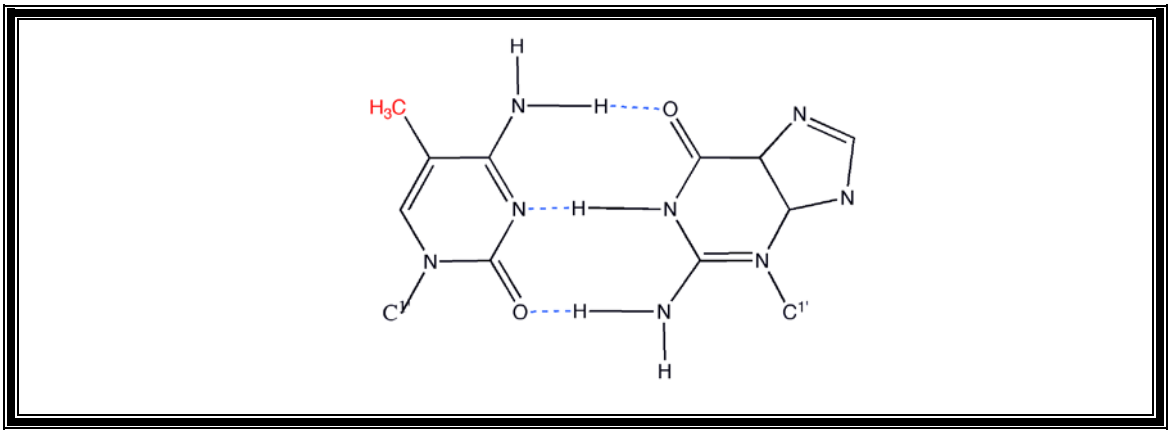

Figure 1-2 Cytosine – Guanine base-pair. The additional 5' methyl group is depicted in red.

How *de novo* methylation enzymes are targeted to some specific gene promoters and not others is a prominent question in cancer epigenetics. It has been proposed that histone modifications may bring about DNA methylation (Schlesinger et al., 2007; W. Zhao et al., 2005) although there is also evidence that the reverse may be true (P. L. Jones, et al., 1998).

1.3 Anti cancer drugs

The aim of chemotherapy is to induce regression of a tumour and its metastasis, therefore allowing the immune system to destroy any remaining malignant cells. There

are a wide variety of chemotherapeutic agents currently available, although most are effective on only a limited range of tumours. As most chemotherapy agents target only those cells in a specific phase of replication, they must often be administered in repeated doses.

Chemotherapy agents can be grouped into a number of broad categories: anti-metabolites, which compete against purines and pyrimidines in the synthesis of DNA/ribonucleic acid (RNA) to block the S phase of mitosis; antitumorigenic agents, which block cell growth by binding to DNA; plant alkaloids, which prevent cell reproduction by disrupting the M phase of cell division; alkylating agents and nitrosoureas, which react with DNA at any stage in cell division to transfer lesions to DNA, resulting in accumulation of DSBs which in turn result in the activation of apoptosis.

1.3.1 Temozolomide

TMZ is an alkylating agent commonly used to treat metastatic melanoma. TMZ has the advantage of freely crossing the blood-brain barrier, proving useful in treating metastases to the brain (Friedman, Kerby, & Calvert, 2000). At physiological pH, TMZ undergoes spontaneous hydrolysis (to produce the active form named 5-(3-methyltriazen-1-yl)imidazole-4-carboxamide (MTIC) (Figure 1-3).

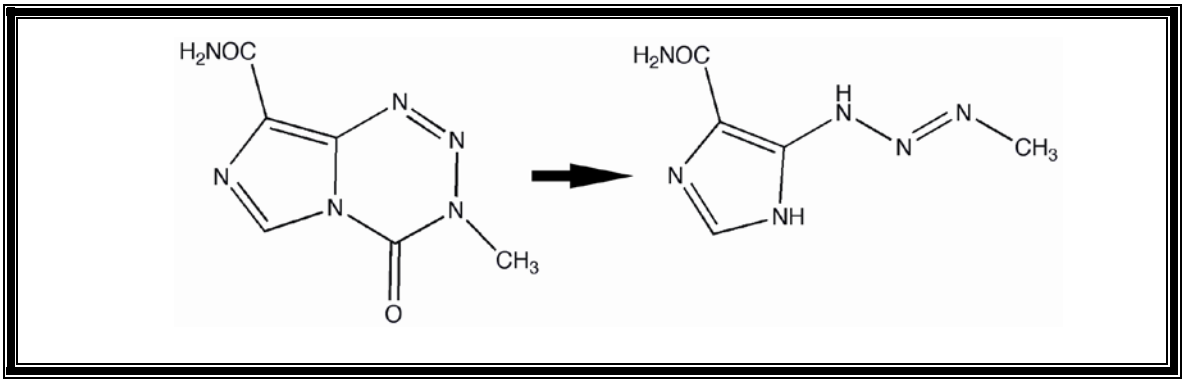

Figure 1-3 Physiological conversion of TMZ (left) to MTIC (right).

MTIC transfers methyl groups to a range of positions on the bases of DNA;
Figure 1-4 shows the methyl lesions in order of decreasing efficiency: N^7 of guanine; O^3 of adenine, and O^6 of guanine (O^6-MG) (Pegg, 1990). Of these adducts only 5% are

O^6-MG, although this is the most potent lesion (Denny, Wheelhouse, Stevens, Tsang, & Slack, 1994).

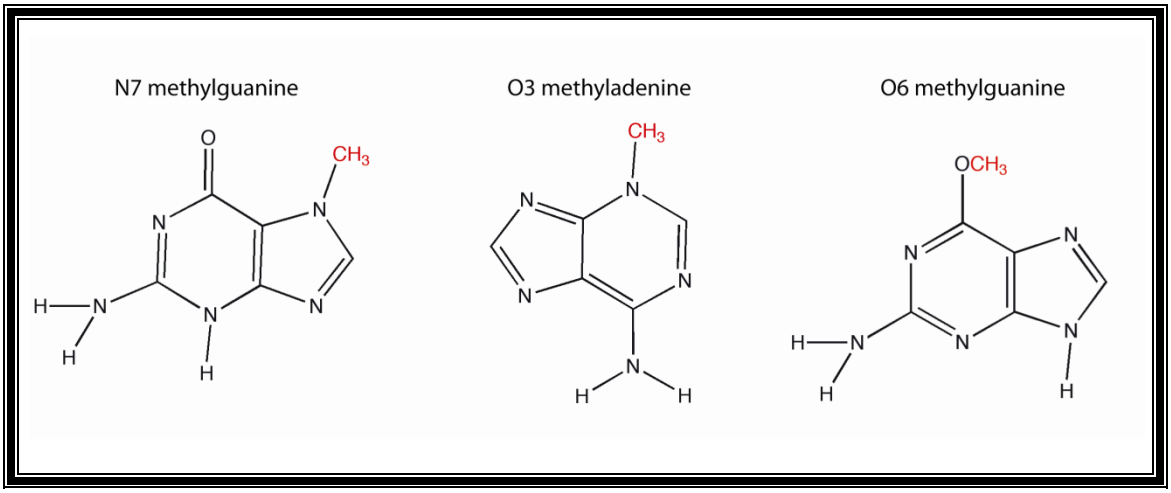

Figure 1-4 MTIC methyl lesions are depicted in red.

There are three main aspects to the O^6-MG to be considered. The first is the ability of O^6-MG to interfere with DNA-protein interactions including transcription factor (TF) (Bonfanti, Broggini, Prontera, & Dincalci, 1991) and DNA methyl-transferase (DNMT) binding (Hepburn, Margison, & Tisdale, 1991). The second is that the O^6-MG adduct has a tendency to pair with thymine during DNA replication, resulting in a guanine-cytosine to adenine-thymine conversion, which can contribute to host DNA infidelity during replication. Lastly, O^6-MG causes lethal cross-links to form between guanine and an opposite cytosine residue, which has the effect of blocking DNA replication (Spratt & Levy, 1997).

Resistance to TMZ and other alkylating agents may arise through two main mechanisms: a defective MMR pathway or through the activity of MGMT. The MMR pathway plays an important role in mediating cytotoxicity to TMZ. When alternative DNA maintenance systems are overloaded, this system recognises and removes O^6-MG bases (D'Atri et al., 1998). Researchers have recently suggested that the MMR removes the O^6-MG base, but cannot find a suitable replacement and instead leaves long-lived nicks/DSBs in DNA. Nicks and DSBs lead to a block at the G_2-M phase of the cell cycle and activation of apoptosis. Liu and colleagues (1996) demonstrated that cells deficient in MMR proteins were resistant to the effects of TMZ (Liu, Markowitz, &

Gerson, 1996). The activity of MGMT is thought to be the primary cause of TMZ resistance.

1.4 O6-methyl-guanine methyltransferase (MGMT)

Direct repair of the O^6-MG lesion by the DNA repair protein MGMT represents the dominant mechanism for TMZ resistance in the cell; no other known proteins remove methyl groups from this residue. In support of this idea, Tentori and colleagues showed that the apoptosis rate in leukemia cell lines treated with TMZ is significantly increased when MGMT is depleted (Tentori et al., 1995). There is some controversy over the nomenclature of MGMT. In the past, alternative names included alkylguanine-alkyltransferase (AGAT), alkylguanine-transferase (AGT) and O^6-alkylguanine transferase (OGAT).

The mechanism of MGMT-mediated O^6-MG repair involves the stoichiometric transfer of a methyl group, from DNA to an internal cysteine residue (Grafstrom, Pegg, Trump, & Harris, 1984) resulting in enzymatic inactivation and degredation. Some other minor targets for mammalian MGMT include O^6-alkyl guanine groups and O^4-methyl thymine residues (Pegg, 1990). The observation that MGMT promoter DNA methylation is directly correlated with expression has led researchers to focus on MGMT as a model gene for DNA methylation and associated gene expression changes.

From an alternative perspective, the O^6 position of guanine is the preferred point of attack for environmental carcinogens such as methylnitrosourea. As MGMT is a DNA repair protein in itself, silencing of MGMT expression leads to the acquisition of a mutator phenotype. Mutations in tumour suppressors such as p53 are common in cells with silenced MGMT, although these cells retain sensitivity to TMZ. Cells with active MGMT however, are resistant to environmental carcinogens but also to TMZ.

1.4.1 MGMT expression and activity

Compared to other tissues, melanoma and glioblastoma often show a low level of MGMT transcription and some tumours show no measurable MGMT transcription at all. Down-regulation of MGMT transcription levels is largely responsible for loss of MGMT activity rather than DNA mutation, messenger RNA (mRNA) instability or post-translational modification (Fornace, Papathanasiou, Hollander, & Yarosh, 1990).

Srivenugopal and colleagues (2000) recently demonstrated that post-translational phosphorylation of the MGMT protein has an effect on its activity. MGMT phosphorylation at specific sites is directly correlated with reduced MGMT activity in brain tumours *in vitro* (Srivenugopal, Mullapudi, Shou, Hazra, & Ali-Osman, 2000). However, the scientific community remains focused on transcriptional control, including elements of promoter DNA methylation and epigenetic changes at the MGMT promoter (Figure 1-5).

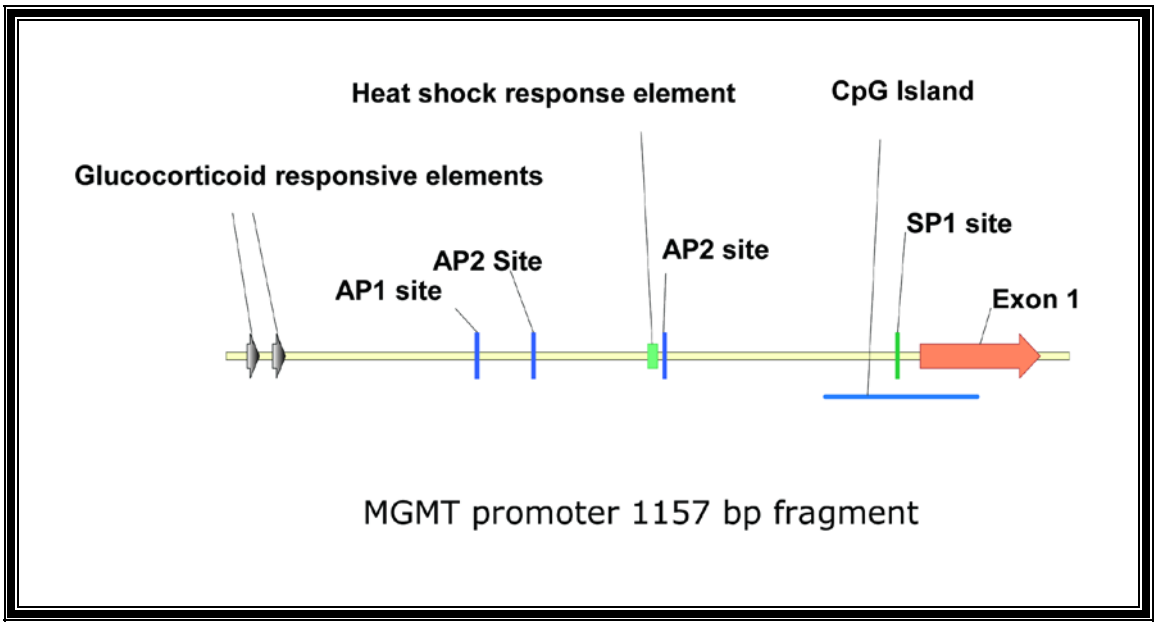

Figure 1-5 1157 bp fragment of the human MGMT promoter and potential regulatory elements (adapted from Harris et al., 1991).

1.5 Transcriptional machinery and MGMT promoter elements

The process of transcription forms the basis for gene expression in the cell and is regulated by a multitude of tissue and locus-specific regulation events. Gene expression is required from specific genes at different times, therefore each gene possesses a different combination of promoter and downstream elements which influence transcription, however the core machinery is shared to some extent.

The core transcription machinery consists of general TFs including the TATA binding protein (TBP) and RNA polymerase II (RNApolII) which assemble at or near the promoter and make up the pre-initiation complex (PIC). In general there are two classes of promoter in the mammalian genome, those that contain a so-called TATA element

and those that do not. Mechanisms for PIC formation differ between these groups somewhat. At TATA promoters it is thought that RNApolII components assemble in a stepwise manner beginning with the binding of the transcription factor $TF_{II}D$ to DNA. At TATA-less promoters the TBP is recruited via protein-protein interactions with the initiator complex located at the transcription start site (TSS) or at upstream enhancer elements. The initiator complex of human pCAF/GCN5 complex then recruits pre-assembled RNApolII complex (Cairns, 2009). pCAF/GCN5 contains factors which interact with the basal transcription machinery and contains a histone lysine acetyl transferase (HAT) module. There is evidence that histone lysine acetylation increases DNA promoter accessibility (discussed in section 1.7.1). The MGMT promoter lacks a TATA element. Notably, many constitutively expressed or housekeeping genes also lack TATA elements.

The largest subunit of RNApolII contains a carboxyl terminal domain (CTD) repeat region which is subject to phosphorylation at serine residues which are known to affect the catalytic properties of the enzyme. The PIC typically contains CTD de-phosphorylated RNApolII. Phosphorylation of the CTD by various kinase enzymes generate an elongation-competent form of the enzyme (RNApolIIo).

The MGMT promoter contains a number of elements which influence silencing or upregulation and may play a role in aberrant MGMT expression in cancer. Elements that present upstream of the MGMT TSS include a glucocorticoid response element (GRE), AP1 (activator protein 1) and AP2 (activator protein 2) elements, a heatshock element and putative CAAT box. The GRE consists of two repeat regions to which the glucocorticoid receptor (GR) binds. The GR is in the nuclear receptor family of TFs which dimerises upon glucocorticoid binding leading to activation, nuclear localisation and GRE binding. MGMT transcriptional upregulation has been observed upon the GR binding steroid hormone and consequently binding the MGMT promoter (Biswas et al., 1999). AP1 and AP2 receptors are responsive to cAMP (cyclic AMP) and phorbol ester signalling. The AP1 transcription factor consists of a dimeric complex comprised of multiple components including JUN, FOS, activating transcription factor (ATF) and masculoaponeurotic fibrosarcoma (MAF) families. Transcriptional activation/repression activity of AP1 is regulated through the concomitant expression

and regulation of its components. In a research article published in 1998, Boldogh and colleagues demonstrated that protein kinase C (PKC) signalling mediates binding of the AP1 receptor to AP1 elements in the MGMT promoter in Hela cells (Boldogh et al., 1998). In 2000 the same researchers used mutational studies and chromatin immunoprecipitation (ChIP) to show that the HAT family member and transcriptional activator p300, and closely related cAMP response element binding protein (CBP) can bind to AP1 elements at or near the MGMT promoter, acetylating nearby lysines on histone H4 and concomitantly up-regulating MGMT expression.

1.5.1 5' cytosine DNA methylation of the MGMT promoter

Several researchers have demonstrated that DNA methylation of the promoter CpG-island of MGMT plays an important role in mediating the silencing of MGMT transcription and activity *in vitro* and *in vivo* (Pieper et al., 1991; Wang et al., 1992). Taken together, attempts to characterize the correlation between DNA methylation and silencing of gene expression suggest that cross-talk between DNA methylation and changes in chromatin architecture changes are responsible for restriction endonuclease inaccessibility at the MGMT promoter and TSP (Ostrowski et al., 1991). Watts and colleagues (1997) used bisulfite sequencing and restriction analysis combined with southern blotting to analyse the compaction state of the MGMT promoter region (Watts et al., 1997). Using cell lines derived from multiple myeloma, their study indicated that in a MGMT silenced cell line there was significant DNA methylation on the MGMT CpG island, and in addition there was a considerable reduction in access to restriction endonucleases. The relevance of this finding has been substantiated in clinical trials. In 2004 Hegi et al. used MGMT promoter methylation as a predictive factor for glioblastoma patient longevity when treated with TMZ (M.E Hegi et al., 2004). A similar study showed a correlation between MGMT promoter methylation and increased survival length in glioblastoma (Martinez et al., 2007). Although MGMT promoter DNA methylation is known to occur in some melanomas (Esteller, Hamilton, Burger, Baylin, & Herman, 1999), the predictive value regarding TMZ sensitivity specifically in melanoma has yet to be examined in detail.

Observed reductions in MGMT expression have been shown to be reversible by treatment with the drug 5-aza-cytidine (Watts, et al., 1997). 5-aza-cytidine is incorporated into the DNA of replicating S-phase cells (P. A. Jones & Taylor, 1980)

where it then forms covalent intermediates with enzymes responsible for *de novo* CpG methylation, blocking further methylation (Baylin & Jones, 2007). One effect is the up-regulation of previously silenced genes by a currently unconfirmed mechanism. The drug 5-aza-cytidine is currently in phase III trials and was recently approved for the treatment of some cancers by the US Food and Drug administration (FDA) (Baylin & Jones, 2007).

1.6 Chromatin modifications

Histone N terminal tails are subjected to a number of post-translational modifications including acetylation, methylation, phosphorylation, adenosine diphosphate (ADP)-ribosylation, ubiquitination and sumoylation. These modifications are known to affect the packing of nucleosomes into higher-order structures and hence affect the condensation state of chromatin, the accessibility of TFs and, consequently, the expression level of genes (M. Shogren-Knaak et al., 2006; Wei, Yu, Bowen, Gorovsky, & Allis, 1999). Chromatin modifications have traditionally been associated with one of two distinct transcriptional states linked to post-transcriptional modifications on the associated histones: euchromatic (active) and heterochromatic (repressed), (Figure 1-6). More recently, a third intermediate (facultatively silenced) state of chromatin has been suggested.

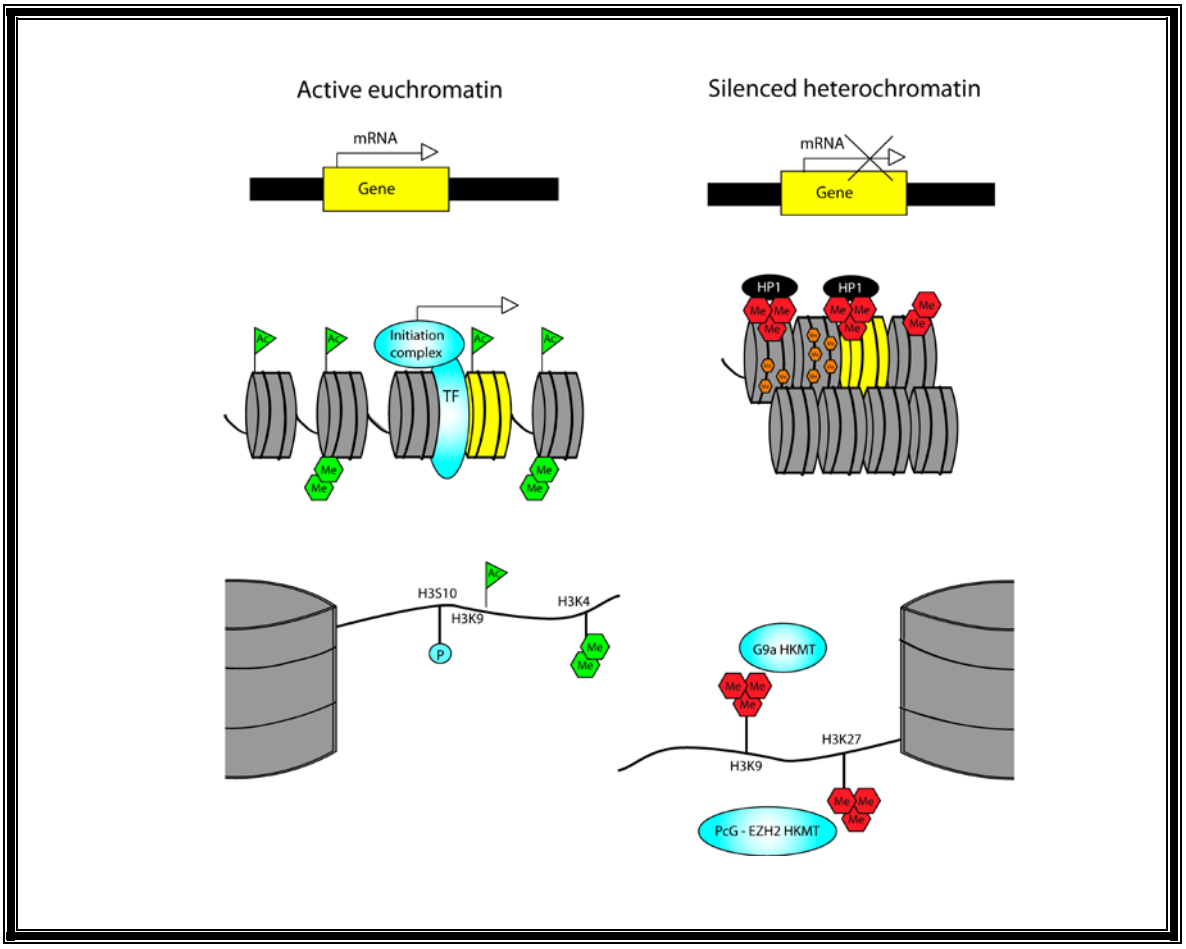

Figure 1-6 Euchromatic and heterochromatic states and associated modifications. Adapted from (Allis, Jenuwein, & Reinberg, 2007).

Chromatin structure and gene expression are not only influenced by histone-modifying enzymes. Another class of enzymes, termed chromatin remodelers, are responsible for influencing the density, composition and positioning of nucleosomes relative to important regulatory sites at the gene promoter. In eukaryotes, actively transcribed genes often display a nucleosome depleted region (NDR) spanning approximately 150 bp upstream of the TSS containing poly (dA:dT) sequences (Struhl, 1985). The biophysical properties of DNA can also affect chromatin architecture. Importantly, poly (dA:dT) sequences are known to deter nucleosome formation and stability.

The composition of nucleosomes is another important aspect of chromatin organisation. Humans have several important H2A and H3 paralogs[9] but none are yet known for H2B and H4. It has been suggested that the different position of histones in the nucleosome has lead to evolutionary diversification of H2A and H3 only. Human histone variants H3.3, H2A.Z and H2A.X have differing roles in nucleosome architecture and can be found on the nucleosome directly upstream or downstream of the NDR at the -1 or +1 nucleosome position respectively in yeast and up to the -3 or +3 position in mammals. One possibility could be that a complex system involving elements of DNA methylation, nucleosome modification, position and composition all play an important role in the regulation of MGMT transcriptional regulation.

1.6.1 De Novo DNA methylation

In mammalian cells, DNA methylation occurs on the 5' position of the ring structure in cytosine within the CpG dinucleotide. DNA methylation is associated with inactive genes and heterochromatin, and is rare in the promoters of active genes (Esteller, Corn, Baylin, & Herman, 2001).

The DNMT proteins catalyse *de novo* DNA methylation and can maintain DNA methylation during replication. The importance of this protein family has been demonstrated by the observation that targeted mutation of DNMT family genes in mice causes embryonic lethality (Li, Bestor, & Jaenisch, 1992). Two general classes of DNA methyltransferases are currently known. Firstly the *de novo* methyltransferases DNMT3A and DNMT3B modify unmethylated CpG sites. Secondly, the maintenance methyltransferase DNMT1 copies hemi-methylated[10] signals to newly replicated DNA strands and is linked to the DNA replication machinery.

DNA methylation is heritable through replication of hemi-methylated DNA coupled to DNMT1 and is thought to be a stable modification, however in 2008, Kangaspeska and colleagues published unexpected findings showing transient cyclic methylation of promoter CpG island DNA in several genes. The authors demonstrate cyclical DNA

[9] A term describing elements derived from common ancestral DNA.

[10] Partially methylated.

methylation turnover with a periodicity of approximately 100 min in MCF-7 cells[11] (Kangaspeska et al., 2008). This observation may be linked to the action of 5-aza-cytidine. Whether this is widespread and whether it applies to MGMT has yet to be examined. Evidence of how *de novo* DNMTs target unmethylated CpGs *in vivo* remains contentious, however a number of possible mechanisms have been proposed in different organisms. The first relates to the suggestion that DNMTs recognise specific domains on DNA or chromatin. Alternatively, DNMTs may be recruited by transcriptional repressors or other protein-protein interactions. Further, antisense non-coding ribonucleic acid (ncRNA) is known to play a role in DNA methylation and silencing of a previously active gene in human cells *in vivo* and murine embryonic stem cells (ES) (Tufarelli et al., 2003). Lastly chromatin modifications may bring about the recruitment of DNMTs. This idea has been demonstrated in plant-based systems (Tamaru & Selker, 2001) and the principle has been demonstrated in mammalian-based systems. Depletion of two histone lysine methyl-transferases (HKMTs) specific for H3K9 has been observed to reduce DNA methylation on sequences within heterochromatic regions in murine ES cells (Lehnertz et al., 2003).

1.6.2 Mechanisms for Methyl-CpG mediated silencing

In recent times, advances in biochemical techniques to study protein-protein interactions have elucidated a number of proteins thought to be involved in linking DNA methylation to chromatin structural changes. Although it was originally thought that CpG methylation prevented binding of TFs directly through steric interference (Watt & Molloy, 1988), more recent research has lead to the hypothesis that a group of proteins containing a methyl binding domain (MBD) are capable of specific methyl-CpG binding. MBD proteins are capable of recruiting histone-modifying and remodelling enzymes as well as playing an important role in transcriptional repression (P. L. Jones, et al., 1998; Wade et al., 1999). One example is the methyl CpG binding protein 2 (MeCP2) complex containing an MBD. MeCP2 is targeted to methylated DNA in a sequence specific manner (Klose et al., 2005) (Figure 1-7). There are currently three MBD proteins/modules that have been linked to methyl-CpG mediated gene silencing: MBD1, MBD2 and MeCP2 (Bird & Wolffe, 1999; Li & Bird, 2007). MBD2 can be coupled to a class of enzyme named histone de-acetylases (HDAC) as part of a large

[11] Human breast cancer cell line.

complex with a role in chromatin organisation and histone variant exchange named Mi-2/NURD (Hendrich, Guy, Ramsahoye, Wilson, & Bird, 2001; Wade, et al., 1999). These results suggest that methyl CpG mediated gene silencing can act through MBD2 binding.

In 2009 the C. David Allis group from Rockefeller University in New York published a landmark paper demonstrating recruitment of DNA methyltransferase by a specific histone modification. It was shown that symmetric dimethylation of arginine 3 on histone H4 by the protein arginine methyltransferase PRMT5 brings about the recruitment of the *de novo* DNA methyltransferase DNMT3A in human erythrocytes. These data provide the first evidence that DNMT3A can simultaneously 'read' histone marks and 'write' DNA methylation marks (Q. Zhao et al., 2009). It remains to be seen whether DNA methylation mediates histone modifications or vice versa, although it seems likely that both mechanisms are present in different cell lines/organisms and involve different loci.

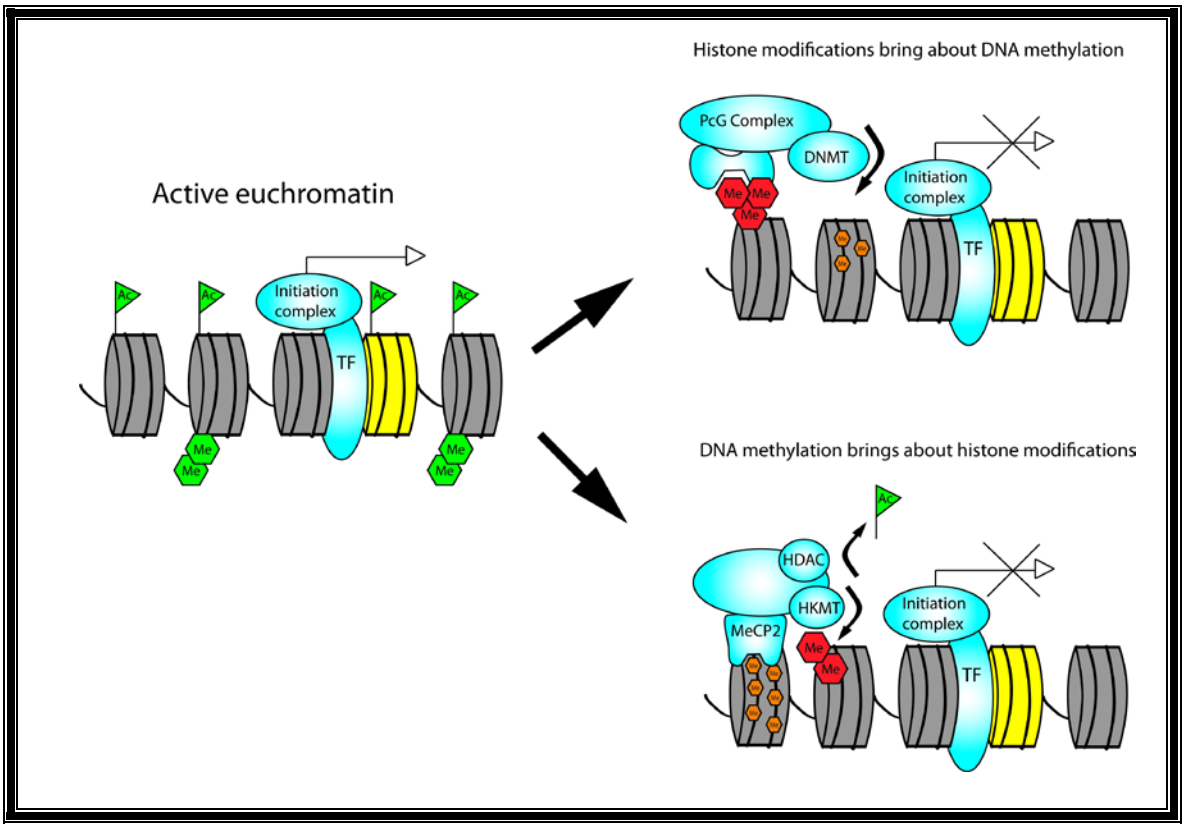

Figure 1-7 Mechanisms for euchromatic gene silencing. Adapted from (Allis, et al., 2007)

1.7 Chromatin modifications and binding domains

There are a variety of histone N-terminal modifications that have been identified, including acetylation, methylation, phosphorylation, ubiquitylation and sumoylation, although very few are well characterised. The hierarchical nature of histone modifications lead the scientist C. David Allis to propose the "histone code" hypothesis in which it is suggested that combinations of different histone modifications are interpreted by chromatin organisation proteins within the cell. Such a system leads to a great deal of complexity, nonetheless, certain modifications associated with active or repressed chromatin have now been established (Jenuwein & Allis, 2001). Evidence supporting the histone code hypothesis comes from studies in which researchers have shown that certain domains such as the bromodomain (Haynes et al., 1992) and chromodomain (Delmas, Stokes, & Perry, 1993) are able to recognise acetylation or methylation respectively at specific histone residues. The bromodomain selectively binds to acetylated histone tails (Winston & Allis, 1999) and is present in members of the mating type switching/sucrose non-fermenting (SWI/SNF) family of transcriptional activators, chromatin remodelling proteins (SNF2/BRM), (Dingwall et al., 1995; Kadam & Emerson, 2003), and components of the transcription machinery including $TAF_{II}250$, GCN5 (Jenuwein & Allis, 2001) and CBP/p300. The chromodomain specifically binds to histone methyl-lysines. The heterochromatin protein 1 (HP1) protein contains a chromodomain displaying specificity for H3K9me2. Additionally, the Mi-2/NuRD HDAC complex contains a double chromodomain (Ahringer, 2000).

1.7.1 Histone lysine acetylation

It is now well established that histone lysine acetylation is important for transcriptional activation, especially in the 5' region of genes (Liang et al., 2004). The HAT family catalyse lysine acetylation while the HDAC family catalyse de-acetylation. All members of the HAT family are thought to confer an activational effect on transcription. Some examples of specific residues which can be acetylated include H3K9, H3K14 and H3K18 (Kouzarides & Berger, 2007). Numerous researchers have used ChIP and other techniques to show that histone acetylation at gene promoters correlates with activation of gene expression, whereas de-acetylation correlates with repression (Hutchins et al., 2002; M. Shogren-Knaak, et al., 2006). In *xenopus*, transcriptional repressors are commonly associated with HDACs (Mi-2/NURD) (Wade, et al., 1999). In addition,

transcriptional activators often possess a HAT domain (PCAF/GCN5), or associate with HAT modules (CBP/p300) (Candau, Zhou, Allis, & Berger, 1997; Grant et al., 1997).

The mechanisms by which acetylation affects transcription have not yet been conclusively established although one hypothesis is that histone lysine acetylation promotes "loosening" of the chromatin by neutralising the positive charge of lysine. This is thought to prevent tight packing of the basic histone tails of the nucleosomes, while allowing access to proteins which may mediate additional histone modification and/or remodelling. In 1999 the Danam group demonstrated that MGMT repression was linked to histone de-acetylation in cells derived from human cervical cancer (Danam, et al., 2005).

1.7.2 Histone methylation

While it is commonly accepted that global acetylation of histone lysines is associated with transcriptional activation (Jenuwein & Allis, 2001), the role of histone methylation is much less clear. To begin with, histone methylation may occur on lysine or arginine residues. A further complication is the presence of multiple methylation states including mono, di and tri methylation (Zhang & Reinberg, 2001). Additionally, histone methylation can either activate or repress transcription, depending on the site and state.

The methyl-lysine histone mark is mediated by HKMT enzymes that are characterised by a catalytically active lysine methyltransferase (SET) domain (Rea et al., 2000). Methylated lysine residues that have been linked to active chromatin include H3K4me, H3K36me and H3K79me. Conversely H3K9me2, H3K9me3, H3K27me3 and H4K20me have been linked to repressed transcriptional activity.

The lysine demethylase (LSD) enzymes contain a recently identified conserved domain named the Jumanji-C (JmjC) domain (Tsukada et al., 2006). The specificity of the prominent LSD family member LSD1 can be altered from methyl H3K4 to methyl H3K9 depending on its binding partner. Of particular interest is the fact that H3K4me is associated with active chromatin, whereas inactive chromatin commonly contains the H3K9me mark (Kouzarides & Berger, 2007).

1.7.2.1 Histone arginine methylation

Arginine methylation is associated with both activation and repression of transcription. The PRMT1/CARM1 protein arginine methyltransferase family (PRMT) can be recruited by TFs including p53 and NFκB and catalyse histone methylation on a number of residues including H3R2, H3R17 and H3R26. Like lysine methylation, mechanistic links to both DNA methylation (as discussed in section 1.6.2) and recruitment of chromatin modification complexes including CBP/p300 have been described for methyl arginine marks (An, Kim, & Roeder, 2004). An arginine demethylase has yet to be discovered, however it is thought that deimination from methyl arginine to citruline may represent the primary mechanism of arginine demethylation. Arginine methylation would seem to be a global mechanism for chromatin regulation, however there are currently no reports of arginine modification at the MGMT locus.

1.7.2.2 Histone lysine methylation

There are a multitude of lysine residues which may be relevant to MGMT expression however there is insufficient space to discuss them all in detail. Methylation of H3K4, H3K36, H327 and H3K9 residues are discussed in further detail. The mixed lineage leukemia (MLL) enzyme mediates the H3K4me mark and are often found at the promoter of active genes in humans. MLL associates with the CTD of RNApolII phosphorylated at serine 5 (Ser5ph) (Ruthenburg, Allis, & Wysocka, 2007). H3K4me3 has been linked specifically to NURF and ISWI histone remodelling complexes in *xenopus* and is thought to be involved in the process of promoter clearance (Wysocka et al., 2006). Notably, methylation of H3K4 prevents methylation of H3K9 by SUV39h (discussed further in section 1.7.2.3) (Kouzarides & Berger, 2007).

The Set2 HKMT mediates the H3K36me mark. Set2 is known to associate with the CTD of RNApolIIo at phosphorylated serine 2 (Ser2ph). Methylation of H3K36 is thought to be important for transcriptional elongation and suppression of cryptic start sites as it is commonly seen within the coding region and at the 3' end of active genes.

The mammalian EZH2 protein [named after *drosophila* enhancer of zeste E(Z)] catalyses methyl transfer to H3K27, however little is known about EZH2 recruitment in mammals. Methylation at H3K27 is linked to a repressive chromatin state and is

observed at discrete regions of the *drosophila* and mammalian genome. Firstly, in *drosophila* and mammals, H3K27me3 has been observed at pericentric[12] heterochromatin. In addition the H3K27 mark is found at polycomb group (PcG) responsive elements throughout the *drosophila* genome. Lastly, the H3K27me3 mark is prevalent on the silenced/inactive X chromosome in mammals. In 2007 the Howard Cedar group published findings which suggest that the H3K27me3 mark is linked to the presence of *de novo* DNMTs and DNA methylation at aberrantly silenced gene promoters in a variety of cancer cell lines (Schlesinger, et al., 2007).

1.7.2.3 H3K9 methylation

H3K9 methylation appears to constitute an important aspect of chromatin silencing because it has direct links to a variety of chromatin organisation events. SUV39h is a HKMT which shows specificity for H3K9 (Rea, et al., 2000). However SUV39h has been shown to primarily be localised to centromeric heterochromatin (Aagaard, Schmid, Warburton, & Jenuwein, 2000). HP1, a well defined marker of inactive heterochromatin, interacts with both SUV39h and the H3K9me2 modification simultaneously (Martin & Zhang, 2005). A second methyltransferase named G9a has been found to catalyse H3K9 methylation. G9a has been demonstrated to be localised to non-centromeric chromatin (Tachibana, Sugimoto, Fukushima, & Shinkai, 2001). Further complicating matters, in 2003 Rice and colleagues demonstrated that pericentric heterochromatin is specifically enriched in H3K9me3, whereas H3K9me1 and H3K9me2 are found in facultatively silenced chromatin (Rice et al., 2003). Scientists Tony Kouzarides and Shelly L. Berger hypothesised that HP1 may act as an anchor which allows for tethering of facultatively silenced chromatin to heterochromatin rich nuclear subcompartments. Previous researchers have suggested heterochromatinisation of the MGMT locus (Watts, et al., 1997). If this is indeed the case, the presence of either H3K9me2 or H3K9me3 could be expected (Figure 1-8). Indeed, in cancer cells, the retinoblastoma protein (RB) has been shown to deliver SUV39h and HP1 to certain genes which are consequently silenced (Kouzarides & Berger, 2007) although this has not yet been demonstrated for the MGMT gene.

[12] Surrounding the centromere

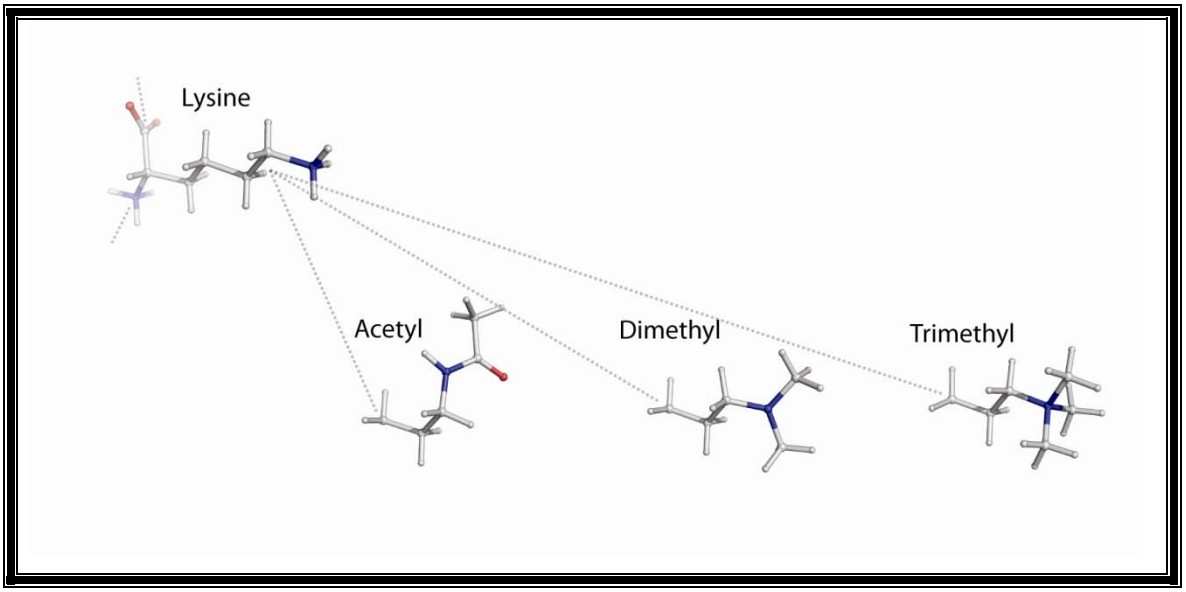

Figure 1-8 Lysine and a selection of post-translational modifications

1.7.3 Histone serine phosphorylation

Protein phosphorylation is among the first described protein modifications and is mediated by a variety of kinases. In 1991 Mehadevan and colleagues demonstrated a correlation between H3 serine phosphorylation by PKC and transcriptional induction (Mahadevan, Willis, & Barratt, 1991). Although phosphorylation of histone 3 at serine 10 (H3S10ph) is not thought to directly affect higher order chromatin folding, H3S10ph has been shown to influence transcription. Using an *in vitro* system, Shrogen-Knaak and colleagues demonstrated that H3S10ph enhances the activity of the HAT complex GCN5 (M. A. Shogren-Knaak, Fry, & Peterson, 2003).

1.7.4 Chromatin remodelers and histone variants

In addition to chromatin modification, chromatin organisation and gene transcription are affected by chromatin remodelling complexes and histone exchange. Chromatin remodelling complexes use ATP to change the composition or position of the nucleosomes in discrete regions near the promoter (Grant, et al., 1997). Remodelling complexes fall into four main classes; ISWI (imitation switch), SWI/SNF (introduced in section 1.7), INO80 (inositol) and CHD (chromodomain helicase DNA-binding) however only the ISWI and SWI/SNF and CHD classes will be discussed.

In general, the ISWI class, including NURF, contain a SANT domain DNA binding module and play a role in chromatin assembly and consistent spatial placement of nucleosomes along replicated DNA. SWI/SNF remodelers on the other hand are distinguished by the presence of a bromodomain and provide access to DNA by sliding or ejecting nucleosomes. Lastly, the CHD family contain a DNA binding domain and two tandem chromodomains which recognise H3K4me2/3. The foremost member of the CHD family, CHD1, is localised throughout the coding regions of genes and acts as a chaperone, catalysing transfer of core histones onto DNA. CHD1 localises with the heterodimeric FACT (facilitates chromatin transcription) complex, the role of which has recently been elucidated. Using an artificial chromatin system developed in *drosophila*, the Reinberg group demonstrated that FACT facilitates the removal of H2A-H2B dimers from within nucleosomes and thus activates transcriptional elongation (Orphanides, LeRoy, Chang, Luse, & Reinberg, 1998). Nucleosome subunit exchange is linked to active and repressive chromatin structures. The H2A.Z histone variant is commonly found at the -1 or +1 histone on the promoter of active genes. It has been proposed that H2A.Z is less stable than H2A leading to efficient ejection by FACT allowing promoter exposure (Tsukiyama, 2002).

1.7.5 A role for ncRNA?

Using a number of systems, researchers have demonstrated that RNA can play a role in heterochromatin assembly and is associated with both DNA methylation and H3K9me specifically (Martiensen & Moazed, 2007). Traditionally, RNA interference (RNAi) is known as the process whereby double stranded RNA (dsRNA) is processed by a ribonuclease named dicer into small interfering RNA (siRNA) molecules of approximately 21-27 nucleotides (nt) in size (Ketting et al., 2001). These small fragments then assist in targeting the RNA-induced silencing complex (RISC) to mRNA or target the RNA-induced transcriptional silencing (RITS) complex to chromosomes to enable CpG-methylation and chromatin modification (Verdel et al., 2004). The RITS complex contains a chromodomain protein Chp1 which binds specifically to methylated H3K9. Notably, recruitment of RITS to methylated H3K9 represents an initial step of siRNA mediated silencing. Spreading and maintenance of silenced chromatin requires additional recruitment of the HKMT Clr4 and the histone remodeller Swi6 (Kouzarides & Berger, 2007). It is a possibility that ncRNA may play an as yet unforeseen role in MGMT silencing.

1.7.6 Epigenetic events involved in MGMT transcription

Melanoma is one of the deadliest types of cancer, and one of the few remaining options for the improvement of treatment is the improvement of current therapies such as TMZ. MGMT expression is the dominant factor influencing patient response to TMZ. It is clear that epigenetic effects play a role in MGMT expression in some cancers, however the epigenetic signature of melanoma specifically has yet to be examined. DNA methylation and chromatin modifications are commonly altered in cancer. In the current study, DNA methylation and chromatin modifications on the H3K9 residue in melanoma cell lines will be examined.

1.8 Hypothesis and aims

The hypothesis under investigation in this research report is as follows:
Promoter DNA methylation, local histone H3 lysine 9 de-acetylation and histone H3 Lysine 9 dimethylation will directly correlate with the silencing of the DNA repair enzyme O^6 methyl-guanine methyltransferase (MGMT) in primary New Zealand melanoma (NZM) cell lines.

A third histone modification (H3K9me3) was hypothesised to correlate with silenced MGMT expression.

The aims of my research project are:

1) To correlate the DNA methylation status of the MGMT locus to MGMT expression levels in melanoma cell lines.
2) To correlate post-translational histone lysine modifications at the MGMT locus to MGMT expression levels in melanoma cell ines.

In order to address these aims the following steps will be taken:

1) Primary melanoma cell lines will be propagated. Then DNA and chromatin will be extracted.
2) Methyl-DNA immuno-precipitation (MeDIP) will be applied using antibodies raised against 5' methyl cytosine to isolate DNA enriched in methyl cytosine residues. Real-time PCR with primers designed to the MGMT promoter CpG island will be carried out on the MeDIP DNA.
3) Chromatin immuno-precipitation (ChIP) will be applied using antibodies raised against acetyl histone H3 lysine 9 (H3K9ac), di-methyl histone H3 lysine 9 (H3K9me2) and tri-methyl histone H3 lysine 9 (H3K9me3) to isolate DNA bound near these modifications. Real-time PCR with primers designed to the MGMT promoter CpG island will be carried out on the ChIP DNA.

2 Materials and methods

2.1 Materials

2.1.1 General chemicals

Stock chemicals were purchased from a number of sources. Dimethyl sulfoxide (DMSO), ethylene-diamine-tetra-acetic acid (EDTA), triton-X-100, sodium dodecyl sulphate (SDS), foetal bovine ferum (FBS), deoxynucleotide triphosphates (dNTPs) and agarose were purchased from Sigma Chemical Company, MO, USA.

2.1.2 Equipment

DNA was quantified using the Nanodrop spectrophotometer ND-1000 or the Qubit fluorometer. PCR was carried out on the MJ research PTC-200 thermal cycler. DNA and chromatin were sonicated using a VirTis Virsonic 600 ultrasonic cell disruptor using a micro-tip.

2.1.3 Cell culture

All sterile culture flasks, scrapers and tubes were purchased from Nunc Inc., IL, USA. Sterile plates were purchased from Greiner Bio-one, Germany. Cells were incubated in a HeraCell 150 incubator. Cells were manipulated in an ESCO biological safety cabinet Model: LA24A1. Acrocap filter unit (0.2 µm) filters were purchased from Pall Corporation, MI, USA. Express stable trypsin-like enzyme plus phenol red (TrypleE) was purchased from Invitrogen Corporation, Auckland, New Zealand. Trypan Blue solution was purchased from Sigma Chemical Company, MO, USA.

2.1.3.1 Media and supplements

Alpha-minimum essential media (α-MEM), FBS and penicillin/streptomycin (5,000 units/mL) were purchased from Invitrogen Corporation, Auckland, New Zealand. Insulin-transferrin selenite (ITS) supplement, (10 mg/ml) was purchased from Roche, Mt. Wellington, Auckland, New Zealand.

2.1.4 Antibodies

All primary antibodies (5-methyl cytosine, H3K9ac, H3K9me2, H3K9me3) were purchased from Abcam inc., MA, USA.

2.1.5 DNA manipulations

2.1.5.1 Restriction endonucleases and DNA modifying enzymes

Restriction endonucleases and buffers were purchased from a number of different sources: New England Biolabs, MA, USA; Roche, Mt. Wellington, Auckland, New Zealand; Boehringer Manheim, Germany.

2.1.5.2 PCR reagents

Oligonucleotides were purchased from Sigma Chemical Company, MO, USA. Faststart *Taq* polymerase, GC rich solution, 10 x PCR buffer, Roche Light Cycler 480 SYBR Green 1 master mastermix, 96-well plates and seals were purchased from Roche, Mt. Wellington, Auckland, New Zealand.

2.1.6 Chromatin manipulations

Complete mini EDTA-free protease inhibitor cocktail tablets were purchased from Roche, Mt. Wellington, Auckland, New Zealand. Protein A/G beads were purchased from Santa Cruz Biotechnology, CA, USA.

2.1.7 Software

LightCycler 480 software release 1.5.0 SP1 and LightCycler probe design software 2.0 version 1.0 R36 were provided by Roche, Mt. Wellington, Auckland, New Zealand. Vector NTI advance software version 11 was purchased from Invitrogen Corporation, Auckland, New Zealand.

2.2 Methods

2.2.1 Cell culture

Primary New Zealand melanoma (NZM) cell lines were acquired from stocks at the Auckland Cancer Society Research Centre, care of Professor Bruce Baguley. Cell lines were cultured for the extraction of genomic DNA (gDNA) and chromatin. All cell lines were grown at 37°C under humid conditions in a 5% CO_2 and 10% O_2 incubator (HeraCell 150). Media was changed every 2-3 days. Cell lines were manipulated aseptically in a biological safety cabinet (ESCO Model: LA24A1).

2.2.1.1 Media preparation

Alpha-minimum essential media (α-MEM), (Invitrogen) was reconstituted from powder according to manufacturer's instructions and adjusted to pH 7.2 using 2.4 g of tissue culture grade sodium bicarbonate per litre. Media was filtered using a 0.2 µm filter (acrocap). A total of 190 mL was dispensed into sterile bottles in a laminar flow hood (Westinghouse Model: Crossflow 1800) and stored at 4°C. Media was supplemented with 5% foetal bovine serum (FBS) (Invitrogen), 1% penicillin/streptomycin (Invitrogen) and 100 µL of insulin-transferrin-selenite (ITS) supplement, (Roche) (10 mg/mL). Media was warmed to room temperature prior to use.

2.2.1.2 Starting cells from frozen stock

Cell cultures were started from 1 mL frozen stocks (prepared by Kelly Senior, Institute of Molecular Biosciences, Massey University, New Zealand). Each frozen aliquot (in 10% DMSO in FBS) was thawed and suspended in 10 mL of supplemented α-MEM. Cells were collected by centrifugation at 200 x g for three minutes. The pellet was re-suspended in 2 mL complete media and 1 mL was added to each of two T25 flasks (Nunc) containing 6 mL of complete media each.

2.2.1.3 Maintenance of cells

Cell cultures were grown as a monolayer in T25 flasks (Nunc) to 80-90% confluence before passaging the cells into new T75 flasks (Nunc). Spent media were removed then the cells were rinsed with 5 mL of express stable trypsin-like enzyme plus phenol red (TrypleE) reagent, (Invitrogen). Flasks were then tapped sharply to aid cell detachment.

Cell detachment was confirmed by examination under an inverted light microscope. Cells were re-suspended in 2 mL of complete media, of which 1 mL was added to a single T75 flask (Nunc) containing 12 mL of complete media. Re-suspension was achieved by repeated uptake and expulsion with a 5 mL pipette.

2.2.1.4 Preparing cells for freezing

Cells for storage were treated as outlined in section 2.2.1.3, following cell detachment cells were re-suspended in 2 mL 10% DMSO in FBS. Next, 1 mL was transferred to each of 2 cryo-vials (Nunc). Cryo-vials were frozen slowly (by wrapping in copious amounts of tissue paper) at -86°C, followed by long-term storage in the gaseous phase of liquid nitrogen at approximately -195°C.

2.2.2 DNA Manipulations

DNA was stored at -20°C and manipulated on ice where appropriate.

2.2.2.1 Phenol-chloroform extraction and ethanol precipitation

DNA was extracted by sequential extraction with equal volumes of phenol, 1:1 phenol/chloroform and chloroform. The aqueous phase was mixed with 1/10 volume of 3 M NaOA pH 5.0 and 2.5 volumes cold 95% EtOH and incubated at -20°C for 30 minutes. DNA was collected by centrifugation at 10,000 x g and washed sequentially in 70% and 95% EtOH. The pellet was air dried and re-suspended in sterile H_2O or Tris-EDTA solution (TE: 10 mM Tris-HCl, 1 mM EDTA pH 8.0).

2.2.2.2 DNA quantification by absorbance at 260 nm or fluorescence

DNA was quantified using either the nanodrop spectrophotometer or the Qubit system using the Quant-it double stranded DNA High Sensitivity Assay kit (Invitrogen) respectively as per the manufacturer's instructions.

2.2.2.3 Block PCR

Sequence-specific primers and a thermostable polymerase such as Faststart *Taq* were used in block PCR reactions. Reactions were set up in thin-walled 0.2 mL PCR tubes in a total reaction volume of 50 µL as outlined in Table 2-1. GC solution was added because it aids GC-rich template denaturation. A negative control (no DNA template)

was included with each PCR. Block PCR was carried out on the MJ research PTC-200 system.

Table 2-1 Block PCR protocol for amplifying MGMT101 product

Initial denaturation	95°C for 5 minutes	
Denaturation	95°C for 20 seconds	45x cycles
Annealing	60°C for 30 seconds	
Extension	72°C for 15 seconds	
Final extension	72°C for 5 minutes	

The PCR mixture contained 3.5 µL (20 µM) of primer F and primer R, 3.5 µL (3 mM) dNTPs, 5 µL 10x PCR buffer (500 mM Tris-HCl, 100 mM KCl, 50 mM $(NH_4)_2SO_4$, 20 mM $MgCl_2$, pH 8.3/ 25°C), 10 µL (5x) GC rich solution, 0.4 µL (5 U/ µL) of Faststart *Taq* DNA polymerase, 2.5 µL of template DNA (100 ng/ µL) and 38.6 µL of sterile H_2O to make the total volume 50 µL.

2.2.2.4 Agarose gel electrophoresis

Varying percentage agarose gels were prepared by melting agarose powder in 50 mL of 1x Tris-Acetate EDTA (TAE: 0.2 M Tris-HCl, 0.2 M Acetic acid, 0.05 M EDTA pH 8.5). Then 1 µL of ethidium bromide [(EtBr) 10 mg/mL] was added to the gel prior to pouring. After allowing to set for approximately 60 minutes at room temperature the gel was covered in 1x TAE. DNA samples were mixed with 6x loading dye (0.22 mM Orange G, 40% sucrose (w/v)) and loaded into the wells. Next 1 µL EtBr (10 mg/mL) was added to the buffer to aid in visualisation. Electrophoresis was carried out at 100 – 105 V for approximately 1 hour followed by visualised under UV illumination on the Gel-Doc system.

2.2.2.5 Restriction endonuclease digestion

Restriction endonuclease digestions were set up in 50 µL reactions in 1.7 mL tubes and carried out according to the enzyme manufacturer's instructions. Following the

digestion, 10-20 µL of sample was examined by agarose gel electrophoresis as outlined in section 2.2.2.4.

2.2.3 Methyl DNA immunoprecipitation

The MeDIP procedure was modified from a protocol developed by Michael Weber and colleagues (Weber et al., 2005).

2.2.3.1 Genomic DNA extraction

Genomic DNA was extracted from 70-90% confluent NZM cell lines. Cells were treated as outlined in section 2.2.1.3 except that they were re-suspended in 6 mL of phosphate buffered saline (PBS) solution (NaCl 140 mM, KCl 2.7 mM, Na_2HPO_4 10 mM, KH_2PO_4 1.8 mM, pH 7.3). The resulting suspension was transferred to a 15 mL tube. Cells were collected by centrifugation at 200 x g for 3 minutes then rinsed in 10 mL of PBS and re-centrifuged at 200 x g for 3 minutes. The cell pellet was suspended in 300 µL of TE followed by lysis in 300 µL of 2x MeDIP lysis buffer (20 mM Tris-HCl, 4 mM EDTA, 20 mM NaCl, 1% SDS) supplemented with 20 µL proteinase K solution (10 mg/mL). Cell lysate was incubated at 55°C for 5 hours or overnight followed by a phenol-chloroform extraction and ethanol precipitation as described in section 2.2.2.1. The precipitated DNA pellet was suspended in 30 µL TE buffer supplemented with RNAse H (final concentration 60 µg/mL) followed by incubation at 37°C for 30 minutes. DNA was subsequently quantified, visualised by agarose gel electrophoresis as outlined in section 2.2.2.4 then stored at -20°C.

2.2.3.2 DNA sonication

Genomic DNA was diluted to a final concentration of 0.05 µg/µL in 400 µL TE. Samples were sonicated on a VirTis virsonic 600, ultrasonic cell disruptor on ice at 1.0 power for 10 seconds at a time with 1 minute breaks in-between. This procedure was repeated 2 x followed by vortex and centrifugation at 3000 x g for less than 30 seconds. This was repeated sequentially until a total of 10 x sonications were achieved. The 7.5 µL samples were examined by gel electrophoresis as outlined in section 2.2.2.4. Samples were precipitated in 1000 µL NaCl-EtOH solution (NaCl 400 mM NaCl, 95% EtOH), washed once 500 µL of ice-cold 98% EtOH, followed by air-drying at room temperature for 1-2 hours. The resulting pellet was suspended in 30 µL autoclaved

milli-Q H_2O and incubated at room temperature (RT) for 30 minutes followed by quantification and storage.

2.2.3.3 Immunoprecipitation

Immunoprecipitation was carried out in 500 µL volumes in 1.7 mL tubes. Then 4 µg of sonicated DNA was suspended in 450 µL of TE. The resulting solution was placed in a boiling water bath for 10 minutes then transferred to ice for 10 minutes. Next 51 µL of cold 10X immunoprecipitation buffer (IP buffer: 0.1 M NaPO4 buffer, 1.4 M NaCl, 0.5% Triton-X) was added and the solution was mixed thoroughly. Following this 4 µg anti-methyl DNA antibody (Abcam Inc.) was added and incubated at 4°C on an orbital shaker for 3-5 hours. Next 25 µL of protein A/G beads (Santa Cruz Biotechnology) were suspended in 25 µL 2 x IP buffer and mixed with the solution or added to a beads-only control sample and incubated at 4°C on a slow orbital shaker over-night. A/G beads were collected by centrifugation at 2000 x g for 5 minutes at 4°C as per manufacturer's instructions. The resulting pellet was washed in 700 µL of cold 1X IP buffer and re-centrifuged three times followed by re-suspension in 250 µL of proteinase K digestion buffer (50 mM Tris-HCl pH 8.0, 10 mM EDTA, 0.5% SDS). Finally 7 µL of proteinase K (10 mg/mL) was added and mixed, the solution was then incubated for 3 hours at 50°C on a shaker.

2.2.4 Chromatin immunoprecipitation (ChIP)

The chromatin immunoprecipitation method used was the ChIP assays protocol (Yan, Chen, & Costa, 2004) with modifications based on those developed by (Irvine & Hsieh, 2004) and (Jallow, Jacobi, Weeks, Dawid, & Veenstra, 2004).

2.2.4.1 Preparing cells for ChIP

NZ melanoma cells were grown to 80-90% confluence in 20 ml supplemented αMEM in 3x 150 mm diameter plates (Nunc). Media was removed from the cells and the plates were washed twice with 5 ml PBS. Cells were scraped into 5 mL PBS and placed into 50 mL tubes. Tubes were centrifuged at 800 x g for 4 minutes. The resulting pellet was re-suspended in 18 mL of PBS.

2.2.4.2 Formaldehyde cross-linking

First, 2 mL of 10x cross-linking buffer (11% Formaldehyde, 0.1 M NaCl, 0.5 mM EGTA, 50 mM Hepes) was added to 18 mL PBS containing approximately $5x10^7$ cells and mixed gently on a rotating shaker at low speed for 5 minutes. Then 1 mL of glycine (2.5 M) was added to quench the cross-linking reaction. Tubes were placed on ice and rinsed twice with ice cold PBS. The resulting pellet was suspended in 1 mL of ChIP lysis buffer (10 mM EDTA, 1% SDS, 50 mM Tris-HCl) in the presence of 1x complete mini protease inhibitors (Roche), and stored at -80°C.

2.2.4.3 Chromatin sonication

A total of 1000 µL of lysed cell extract was sonicated using a VirTis Virsonic 600 ultrasonic cell disruptor on ice in a 1.7 mL tube at 1.0 power for 35-50 sets of 5 x 10 second bursts. Samples were held on ice for 1 minute between sonications to prevent excessive heating which may reverse cross-links. Samples were briefly vortexed and centrifuged between each set of 5 x 10 sonications to ensure homogenization. When the lysate was sonicated to the desired size a 50 µL sample was removed to check sonication efficiency and for DNA quantification. Sonicated extract was centrifuged at 10,000 x g for 15 minutes at 4°C to remove cellular debris.

Approximately 950 µL samples were stored at -80°C for immunoprecipitation. A 50 µL aliquot from this stock was added to 350 µL ChIP Elution Buffer (1% SDS, 100 mM $NaHCO_3$) containing 0.5 mg/mL RNAse and 0.5 mg/mL proteinase K followed by incubation at 37°C for 30 minutes. Cross-link reversal was achieved by incubation at 65°C over-night in the presence of 200 mM NaCl. The DNA was phenol-chloroform extracted and EtOH precipitated as previously described in section 2.2.2.1 and resuspended in 100 µL H_2O. The 5 µL of sample was examined by agarose gel electrophoresis as described in section 2.2.2.4. Finally, 1 µL of sample was quantified on the nanodrop spectrophotometer.

2.2.4.4 Chromatin immunoprecipitation

For each cell line four aliquots of 200 µL of chromatin were added to 800 µL cold RIPA buffer (50 mM Tris-HCl, 150 mM NaCl, 2 mM EDTA, 1% NP-40, 0.5% Na deoxycholate, 0.1% SDS) each in the presence of 1x protease inhibitor cocktail in pre-

cooled 1.7 mL microcentrifuge tubes. Next 4 µg of primary antibody was added to all samples except the beads-only control. Samples were incubated at 4°C on a rotating shaker at low speed for two hours. Simultaneously, 150 µL protein A/G beads (Santa Cruz Biotechnology) were prepared by washing three times in 500 µL RIPA buffer followed by resuspension in 150 µL RIPA buffer containing herring sperm ssDNA (Invitrogen) to a final concentration of 75 ng/µL and BSA (NEB) to a final concentration of 0.1 µg/µL. Beads were incubated shaking at RT for 30 minutes. Beads were washed in 500 µL of RIPA buffer followed by re-suspension in 150 µL RIPA buffer. Then 20 µL of pre-adsorbed beads were added to each IP sample followed by incubation at 4°C on a rotating shaker at low speed over night. Beads were collected by centrifugation at 1500 x g for 1 minute. Beads were washed 4 times by inversion (10 x) in chilled wash buffer 1 (0.1% SDS, 1% Triton X-100, 2 mM EDTA, 150 mM NaCl, 20 mM Tris HCl pH 8.0) followed by a single wash by inversion (10 x) in chilled wash buffer 2 (0.1% SDS, 1% Triton X-100, 2 mM EDTA, 500 mM NaCl, 20 mM Tris HCl pH 8.0). Antibodies were eluted by the addition of 400 µL elution buffer (1% SDS, 100 mM $NaHCO_3$) in the presence of 0.5 mg/mL proteinase K and 0.5 mg/mL of RNAse A followed by incubation at 37°C for 30 minutes. Samples were centrifuged for 1 minute at 1500 x g and the supernatant transferred to fresh tubes. Cross-link reversal was achieved by incubation at 65°C for 4 hours in the presence of 200 mM NaCl. The DNA was phenol-chloroform extracted and EtOH precipitated as previously described in section 2.2.2.1 and re-suspended in 80 µL of H_2O.

3 Real-time quantitative PCR assay development

3.1 Introduction

In order to examine DNA methylation and histone modifications at the MGMT promoter, two robust real time-quantitative quantitative PCR (RT-qPCR) assays were developed. The MeDIP relative quantification assay required three primer sets, however the ChIP absolute quantification assay required only two primer sets.

Primers were designed using the Lightcycler probe design 2 software (Roche) to amplify a region near the MGMT promoter and regions within two reference genes (β-actin and H19) selected from the literature (Weber, et al., 2005). Short amplicons were designed to amplify regions no greater than 200 bp in size to increase sensitivity of the assay. Primer pairs were shown to be specific for the intended sequence by restriction endonuclease digestion. Primers were first optimised on the MJ research block PCR thermal cycler as previously described in section 2.2.2.3. Primer pairs were then optimised for RT-qPCR reactions using the SYBR green 1 master solution on the lightcycler 480 instrument to find optimal shared reaction parameters. Primer pairs were found to produce efficient linear PCR amplification in RT-qreactions.

Amplicons were analysed by melting characteristics and gel electrophoresis to ensure amplification of single products. A dilution series of sonicated DNA template was carried out and amplified by RT-qPCR in duplicate for each primer pair. Reaction efficiency and linearity were calculated by plotting crossing points (Cp) against template concentration for each reaction.

3.2 MGMT promoter PCR

The MGMT promoter contains a CpG island which contains a number of CpG sites capable of accepting a methyl group from cellular DNMTs. The CpG island itself is very GC-rich which poses significant problems for designing feasible primers, therefore primers were designed to amplify genomic DNA either upstream or downstream of the CpG island.

Primers were designed to amplify a region upstream of exon 1 of the MGMT gene. All primers shared a similar GC content and a similar annealing temperature (as shown in Table 3-1). Secondary structure formation and inter/intra primer dimerisation was avoided by checking potential interactions *in silico* using the Lightcycler probe design 2 software. After initial testing it was found that purines at the 3' end of each primer improve reaction efficiency.

Table 3-1 Primers designed to amplify a 101 bp fragment upstream of exon 1.

Primer name	Primer sequence	Tm (°C)	Amplicon size (bp)
MGMT101 F	5' CGCTTTCAGGACCACTC 3'	57.8	101
MGMT101 R	5' CTGTGCCTTAGTTTGCC 3'	58.2	

Figure 3-1 shows the GC-rich CpG island and exon 1 of the MGMT promoter in relation to MGMT101F and MGMT101R primer binding sites. Appendix I shows the features at the sequence level.

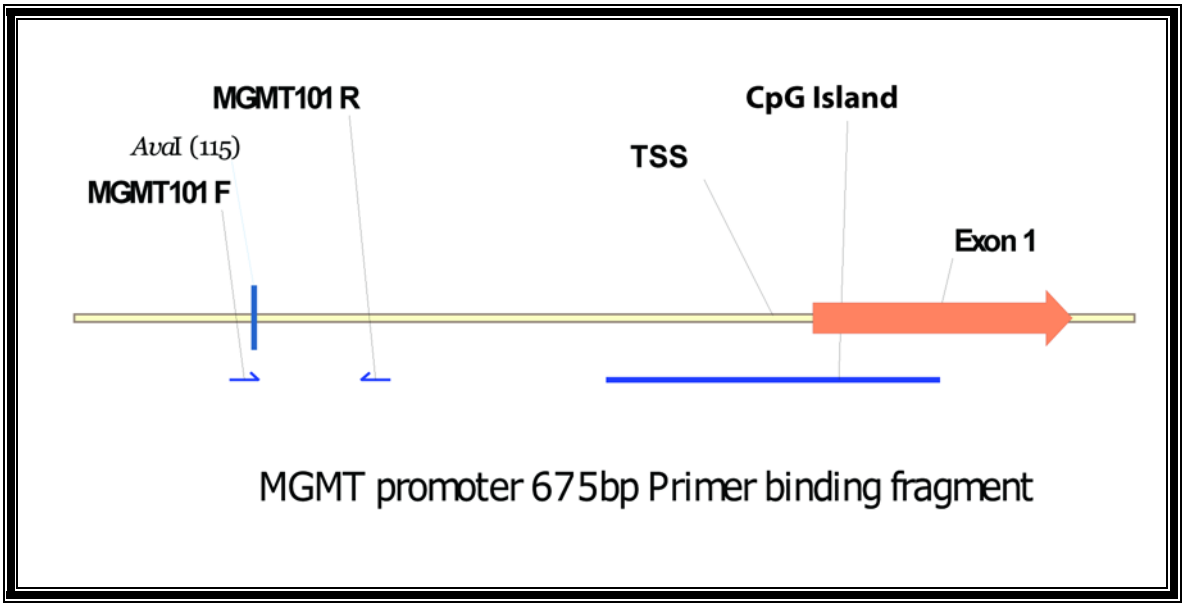

Figure 3-1 Schematic representation of restriction endonuclease cutting site and primer binding sites within a 675 bp MGMT promoter fragment of genomic DNA. Accession # NT_008818.16.

Forward (MGMT101 F) and reverse (MGMT101 R) primers (thin blue arrows) were designed to target a region upstream of the GC-rich CpG island (thick blue lines) within the MGMT promoter upstream of exon 1 (orange block arrow). Restriction endonuclease digestion (vertical blue line) with the *Ava*I enzyme was used to validate the MGMT101 amplicon.

3.2.1 Amplification of the MGMT101 sequence by block PCR

Block PCR reactions were carried out to test PCR parameters. The reaction mixture contained Faststart *Taq* DNA polymerase (Roche) and human genomic DNA template as previously described in section 2.2.2.3. A range of annealing temperatures (54 - 60°C) and magnesium chloride concentrations were tested to optimise the PCR conditions. The correct products were formed at 60°C using native buffered $MgCl_2$ concentration. GC rich solution was found to improve specificity and efficiency of MGMT101 amplification. The final amplification protocol and reaction mix are shown in Table 3-2.

Table 3-2 Block PCR protocol for amplifying MGMT101 product.

Initial denaturation	95°C for 5 minutes	
Denaturation	95°C for 20 seconds	45x cycles
Annealing	60°C for 30 seconds	
Extension	72°C for 15 seconds	
Final extension	72°C for 5 minutes	

The PCR mixture contained 3.5 µL (20 µM) of each primer MGMT101 F and MGMT101 R, 3.5 µL (3 mM) dNTPs, 5 µL 10x PCR buffer (500 mM Tris-HCl, 100 mM KCl, 50 mM $(NH_4)_2SO_4$, 20 mM $MgCl_2$, pH 8.3/ 25°C), 10 µL (5x) GC rich solution, 0.4 µL (5 U/ µL) of Faststart *Taq* DNA polymerase, 2.5 µL of template DNA (100 ng/ µL) and 38.6 µL of sterile H_2O to make the total volume 50 µL.

Block PCR using MGMT101F and MGMT101R primers was expected to produce amplicons of 101 bp in size. The resulting PCR products were electrophoresed on an agarose gel (Figure 3-2). Lanes 2 and 3 contain the desired MGMT101 product 101 bp in size.

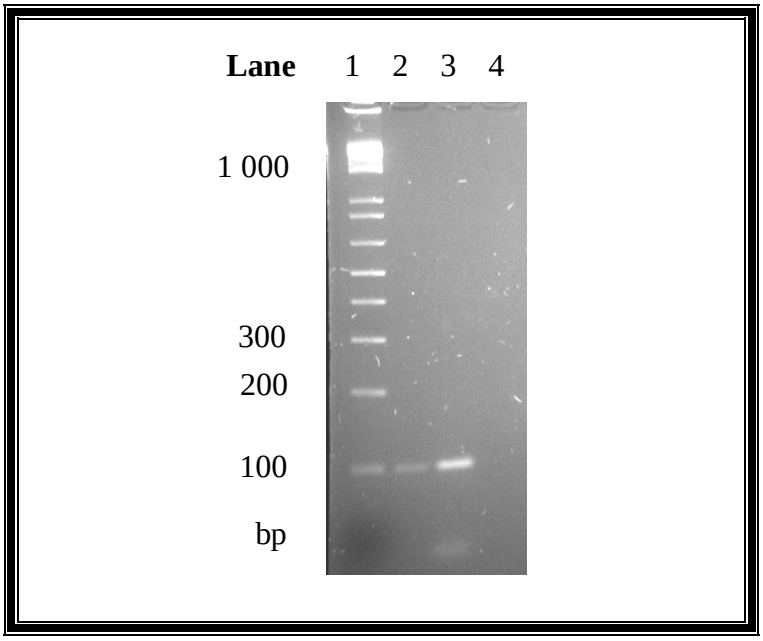

Figure 3-2 MGMT101 amplification by block PCR.

Samples were analysed using electrophoresis on a 3% agarose gel in 1x TAE buffer for approximately 1 hr at 100 V. DNA was visualised by staining with EtBr as described in section 2.2.2.4, followed by illumination under UV light. Molecular size markers are shown to the left in base pairs.

Lanes 1) 0.4µg (4 µL) 1kb plus ladder
2) 10% (5 µL) standard PCR reaction
3) 10% (5 µL) standard PCR reaction with additional 1 µL (50 mM) MgCl
4) 10% (5 µL) negative control (no template added)

3.2.2 Restriction endonuclease digestion of MGMT101 amplicon

To confirm that the sequence of the MGMT101 was correct, a restriction endonuclease digestion was performed. Initially 1 µg of product was digested with 5 U of *Ava*I for 1 hour in a total of 50 µL (as described in section 2.2.2.5) which resulted in an unclear separation of digestion products. The digestion was repeated with 20 U for 3 hours which resulted in a clear differentiation of products. The size of each product was determined relative to the molecular size marker ladder. *Ava*I digestion was expected to produce two bands of 17 and 84 base pairs in size. The result of the digestion is shown in (Figure 3-3). Lane 3 contains the desired MGMT101 restriction fragments.

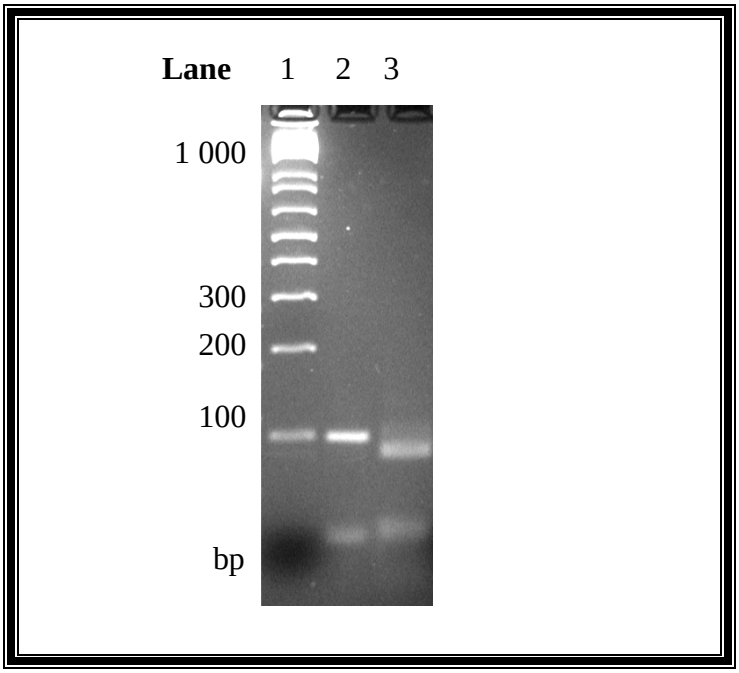

Figure 3-3 MGMT101 amplicon restriction endonuclease digest.

Samples were separated by electrophoresis on a 4% agarose gel in 1x TAE buffer for approximately 1 hr at 100 V. DNA was visualised by staining with EtBr as described in section 2.2.2.4, followed by illumination under UV light. The sizes of molecular size markers are shown to the left in base pairs.

Lanes 1) 0.4 µg (4 µL) 1kb plus ladder
2) 40% (20 µL) of negative control MGMT101 product (no enzyme added)
3) 40% (20 µL) of digestion reaction

3.3 Reference primer design and validation

3.3.1 β-actin primer design and Bact114 restriction endonuclease digestion

The β-actin gene is constitutively expressed consistently among many different cell types. It is well established that DNA methylation is low or absent on constitutively active genes (Li & Bird, 2007). This makes the β-actin gene suitable as a negative reference for DNA methylation. Figure 3-4 shows the region of the β-actin gene used to design primers. Appendix II shows the features at the sequence level.

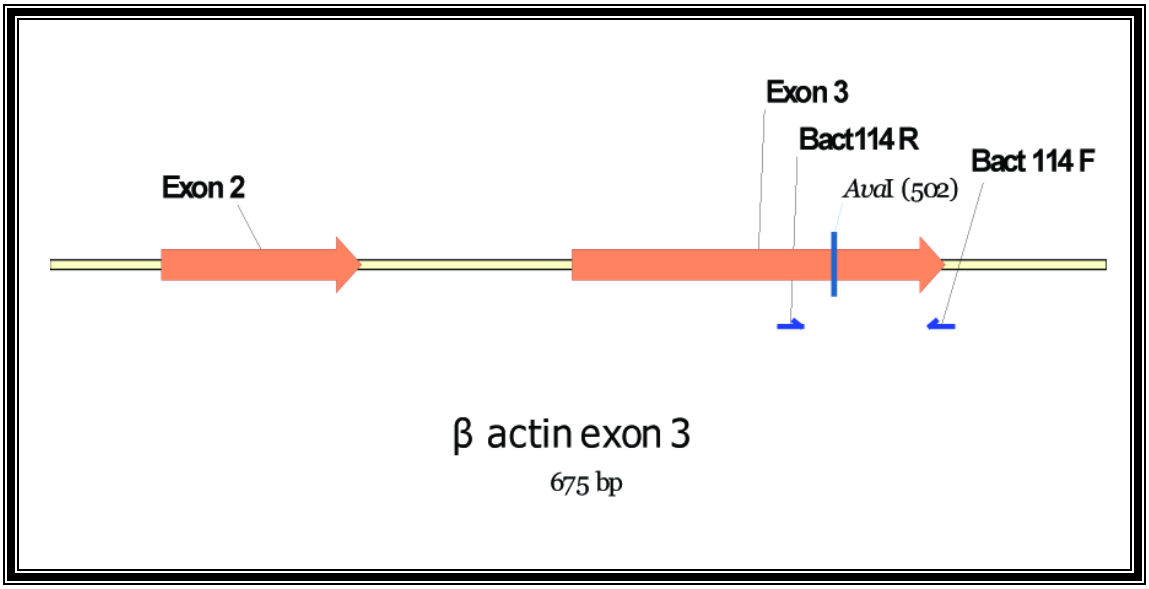

Figure 3-4 Schematic representation of restriction endonuclease cutting site and primer binding sites within a 675 bp β-actin gene fragment showing exons 2 and 3. Accession # NC_000007.13.

Forward (Bact114 F) and reverse (Bact114 R) primers (thin blue arrows) were designed to target a region within the body of the β-actin gene. Exons 2 and 3 are shown as orange block arrows. Restriction endonuclease digestion (vertical blue line) with the *Ava*I enzyme was used to validate the Bact114 amplicon.

*Ava*I digestion was expected to produce two bands of 37 and 77 bp in size. The result of the digestion is shown in Figure 3-5. Lane 3 contains products of a partial digestion reaction. A partial digestion could be due to insufficient enzyme activity or sub-optimal reaction conditions. Due to the partial digestion, the size of the product and the contrast of the EtBr the 37 bp fragment is difficult to see. However the 114 bp amplicon and 77 bp Bact114 restriction fragment were observed.

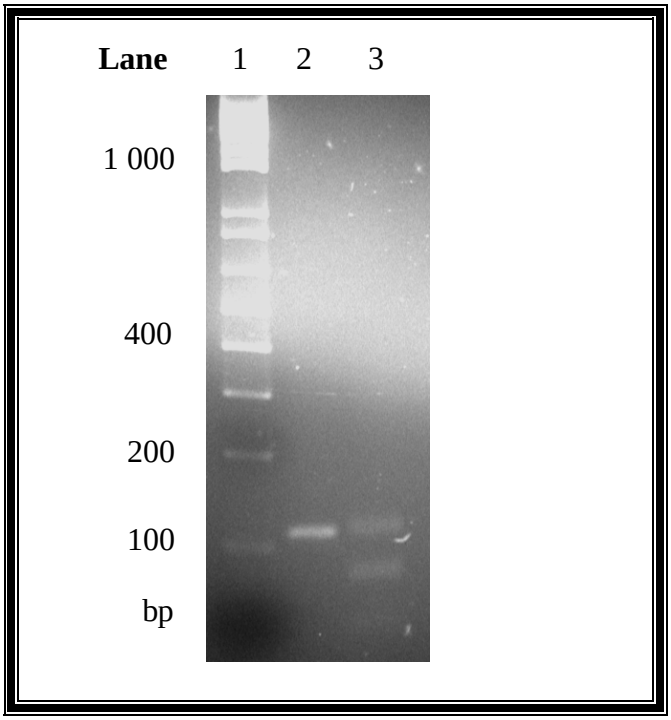

Figure 3-5 Bact114 amplicon restriction endonuclease digest.

Samples were separated by electrophoresis on a 4% agarose gel in 1x TAE buffer for approximately 1 hr at 100 V. DNA was visualised by staining with EtBr as described in section 2.2.2.4, followed by illumination under UV light. The sizes of molecular size markers are shown to the left in base pairs.

Lanes 1) 0.4µg (4 µL) 1kb plus ladder
2) 40% (20 µL) of negative control Bact114 product (no enzyme added)
3) 40% (20 µL) of digestion reaction

3.3.2 H19 primer design and H19155 restriction endonuclease digestion

H19 genomic DNA is transcribed into non-coding RNA. The H19 gene is methylated on the paternal allele as a result of embryonic imprinting (Davis, Yang, McCarrey, & Bartolomei, 2000). This feature makes the H19 gene a suitable positive DNA methylation control. Figure 3-6 shows the region of the H19 gene used to design primers. Appendix III shows the features at the sequence level.

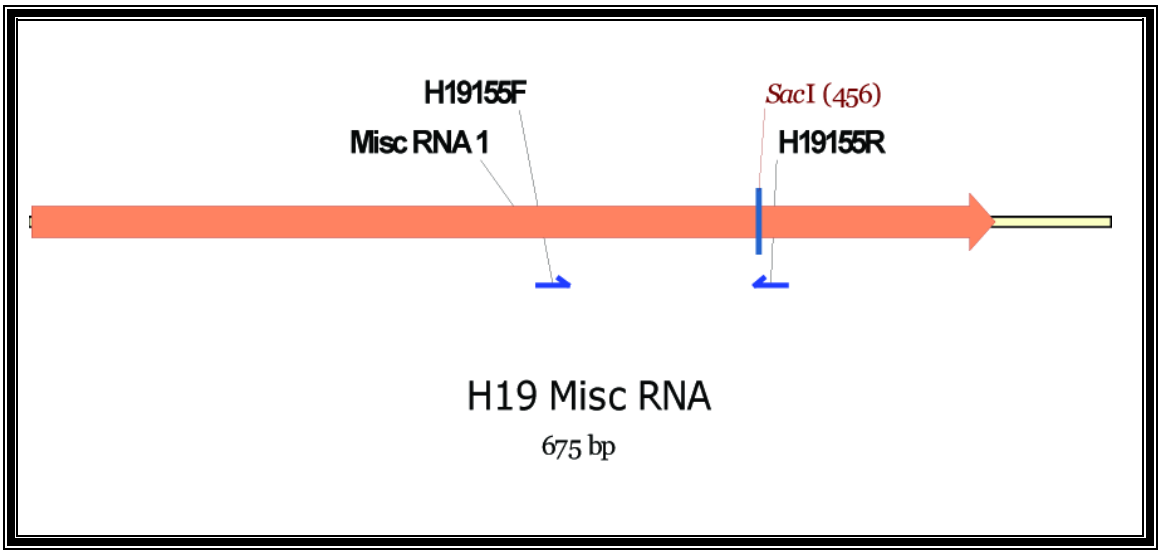

Figure 3-6 Schematic representation of restriction endonuclease cutting site and primer binding sites within a 675 bp fragment within the H19 gene. Accession # NC_00001.9.

Forward (H19155 F) and reverse (H19155 R) primers (thin blue arrows) were designed to target a region within the body of the non-coding mRNA region (orange block arrow). Restriction endonuclease digestion (vertical blue line) with the *Sac*I enzyme was used to validate the H19155 amplicon.

*Sac*I digestion was expected to produce two bands of 138 and 17 bp in size.

The result of the digestion is shown in Figure 3-7. Lane 3 contains products of a partial digestion reaction. Due to the small size of the 17 bp product, it is likely that this product over-ran the length of the gel and therefore cannot be seen. However the 155 bp amplicon and 138 bp H19155 restriction fragment were observed in lane 3.

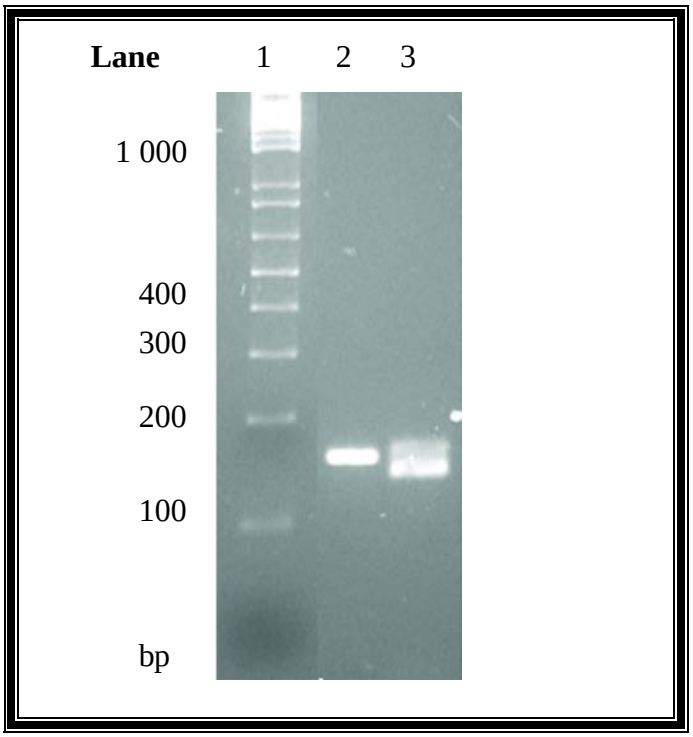

Figure 3-7 H19155 amplicon restriction endonuclease digest.

Samples were separated by electrophoresis on a 4% agarose gel in 1x TAE buffer for approximately 1 hr at 100 V. DNA was visualised by staining with EtBr as described in section 2.2.2.4, followed by illumination under UV light. The sizes of molecular size markers are shown to the left in base pairs.

Lanes 1) 0.4µg (4 µL) 1kb plus ladder
2) 40% (20 µL) of H19155 product (no enzyme added)
3) 40% (20 µL) of digestion reaction

3.4 Real time quantitative PCR

RT-qPCR is a method for accurately measuring the concentration of an unknown DNA sample (or target DNA sequence) through amplification. Firstly, a standard curve is generated by diluting a series of DNA of a known concentration. PCR parameters such as reaction linearity and efficiency can be measured and applied to the amplification curves of an unknown DNA sample. These parameters can be used to determine the concentration of original template. On the lightcycler 480 system, an entire experiment can be carried out in a 96-well plate and analysed within 1.5 hours.

The fluorescent dye SYBR Green I fluoresces when bound to dsDNA (Zipper, Brunner, Bernhagen, & Vitzthum, 2004). Therefore as DNA is amplified in a RT-qPCR reaction an increase in fluorescence over cycle number is observed. The point at which the fluorescence increases above a calculated threshold is called the crossing point (Cp). The Cp for a given sample is directly proportional to the concentration of PCR template. Figure 3-8A shows a single amplicon (MGMT101) amplified using serial dilutions of known template.

After the final annealing cycle products are melted by increasing reaction temperature (65 – 97 °C) while fluorescence is monitored. Heterologous sequence will melt over a wide temperature range. Homologous sequence will melt within a tight temperature range resulting in a single melt curve. To visualise melt curves easily they are transformed by derivation resulting in melt peaks. Melt curves (Figure 3-8B) and derivative melt peaks (Figure 3-8C) for the MGMT101F + MGMT101R reaction show that a single product was formed.

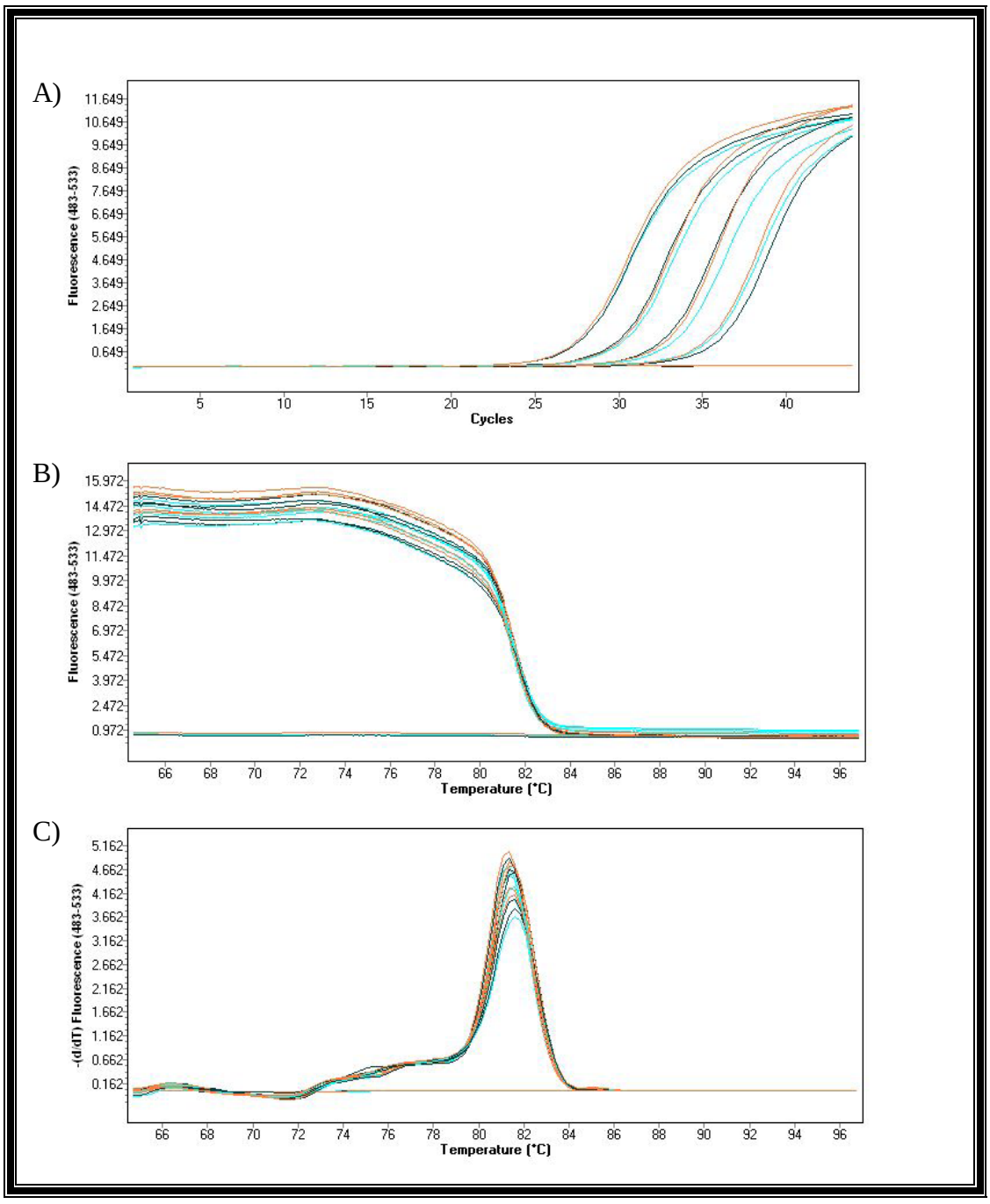

Figure 3-8 A) Amplification curves, B) melt curves and C) melt peaks of the MGMT101 amplicon.

A) Amplification curves for the MGMT101F + MGMT101R RT-qPCR reaction.

B) Melt curves for the MGMT101F + MGMT101R RT-qPCR reaction.

C) Melt peaks for the MGMT101F + MGMT101R RT-qPCR reaction.

3.4.1 Amplification of target and reference sequences by RT quantitative PCR

MGMT101, Bact114 and H19155 products were amplified with their respective primer sets according to Table 3-3. The LC480 provides sensitive detection of 2° product amplification by melt curve analysis. Melt peaks (Figure 3-9A) were analysed and their respective aliquots were visualised by gel electrophoresis (Figure 3-9B) to further check that the correct product is being amplified.

Table 3-3 LC480 protocol for amplifying MGMT101, Bact114 and H19155 products

Initial denaturation	95°C for 5 minutes	
Denaturation	95°C for 10 seconds	45x cycles
Annealing	60°C for 15 seconds	
Extension	72°C for 07 seconds	
Melt analysis	65 – 97 °C	

The PCR mixture contained 0.5 µL (20 µM) of each primer (Primer F and Primer R, 2 µL of SYBR green 1 master (Roche), 10 µL (5x) GC rich solution (Roche), 1.5 µL of template DNA (100 ng/ µL) and 3.5 µL of sterile H_2O to make the total volume 10 µL.

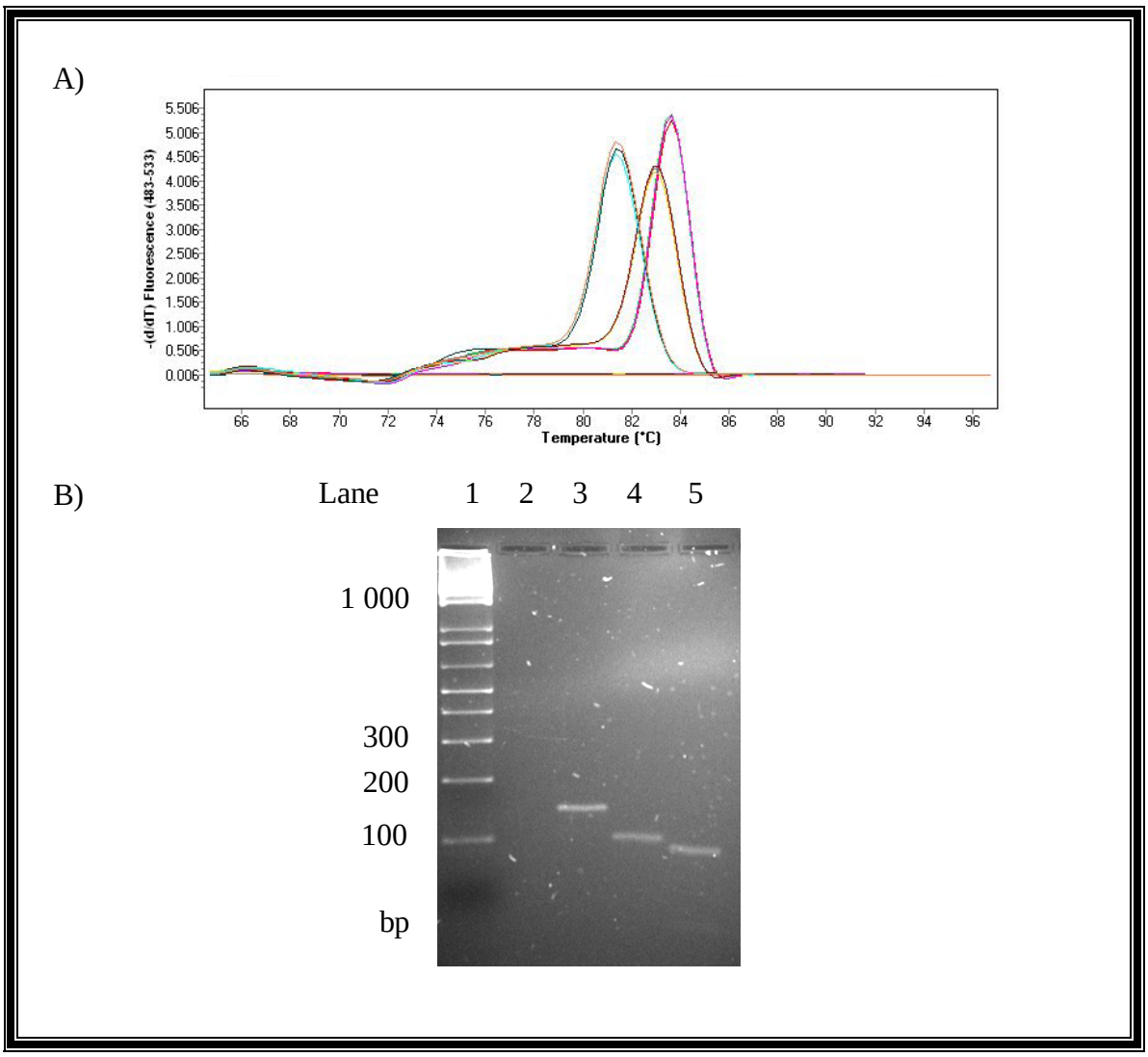

Figure 3-9 Results of RT-qPCR for H19155, Bact114 and MGMT101 products.

A) Melt peaks for three primer sets MGMT101 (81°C), Bact114 (83°C) and H19155 (84°C).

B) Samples were separated by electrophoresis on a 4% agarose gel in 1x TAE buffer for approximately 1 hr at 100 V. DNA was visualised by staining with EtBr as described in section 2.2.2.4, followed by illumination under UV light. The sizes of molecular size markers are shown to the left in base pairs.

Lanes 1) 0.4 µg (4 µL) 1kb plus ladder
2) 50% (5 µL) No template control reaction
3) 50% (5 µL) H19155 reaction
4) 50% (5 µL) Bact114 reaction
5) 50% (5 µL) MGMT101 reaction

3.5 PCR amplification efficiency determination

PCR amplification efficiencies of all three primer pairs (H19155, Bact114 and MGMT101) were determined by making five serial dilutions of sonicated genomic DNA in 1:5 steps. Figure 3-10A shows a 5-point standard curve for the Bact114 reaction and the corresponding melt peaks (Figure 3-10B) showing a single product. The NTC is shown in brown.

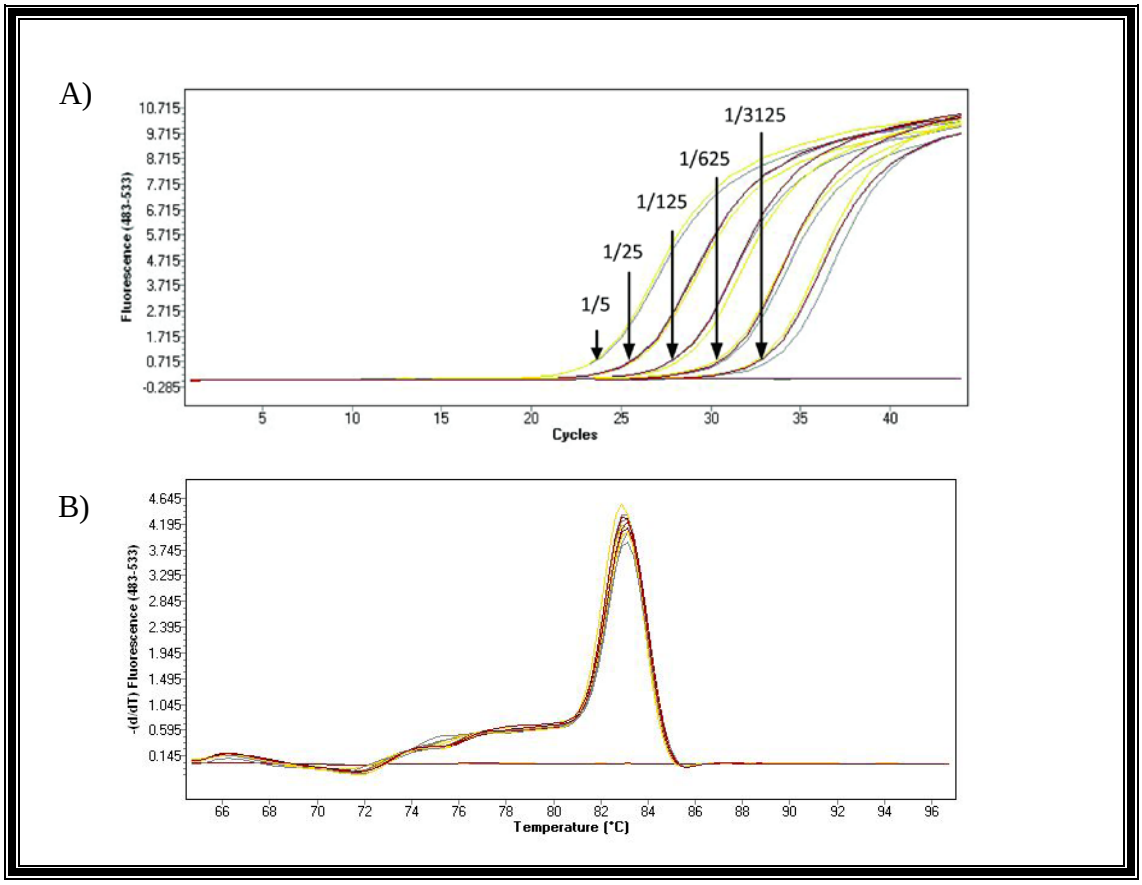

Figure 3-10 Standard curve for the Bact114 amplicon for determination of PCR linearity. A) Amplification curves showing dilutions from stock. B) Corresponding melting peaks.

(A) Amplification curves were generated by the amplification of sonicated genomic DNA using Bact114 primers.
(B) Melt peaks for the Bact114 reaction.

For each primer pair the linearity of amplification was determined by plotting the average of the Cps (y axis) against log concentration (x axis), (Figure 3-11). Amplification efficiency (E) for each reaction was calculated using Equation 1. A theoretical maximum reaction efficiency of 2 indicates a doubling of product for each cycle. For RT-qPCR the reaction efficiencies should be between 1.8 and 2.0.

Equation 1 Efficiency of PCR reaction.

$$E = 10^{-1/slope}$$

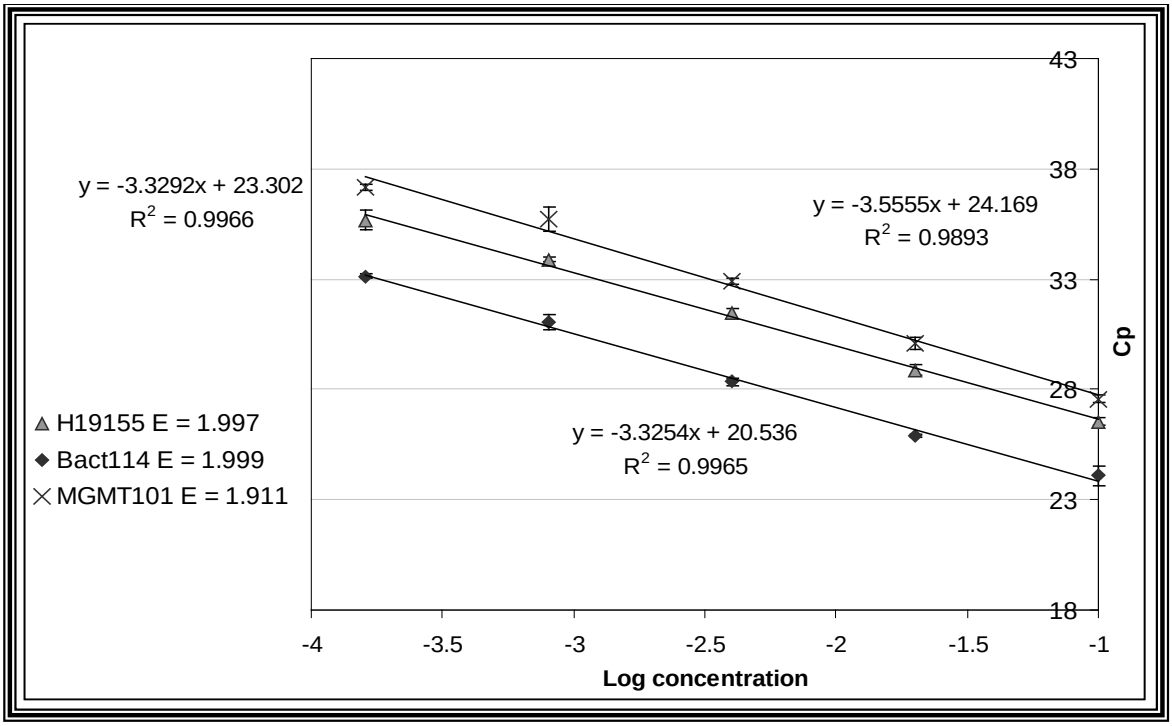

Figure 3-11 Standard curves for H19155, Bact114 and MGMT101amplification reactions.

Standard curves shown are the average of two curves with error bars shown as standard deviation. Equations are shown near each line. The regression coefficient was >.9 in all cases indicating a very strong association between the trendline and data points.

3.6 Chapter summary

Primers were designed to amplify three regions of genomic DNA. MGMT101, Bact114 and H19155 primers were optimised for block PCR and validation by restriction endonuclease digestion. Reaction conditions for each primer pair were optimised to generate single products when run simultaneously in a RT-qPCR assay. This is significant because it indicates that the assay is specific for the desired amplicons. PCR parameters including reaction efficiency and linearity were established by amplifying a dilution series of sonicated DNA for each primer pair. Reaction efficiencies were consistent and fell within the desired range. Taken together, these results indicate that the assay is robust and reliable.

4 Methyl DNA immunoprecipitation

4.1 Introduction

Cytosine methylation at the 5' position of CpG dinucleotides represents an important process in mammalian development and cancer. In the human genome CpG dinucleotides are often enriched at discrete regions named CpG islands. CpG islands are commonly found at gene promoters and the MGMT promoter contains over 95 CpG dinucleotides (Nakagawachi et al., 2003). In non-cancerous cells intergenic CpG dinucleotides are commonly methylated, meanwhile CpG islands at gene promoters remain largely unmethylated resulting in an open chromatin structure (Keshet, Liemanhurwitz, & Cedar, 1986) that is transcription competent. In cancer cells, however, a global reversal of methylation has been observed whereby CpG islands throughout the genome undergo methylation. It is thought that this shift results in changes in expression of genes relevant to cancer progression by inducing and/or maintaining a repressive chromatin structure (Baylin & Jones, 2007).

A number of methods are available for assessing DNA methylation. Bisulfite treatment followed by DNA sequencing is regarded as the gold standard for methylation detection. Bisulfite conversion of unmethylated cytosine residues converts cytosine to uracil, leaving methylated cytosine residues unaffected. However, if the bisulfite treatment is not highly efficient an erroneous read-out in the subsequent DNA-sequencing analysis is obtained. Alternative methods such as methylation-sensitive restriction endonuclease digestion require southern blotting, can be limited by surrounding sequence context and can be prone to false-positive results due to incomplete digestion (Yegnasubramanian, Lin, Haffner, DeMarzo, & Nelson, 2006). Mtheylation-sensitive PCR can also be used which combines bisulfite treatment with PCR using primers designed to bind at the converted cytosine sequence. This method can also be limited by the surrounding sequence context and inefficient conversion (Herman, Graff, Myohanen, Nelkin, & Baylin, 1996).

MeDIP is an efficient method to assess DNA methylation at a given locus as it does not require chemical treatment and specificity is determined by primer design. MeDIP has the additional advantage of being amenable to future large scale analysis such as DNA

microarray or genome wide sequencing (Weber, et al., 2005). Drawbacks of the MeDIP method are that it cannot easily be used to differentiate between alleles and it cannot determine which exact CpGs are methylated at a given CpG island. MeDIP can however, be used to quantify CpG methylation at specific loci.

MeDIP was used to estimate the methylation status of the MGMT promoter in seven melanoma cell lines that had previously been characterised for MGMT expression by RT-qPCR. Genomic DNA was extracted and sheared randomly by sonication to between 300-1000 bp in size. This size range is optimal for the separation of methylated and unmethylated DNA while still allowing sufficient lengths of potential templates for PCR. Antibodies against 5-methylcytosine (5mC) were added, followed by precipitation assisted by the inclusion of protein A/G beads. This step separates methylated DNA fragments from those that are unmethylated by precipitation.

Precipitated DNA was purified and subsequently analysed by RT-qPCR. Two reference genes were chosen, and primers were designed such that the methylation state of the MGMT promoter could be estimated by relative quantification. The constitutively active β actin gene was selected as a non-methylated reference and the paternally imprinted H19 gene was selected as a methylated reference.

A PCR-based sonication control test was developed to ensure sufficient sonication of each DNA sample. Primers were designed to amplify an approximately 2000 bp fragment of genomic DNA, a sub-optimal target length for immunoprecipitation. As determined by PCR, samples containing sonicated DNA fragments of less than approximately 2000 bp in length were used for immunoprecipitation to ensure optimal reaction conditions.

4.2 MeDIP optimisation

4.2.1 Isolation and sonication of genomic DNA

Genomic DNA was isolated from New Zealand melanoma cell lines by phenol-chloroform extraction followed by ethanol precipitation as described in section 2.2.2.1 and then sonicated as described in section 2.2.3.2. To investigate the optimal number of cycles for sonication, 10 µL samples were taken at time points during sonication and analysed by gel electrophoresis (Figure 4-1) as described in section 2.2.2.4. Lane six contains sonicated DNA fragments of between 300-1000 bp in size.

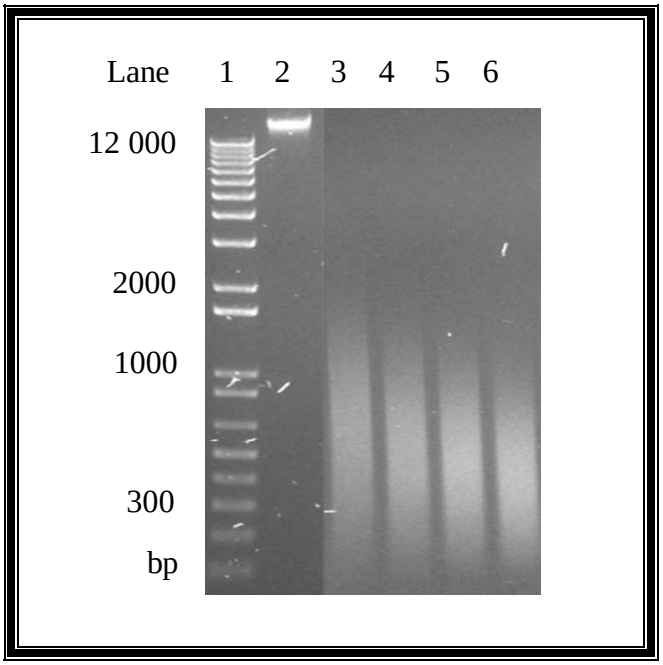

Figure 4-1 Genomic DNA isolated from melanoma cell lines and sonicated DNA respectively.

Samples were separated by electrophoresis on a 2% agarose gel in 1x TAE buffer for approximately 1 hr at 100 V. DNA was visualised by staining with EtBr as described in section 2.2.2.4, followed by illumination under UV light. The sizes of molecular size markers are shown to the left in base pairs.

Lanes 1) 0.5 µg (5 µL) 1kb plus ladder
2) approximately 500 ng Genomic DNA
3) 2.5% (10 µL) genomic DNA sonicated 4 x 10 s @ power setting 1
4) 2.5% (10 µL) genomic DNA sonicated 6 x 10 s @ power setting 1
5) 2.5% (10 µL) genomic DNA sonicated 8 x 10 s @ power setting 1
6) 2.5% (10 µL) genomic DNA sonicated 10 x 10 s @ power setting 1

4.2.2 PCR-based control for sonication efficiency

4.2.2.1 Primer design

A PCR-based sonication efficiency control assay was developed to ensure each DNA sample was sonicated to the correct size of between 300-1000 bp in size (Weber, et al., 2005) and to ensure consistent sonication between genomic DNA samples. Primers were designed to amplify a 1966 bp region upstream of the MGMT promoter. Figure 4-2 shows the region of the MGMT promoter used for primer design. Appendix I shows features at the DNA level.

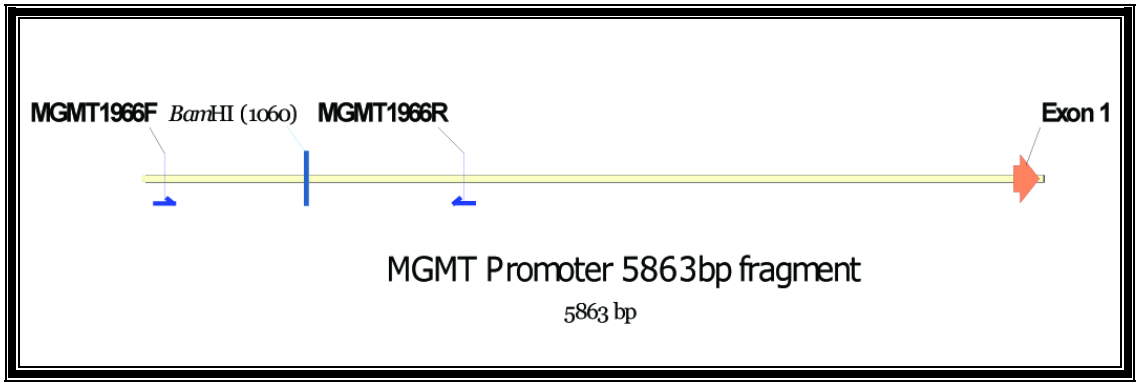

Figure 4-2 Schematic representation of restriction endonuclease cutting site and primer binding sites within a 5863 bp fragment upstream of the MGMT gene. Accession NT_008818.16.

Forward (MGMT1966 F) and reverse (MGMT1966 R) primers (thin blue arrows) were designed to target a region upstream of exon 1 (orange block arrow). Restriction endonuclease digestion (vertical blue line) with the *Bam*HI enzyme was used to validate the MGMT1966 amplicon.

4.2.2.2 PCR amplification and restriction endonuclease digestion

To ensure specificity of the desired primers a restriction analysis was carried out on the amplicon generated by a PCR reaction with 1966F and 1966R primers. *Bam*HI digestion was expected to produce two bands of 922 bp and 1044 bp and in size. The result of the digestion is shown in Figure 4-3. Lane 3 contains the desired MGMT1966 restriction fragments. A number of secondary products were generated in the PCR reaction indicating some degree of non-specific amplification, however the 1966 bp band is the dominant product.

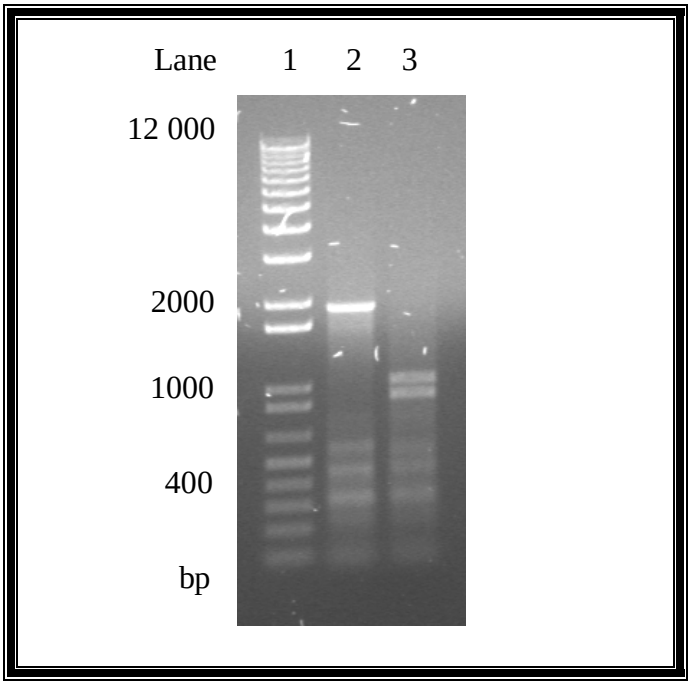

Figure 4-3 MGMT1966 amplicon restriction endonuclease digestion with *Bam*HI.

Samples were separated by electrophoresis on a 1% agarose gel in 1x TAE buffer for approximately 1 hr at 100 V. DNA was visualised by staining with EtBr as described in section 2.2.2.4, followed by illumination under UV light. The sizes of molecular size markers are shown to the left in base pairs.

Lanes 1) 0.5 µg (5 µL) 1kb plus ladder
2) 40% (20 µL) of MGMT1966 product (no enzyme added)
3) 40% (20 µL) of digestion reaction

4.2.2.3 Determination of sensitivity of sonication control

In order to assess the sensitivity of the sonication efficiency control a series of PCR reactions were carried out on sonicated and unsonicated genomic DNA template standards of known concentrations. Sonicated DNA was spiked with serial 2.5 fold dilutions of unsonicated genomic DNA from a 37 ng/µL stock. A total of 5 µL of spiked template was added to 45 µL PCR reactions as previously described in section 2.2.2.3. Figure 4-4 shows the sonication control test can detect as little as 0.4 ng of genomic DNA in a background of sonicated DNA. Again some degree of non-specific amplification is present as indicated by brackets, however the 1966 bp band remains the dominant product.

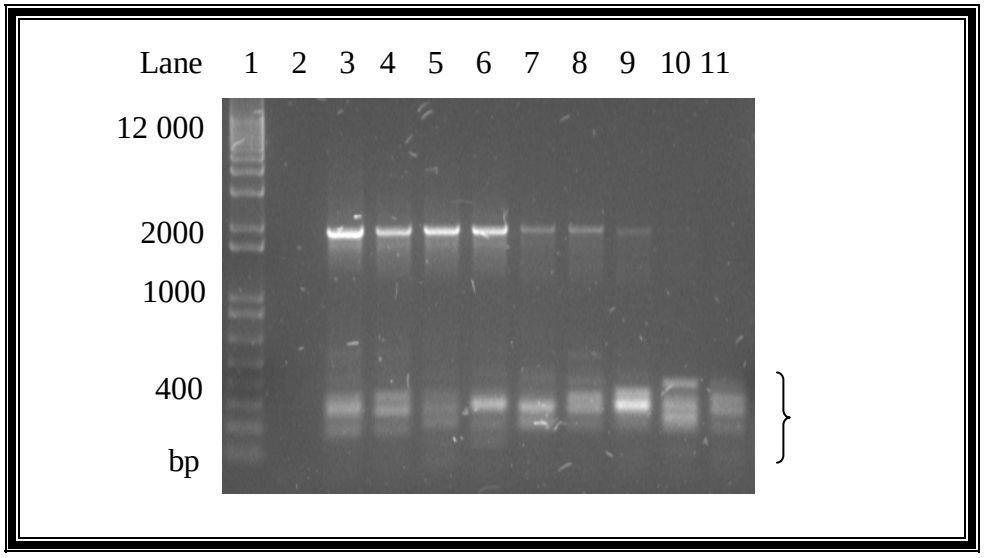

Figure 4-4 PCR reactions on sonicated DNA spiked with serial dilutions of genomic DNA template.

PCR reactions were carried out in a total of 50 µL using MGMT1966 primers and 5 µL of template (amount indicated below). 5% samples of each reaction were separated by electrophoresis and stained with EtBr as previously described in 2.2.2.4, followed by illumination under UV light. The sizes of molecular size markers are shown to the left in base pairs.

Lanes 1) 0.4 µg (4 µL) 1kb plus ladder
2) No template PCR control
3) 10 ng sonicated DNA + 92.5 ng gDNA
4) 10 ng sonicated DNA + 37.0 ng gDNA
5) 10 ng sonicated DNA + 14.8 ng gDNA
6) 10 ng sonicated DNA + 5.9 ng gDNA
7) 10 ng sonicated DNA + 2.4 ng gDNA
8) 10 ng sonicated DNA + 1.0 ng gDNA
9) 10 ng sonicated DNA + 0.4 ng gDNA
10) 10 ng sonicated DNA + 0.2 ng gDNA
11) 10 ng sonicated DNA + 0.1 ng gDNA

4.2.2.4 PCR to control for sonication efficiency

The sonication control PCR was carried out on each sonicated DNA sample prior to immunoprecipitation. Figure 4-5 shows unsonicated genomic DNA (lane 2) and sonicated DNA (Lane 4) and PCR products generated in the sonication control PCR reaction in the presence of genomic template (Lane 3) or sonicated template (Lane 5). The absence of a band in lane 5 indicates that the sonicated template contains approximately < 0.38 ng of unsonicated genomic DNA.

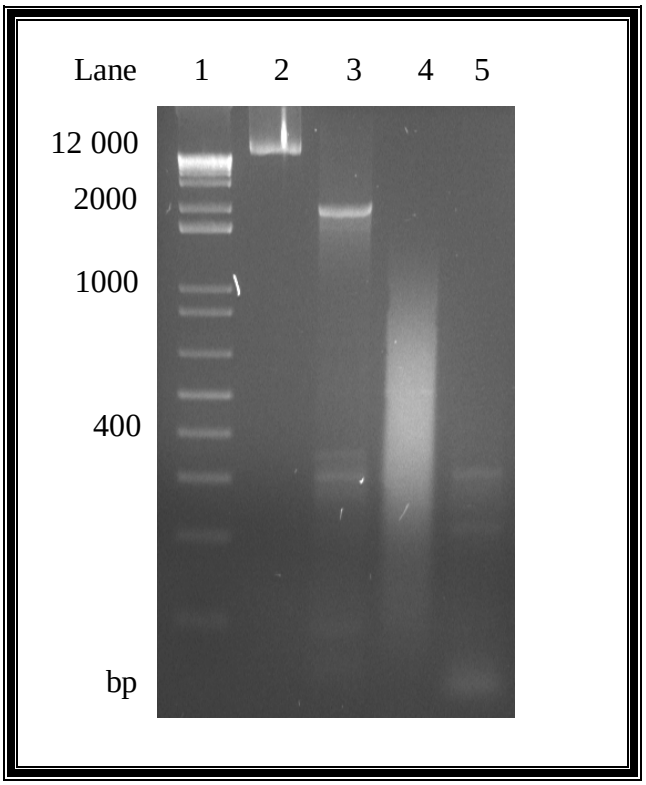

Figure 4-5 Template and PCR reactions using MGMT1966 primers for sonicated DNA prior to MeDIP procedure.

Samples were separated by electrophoresis on a 2% agarose gel in 1x TAE buffer for approximately 1 hr at 100 V. DNA was visualised by staining with EtBr as described in section 2.2.2.4, followed by illumination under UV light. The sizes of molecular size markers are shown to the left in base pairs.

Lanes 1) 0.4 µg (4 µL) 1kb plus ladder
2) approximately 1 µg genomic DNA
3) PCR carried out using approximately 1 µg of genomic DNA template
4) approximately 1 µg sonicated DNA
5) PCR carried out using approximately 1 µg of sonicated DNA template

4.3 MeDIP results

Genomic DNA prepared from seven cell lines was sonicated and immunoprecipitated with anti–5mC antibodies or without antibody (beads-only control). The resulting DNA was purified by phenol-chloroform extraction and ethanol precipitation as described in 2.2.2.1. Input DNA, beads-only control, immunoprecipitated DNA and calibrator DNA template (arbitrarily chosen NZM3 DNA) were amplified using MGMT101, Bact114 and H19155 primers on 96-well plates in triplicate. Appendix IV shows the 96-well plate template for the MeDIP assay. The average crossing points were used in Equation 2 to calculate the enrichment of target MGMT template compared to unmethylated β actin template and to methylated H19 template, respectively.

Equation 2 Enrichment of MGMT promoter template compared to reference gene template

$$\text{Enrichment} = \frac{\text{MGMT efficiency}^{(\text{MGMT calibrator Cp - MGMT sample Cp})}}{\text{Reference efficiency}^{(\text{reference calibrator Cp - reference sample Cp})}}$$

4.3.1 Real time quantitative PCR and enrichment for NZM11 (1 of 3 replicates)

Technical replicates were amplified in triplicate in 96-well plates. Enrichments were calculated for each 96-well plate independently and the average enrichment values of three or more plates were used to generate the final data set. Amplification curves and enrichments from a single 96-well plate amplifying the arbitrarily chosen NZM11 template are shown in Figure 4-6 and Figure 4-7. Figure 4-6A-C shows MGMT enrichment relative to β actin (low methylation), while Figure 4-7A-C shows MGMT enrichment relative to H19 (high methylation).

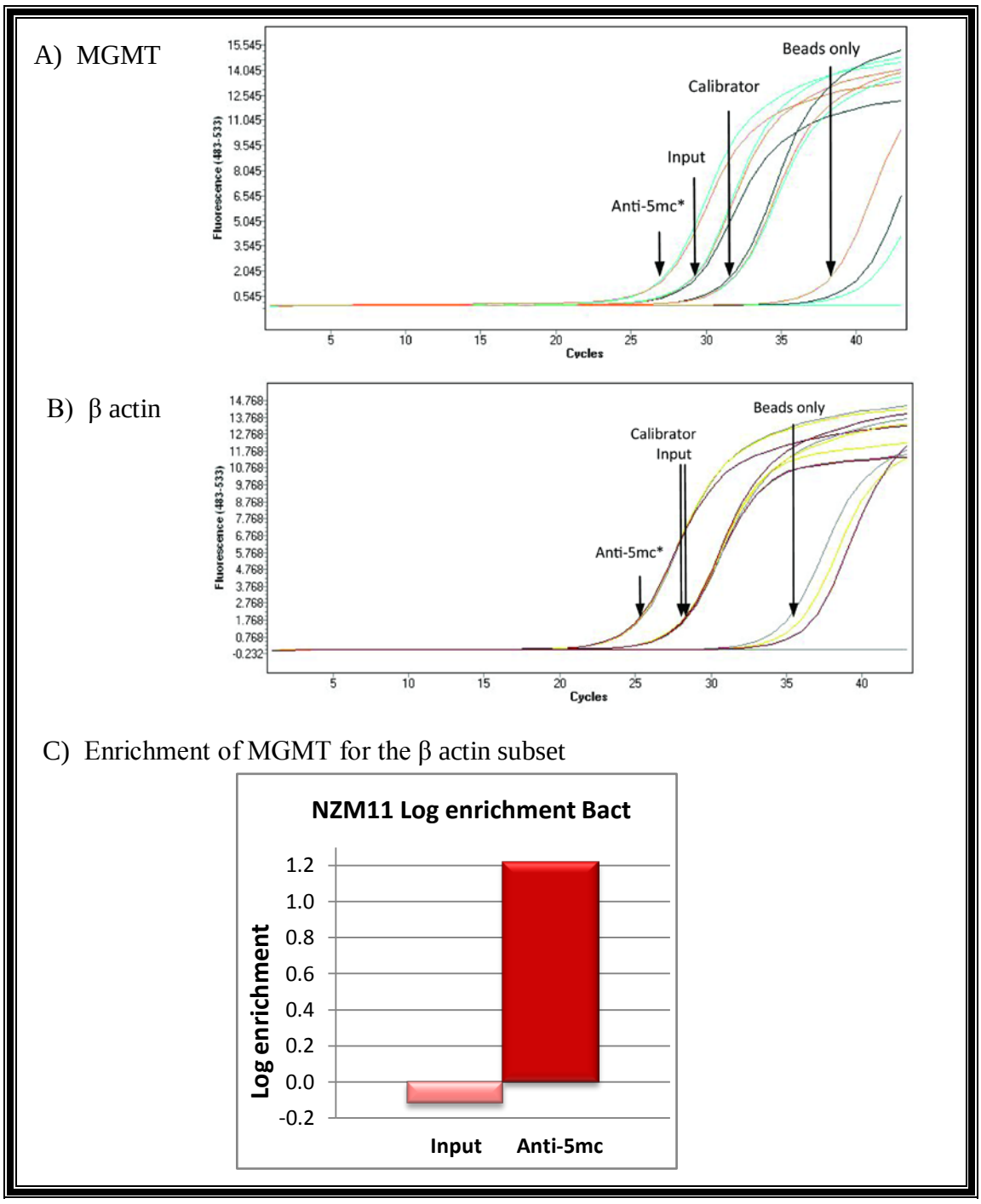

Figure 4-6 Amplification curves and enrichment for NZM11 β actin subset (replicate 1 of 3).

Figure 4-6A) Amplification curves for MGMT101 in triplicate. Crossing points are approximate.
Figure 4-6B) Amplification curves for Bact114 in triplicate.
Figure 4-6C) Light red bars show enrichment of input MGMT template compared to β actin reference template. A 0 value indicates no difference between input concentrations between templates. Dark red bars indicate enrichment of 5mC purified MGMT template relative to β actin template. A 0 value indicates no change in MGMT101 template concentration relative to β actin.

A) MGMT

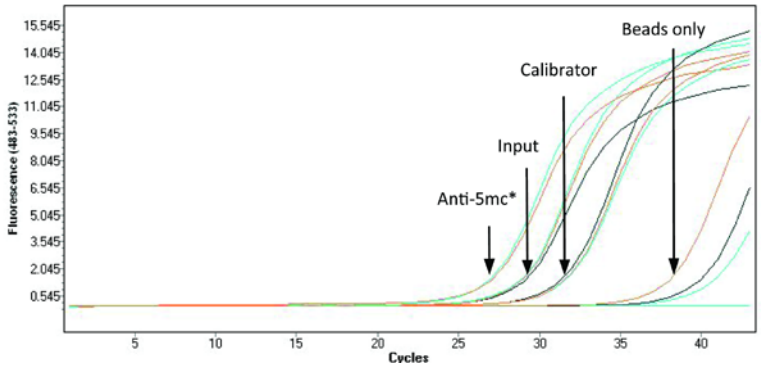

B) H19

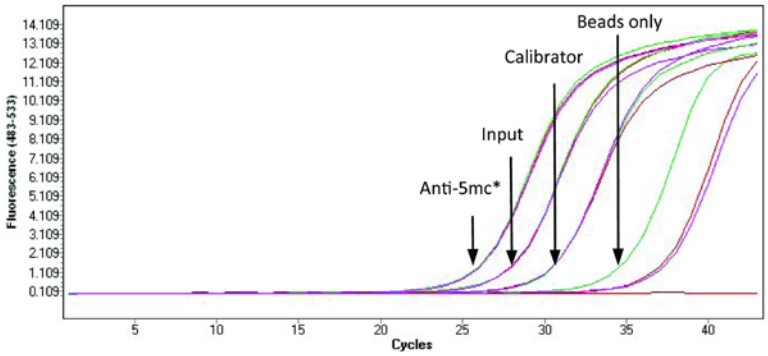

C) Enrichment of MGMT for the H19 subset

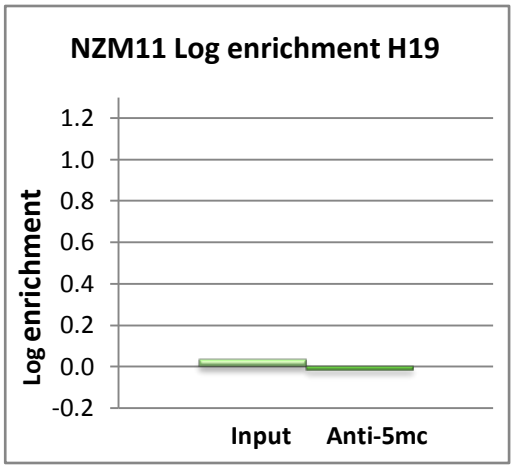

Figure 4-7 Amplification curves and enrichment for NZM11 H19 subset (replicate 1 of 3).

Figure 4-7A) Amplification curves for MGMT101 in triplicate.

Figure 4-7B) Amplification curves for H19155 in triplicate.

Figure 4-7C) Light green bars show enrichment of input MGMT template compared to H19 reference template. Dark green bars indicate enrichment of 5mC purified MGMT template compared to H19 template. Similarly to

Figure 4-6, the beads-only value has been excluded.

A calibrator template (NZM3) was amplified along with the NZM11 template series to normalise results between cell lines. After adjusting for differences in reaction efficiency, input, beads-only and anti-5mc purified MeDIP templates were amplified and their respective crossing points used in Equation 2 to calculate enrichment between MGMT101 and either Bact114 or H19155 reference template series.

The beads-only control resulted in a large depletion (Cp > 35) with high variability, as would be expected for a negative control. Therefore it was excluded from the graph.

Input Cps were used to calculate input enrichment of MGMT101 relative to Bact114 and H19. In theory, each genome should contain two copies of MGMT and two copies of each of β actin and H19, therefore the difference in enrichment should be zero for all input samples. A significant deviation from zero indicates that the assay is detecting an unequal enrichment before immunoprecipitation is carried out which is not expected. This could mask the true anti-5mc enrichment result for any cell line and primer subset where input enrichments are significantly different from zero. This effect should be taken into account when comparing MeDIP data between subsets where the input enrichment value is significantly different from zero.

For the immunoprecipitated samples, enrichment of MGMT101 relative to Bact114 indicates methylation on the MGMT promoter. An enrichment of zero indicates no significant difference in methylation between the MGMT promoter and the unmethylated β actin gene and hence indicates no significant methylation on the MGMT promoter. A depletion of MGMT101 relative to H19 indicates the MGMT promoter has less methylation than the H19 gene. An enrichment of zero indicates no significant difference in methylation between the MGMT promoter and the methylated H19 gene and hence indicates methylation on the MGMT promoter.

4.3.2 MeDIP results for seven cell lines

The average enrichment values of three RT-qPCR assays for each cell line were plotted for seven melanoma cell lines (Figure 4-8A). MeDIP results were compared to expression levels of MGMT mRNA relative to β actin (Figure 4-8B) to address links between MGMT promoter methylation state and MGMT expression (M. Aalderink, personal communication, Nov, 2007). In addition, IC_{50} values for TMZ (Figure 4-8C) demonstrate the clinical relevance of MGMT expression (B. Baguley, personal communication, Nov, 2007).

MeDIP data from MGMT expressing cell lines (NZM2, NZM4, NZM5) indicates a low level of methylation at the MGMT promoter. Data from MGMT silenced cell lines (NZM3, NZM11, NZM14, NZM58) indicates a significant level of methylation at the MGMT promoter.

MGMT expression values were normalized to the NZM2 cell line, the first cell line measured. The expression value of this cell line was set at one. IC_{50} values represent the concentration of TMZ (μM) required to reduce thymadine incorporation (into DNA) by 50%.

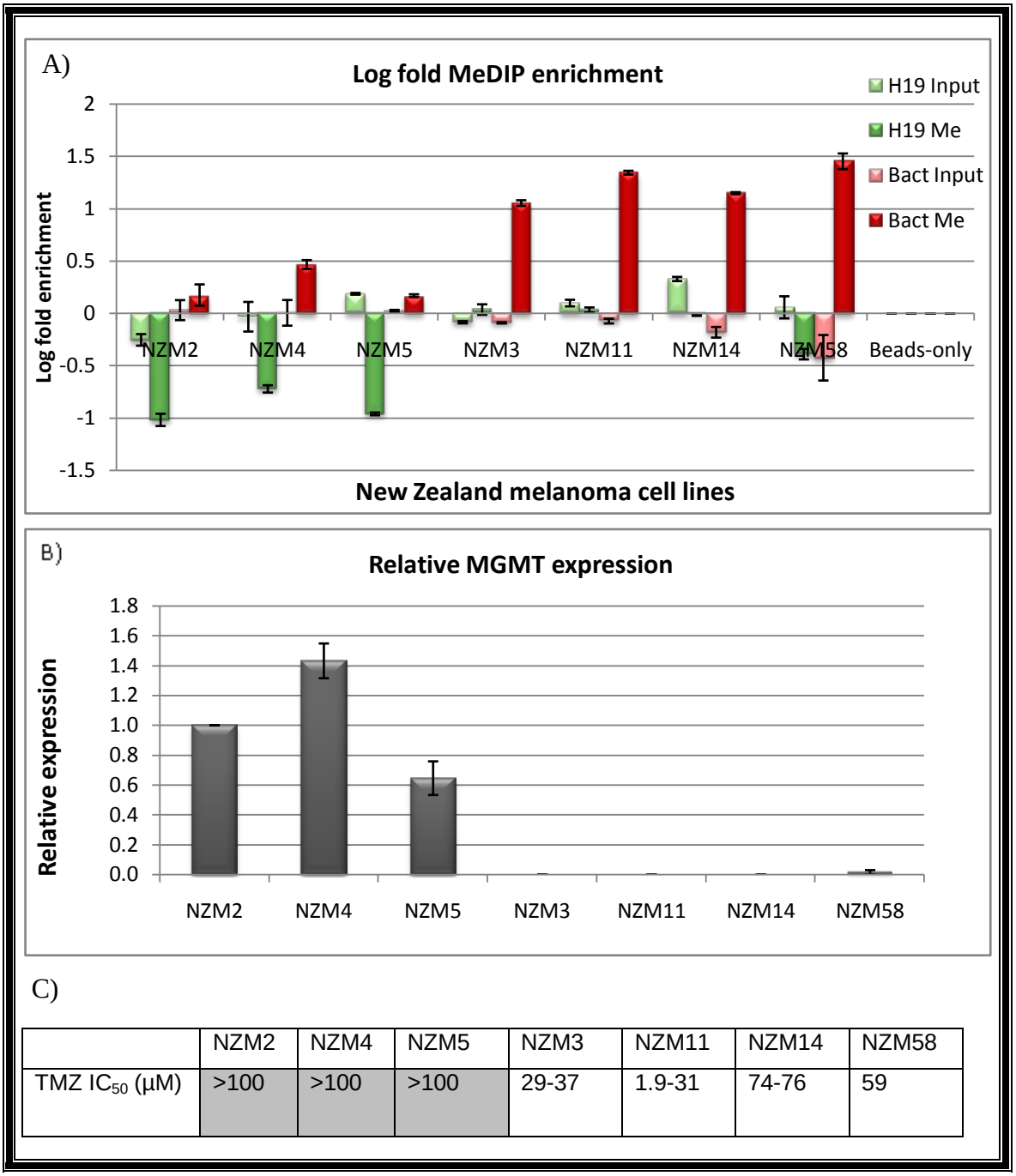

C)

	NZM2	NZM4	NZM5	NZM3	NZM11	NZM14	NZM58
TMZ IC_{50} (µM)	>100	>100	>100	29-37	1.9-31	74-76	59

Figure 4-8 MeDIP enrichment values and previously established MGMT expression values.

A) MeDIP results showing enrichment of MGMT 101 template relative to H19155 and Bact114 respectively. Error bars are depicted as standard error. $n = 3$.

B) MGMT mRNA expression levels relative to B actin mRNA expression (M, Aalderink, personal communication, Nov, 2007). Error bars depicted are standard deviation. $n = 3$.

C) IC_{50} values for TMZ (B. Baguley, personal communication, Nov, 2007). $n = 3$.

Figure 4-8A)
Light red bars show enrichment of input MGMT template compared to β actin reference template.
Dark red bars indicate enrichment of 5mC purified MGMT template relative to β actin template.
Light green bars show enrichment of input MGMT template compared to H19 reference template.
Dark green bars indicate enrichment of 5mC purified MGMT template relative to H19 template.

Figure 4-8B) Grey bars show MGMT mRNA expression relative to β actin mRNA.

Figure 4-8C) IC50 values for TMZ were measured. A value of >100 indicates resistance to TMZ and a value of <100 indicates sensitivity (B. Baguley, personal communication, Oct, 2009). Shaded cells represent TMZ resistance.

A student's *t*-test (independent 1-sample) was carried out using a 95% confidence interval to test whether the mean input sample enrichment was equal to zero for each cell line and subset. Using this technique five input subsets; NZM2 H19, NZM5 H19, NZM3 H19; β actin and NZM14 H19 were different from zero ($p < 0.05$), (-0.252 ± 0.06, 0.118 ± 0.01, -0.084 ± 0.01, -.090 ± 0.01 and 0.329 ± 0.02 respectively).
However, these differences were small (< 0.15) in most cases. Differences observed for input sample enrichment for other subsets were not significantly different from zero. Deviation from zero may indicate experimental error, may be due to cellular changes such as allelic loss/gain, allele specific differences or mutation (which may result in altered amplification efficiency) or may be a result of an unequal rate of primer degradation over time.

The beads-only control was negative ($Cp \geq 35$) for most cell lines indicating that the observed results were not due to non-specific interactions between DNA and protein or protein A/G beads. In the NZM5 and NZM11 cell line the beads only control amplified slightly earlier than expected for the β actin subset ($Cp \geq 34$) however, when considering multiple replicates the Cp remained≥ 35.

Traditionally CpG methylation at gene promoters is thought to be associated with gene silencing, whereas an absence of CpG methylation is thought to be associated with an active transcriptional state. Therefore MGMT promoter CpG methylation was expected in cell lines with silenced MGMT mRNA expression. Conversely, the absence of

methylation at the MGMT promoter was expected in cell lines with active MGMT mRNA expression.

It was observed that in 3/3 (100%) cell lines expressing MGMT there was a net depletion in DNA methylation at the MGMT promoter. In addition, in 4/4 (100%) of MGMT silenced cell lines there was a net enrichment in DNA methylation at the MGMT promoter. Overall, these findings are consistent with the expected results. However there are some inconsistencies arising in the NZM4 cell line. The NZM4 cell line shows relatively high levels of MGMT expression. Suprisingly, the NZM4 MGMT promoter displays an intermediate state of DNA methylation and expresses MGMT mRNA. This result suggests that intermediate levels of methylation may be insufficient to bring about MGMT silencing. Notably, the NZM4 cell line is resistant to TMZ.

A number of researchers have described similar findings in cells derived from colon cancer. Esteller and colleagues used MSP and immuno-histochemistry techniques to investigate the correlation between MGMT expression and promoter CpG methylation (Esteller, et al., 1999). Of 14 cancer cell lines, 6/7 (85%) MGMT non-expressing lines showed significant MGMT CpG island methylation. 7/7 (100%) MGMT expressing cell lines showed an absence of CpG methylation at the MGMT promoter. Notably, for primary tumours of melanoma specifically, Esteller and colleagues reported an overall rate of promoter methylation of 2/18 (11%). In contrast, preliminary MSP findings by Baguley and colleagues (B. Baguely, unpublished data, 2007) report the much higher rate of promoter methylation of 15/32 (47%) in primary melanoma cell lines. The current study examines a selected subset of these cell lines therefore the reported rate 4/7 (57%) of promoter methylation does not reflect the true rate.

Chapter summary

DNA sonication was optimised to generate DNA fragments of 300-1000 bp in size. A PCR-based sonication control was developed to ensure consistent sonication between DNA samples. MeDIP of sonicated DNA from seven cell lines was carried out. Immunoprecipitated DNA was analysed by relative quantification of MGMT target compared to H19 and β actin references respectively. Importantly, the beads-only control was negative and the majority of input controls showed no significant difference from zero at the 95% confidence level.

Comparison with MGMT expression levels indicates a strong correlation between DNA methylation at the MGMT promoter and MGMT silencing. These data are in concordance with previously reported data on MGMT promoter methylation among MGMT expressing and silenced primary tumour samples. However, evidence from the NZM4 cell line indicates that DNA methylation of the MGMT promoter alone may not account for the observed on/off expression state of MGMT.

5 Chromatin immunoprecipitation

5.1 Introduction

The primary repeating unit of DNA orgnisation in each eukaryotic cell is the nucleosome. Each nucleosome consists of 150 bp of DNA wound around a core of histone proteins. Each nucleosome contains a Histone 3 and 4 (H3-H4) tetramer and two histone 2A and 2B (H2A-H2B) dimers (Luger, et al., 1997). Collectively, nucleosomes make up chromatin, which undergoes condensation and expansion in certain regions of the genome depending on the gene expression requirements of the cell (Allis, et al., 2007). Exposed histone N terminal tails are targets for a variety of post-translational modifications which influence the higher order structure of chromatin. ChIP experiments allow for the examination of specific histone modifications over particular areas of the genome.

H3K9 is an amino acid which can be modified to form acetyl, methyl, dimethyl or trimethyl lysine moieties. It has been proposed that acetylation of H3K9 correlates with an open chromatin structure amenable to transcription, however little is known about the functions of different methylation states of H3K9. Various groups have proposed that the modifications of the H3K9 position may act as part of a switch mechanism to control the conversion from active euchromatin to silenced heterochromatin (Jenuwein & Allis, 2001). In the present study, three states of the H3K9 residue were examined: H3K9ac, H3k9me2 and H3K9me3. These states are thought to correlate with active, facultatively silenced and constitutively silenced states of gene expression respectively (Kouzarides & Berger, 2007). Modifications cannot occur simultaneously on the same residue, however as there are two H3 histones within each nucleosome, it is possible that there may be different H3K9 modifications on each H3 histone within each nucleosome.

In the current study, the histone modification state of the MGMT promoter was analysed by ChIP experiments using cross-linked chromatin extracted from melanoma cell lines as described in section 2.2.4.2. The ChIP assay began with the fixation of chromatin *in vivo* by formaldehyde cross-linking. This step ensures a strong interaction between DNA and histones. Crosslinked chromatin was then sheared randomly by

sonication. Sonicated chromatin was incubated with selected antibodies to immunoprecipitate modified nucleosomes complexed with short fragments of DNA. Antibody-nucleosome-DNA complexes were immunoprecipitation with protein A/G beads.

RT-qPCR was carried out on undiluted immunoprecipitated DNA and serially diluted input DNA as described in section 3.4.1. The constitutively active β actin gene and the MGMT promoter were examined for the presence of H3K9ac, H3K9me2 and H3K9me3 modifications. The β actin gene was expected to contain the H3K9ac modification and little or none of the H3K9me2 and H3K9me3 modifications.

5.2 Optimisation of the ChIP assay

Initial testing of the ChIP assay involved testing the relationship between chromatin concentration, formaldehyde cross-linking time and sonication time. Melanoma cell lines vary in cell density when grown in culture and in their DNA/chromatin yield per cell. These properties can affect the optimisation of ChIP assays.

Initially, a relative quantification assay similar to that used in the MeDIP experiment was used to measure ChIP DNA. However, in order to be able to compare results against other researchers in the field, the relative quantification approach was abandoned in favour of absolute quantification. This assay method allows monitoring of ChIP DNA recovery as a percentage of input. A control consisting of beads-only was included to control for non-specific interactions between DNA and protein A/G beads.

5.2.1 Chromatin isolation, cross-linking and sonication

Cross-linking and sonication times were simultaneously optimised. It was found that a cross-linking time of 5 minutes combined with 30 x sonications consistently produced chromatin fragments within the appropriate size range of 200 – 700 bp.

New Zealand melanoma cells were cross-linked in solution followed by sonication as described in section 2.2.4.2. Samples of 50 µL (5%) were taken at time points to assess cross-linking and sonication efficiency. The resulting DNA fragments were electrophoresed on an agarose gel after cross-link reversal (Figure 5-1). Lane 2 (30 sonications) shows an average size of approximately 400 bp.

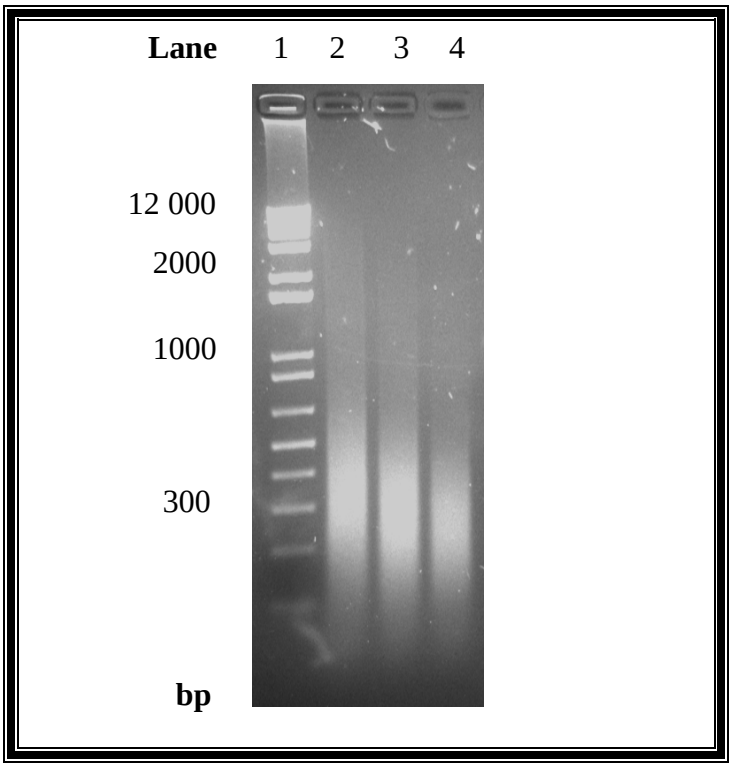

Figure 5-1 DNA purified from sonicated chromatin at 30 - 50 sonications.

Samples were separated by electrophoresis on a 2% agarose gel in 1x TAE buffer for approximately 1 hr at 100 V. DNA was visualised by staining with EtBr as described in section 2.2.2.4, followed by illumination under UV light. The sizes of molecular size markers are shown to the left in base pairs.

Lanes 1) 0.5 µg (5 µL) 1kb plus ladder
2) 25% (7 µL) purified DNA isolated from 5% (50 µL) samples of chromatin sonicated 30 x
3) 25% (7 µL) purified DNA isolated from 5% (50 µL) samples of chromatin sonicated 40 x
4) 25% (7 µL) purified DNA isolated from 5% (50 µL) samples of chromatin sonicated 50 x

5.3 ChIP results

Fixed chromatin from melanoma cell lines was formaldehyde crosslinked, sonicated and immunoprecipitated with selected antibodies or with no anibody (beads-only control). After reversal of cross-links, immunoprecipitated DNA was purified by phenol-chloroform extraction and ethanol precipitation as described in 2.2.2.1. Serially diluted input DNA, anti-H3K9Ac, anti-H3K9me2, anti-H3K9me3 and beads-only control immunoprecipitated DNA were amplified using primers against the MGMT promoter and the β actin gene on 96-well plates in triplicate. Appendix IIV shows the 96-well plate setup for the ChIP assay. Sample crossing points were analysed by the LC480 software (Version 1.5.0 SP1). Percentage enrichments were calculated by interpolation using the LC480 software and plotted for each cell line and primer subset.

5.3.1 ChIP real time quantitative PCR and enrichment for NZM5 (1 of 3 replicates)

Amplification reactions were carried out in triplicate on each 96-well plate.
Enrichments were calculated for each 96-well plate independently and the average enrichment values of three or more plates were used to generate the final data set.
Amplification curves and enrichments from a single 96-well plate amplifying NZM5 template is shown in Figure 5-2 and Figure 5-3. Figure 5-2A-C shows data for the MGMT amplicon while Figure 5-3A-C shows data for the β actin amplicon.

Standard curves of serially diluted input sample were run on plates alongside ChIP samples for each cell line. After adjusting for differences in reaction efficiency, enrichment of target MGMT and reference β actin were calculated based on the Cp of samples as a percentage of input recovery.

A) MGMT standard curve for input

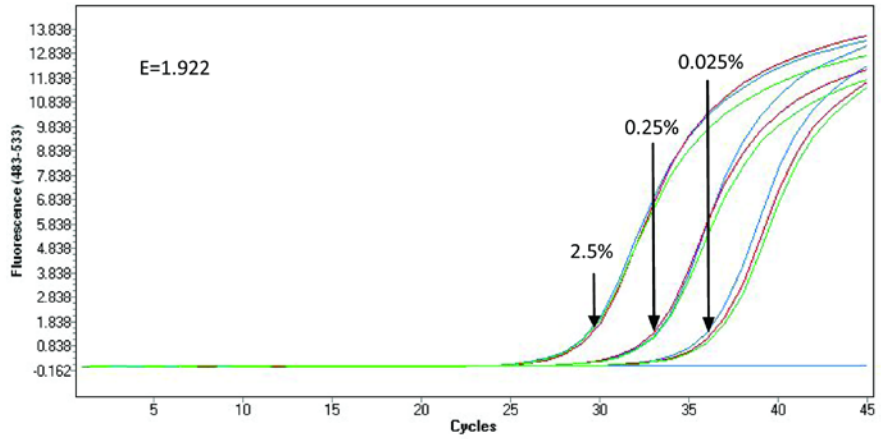

B) MGMT ChIP samples

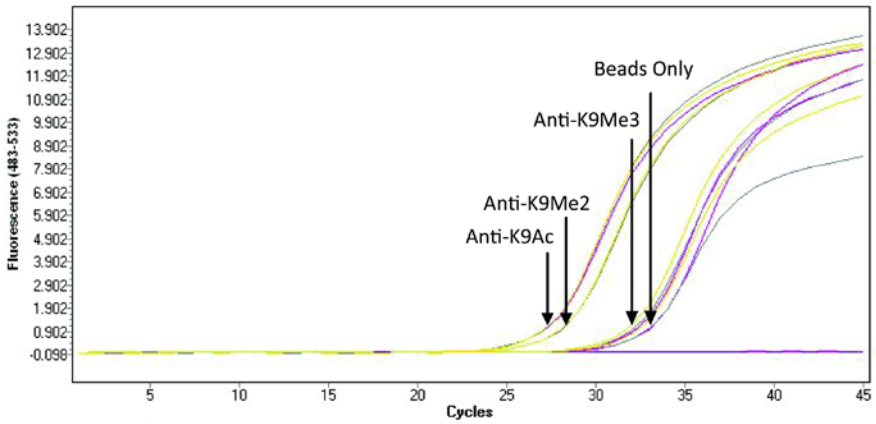

C) MGMT enrichment

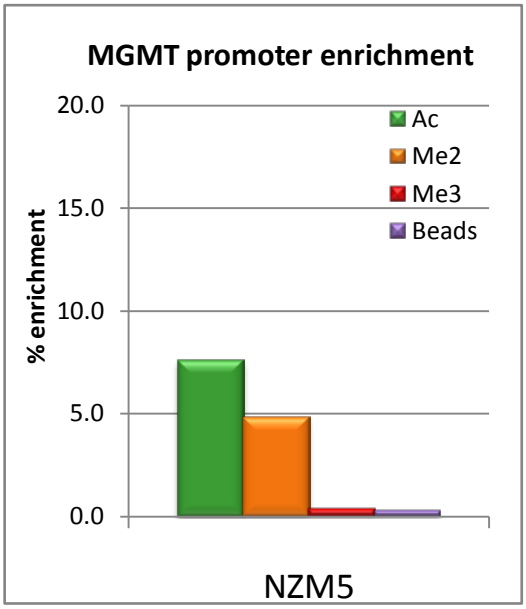

Figure 5-2 Amplification curves and enrichment for NZM5, MGMT subset (1 of 3).

A) β actin standard curve for input

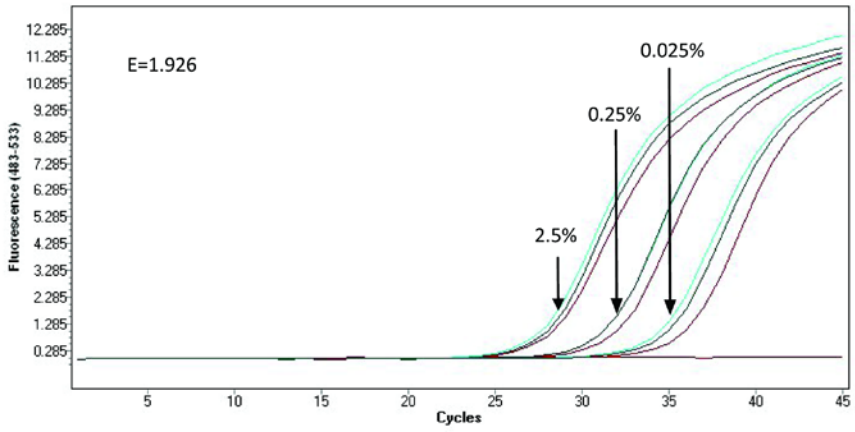

B) β actin ChIP samples

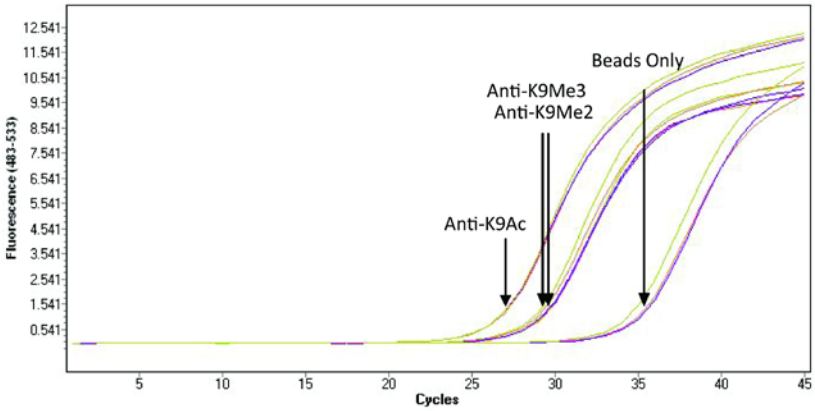

C) β actin enrichment

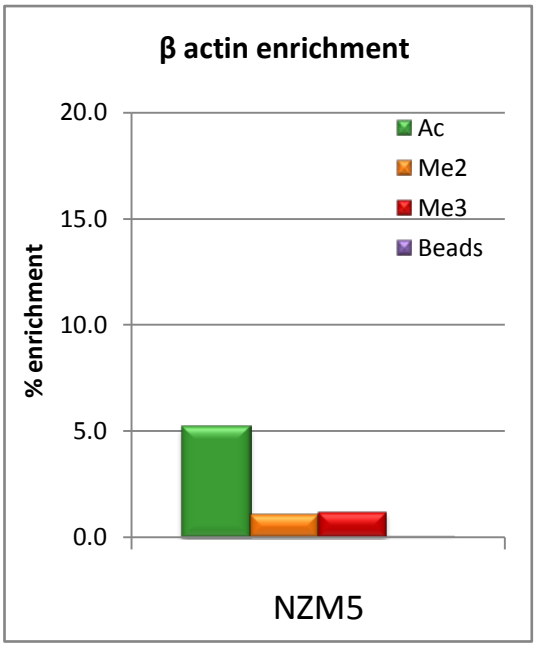

Figure 5-3 Amplification curves and enrichment for NZM5, β actin subset (1 of 3).

Figure 5-2A) Amplification curves for MGMT input standard curve series.
Figure 5-2B) Amplification curves for MGMT ChIP samples.
Figure 5-2C) Enrichment of the MGMT promoter for respective antibodies.
Green bars show enrichment of H3K9ac at the MGMT promoter with respect to input.
Orange bars indicate enrichment of H3K9me2 at the MGMT promoter with respect to input.
Red bars show enrichment of H3K9me3 at the MGMT promoter with respect to input.
Purple bars indicate enrichment of beads-only at the MGMT promoter with respect to input.

Figure 5-3A) Amplification curves for β actin input standard curve series.
Figure 5-3B) Amplification curves for β actin ChIP samples.
Figure 5-3C) Enrichment of the β actin gene for respective antibodies.
Colours are the same as above.

The NZM5 cell line expresses MGMT mRNA and was shown to display the active histone modification of H3K9ac at the MGMT promoter as expected. The absence of both H3K9me2 and H3K9me3 was also as expected. However, inconsistent with an active gene promoter, a low level of enrichment for H3K9me2 was also observed.

Significantly, the β actin gene shows enrichment in the ChIP assay for acetylation of H3K9 and near background levels of enrichment for both H3K9me2 and H3K9me3 reactions. This was expected for the β actin gene as this gene is constitutively active.

The beads-only control resulted in negligible enrichment <0.025% input for both the MGMT promoter and β actin gene indicating that the observed results are not due to non-specific interactions between histone-DNA complexes and protein A/G beads.

5.3.2 ChIP assay results for five cell lines

ChIP assays were carried out on aliquots of fixed chromatin extracted from five melanoma cell lines. ChIP grade antibodies against H3K9ac, H3K9me2, H3K9me3 were used in addition to protein A/G beads.

Data from MGMT expressing cell lines (NZM4, NZM5) indicated the presence of H3K9ac on the MGMT promoter as expected, although the overall signal for the NZM4 cell line was low. The H3K9ac signal was also observed on the constitutively expressed β actin gene. Both H3K9me2 and H3K9me3 were near-background levels on both the MGMT promoter and the β actin gene in MGMT expressing cell lines.

In MGMT silenced cell lines (NZM3, NZM11, NZM14) the H3K9ac mark was low or absent at the MGMT promoter with the exception of NZM14. The H3K9ac mark was present on the β actin gene in NZM3, NZM11 and NZM14. The H3K9me2 was present on the MGMT promoter in all cases and was absent on the β actin gene with the exception of NZM14. However, in this cell line there is large variability for the H3K9ac and H3K9me2 marks on the β actin gene (6.94 ± 3.9, 8.24 ± 4.8 respectively).

Notably the H3K9me3 mark was present on the MGMT promoter in all cell lines which do not express MGMT and in none of the cell lines expressing MGMT. In addition, the H3K9me3 mark was low or absent on the β actin gene in all cases as expected.

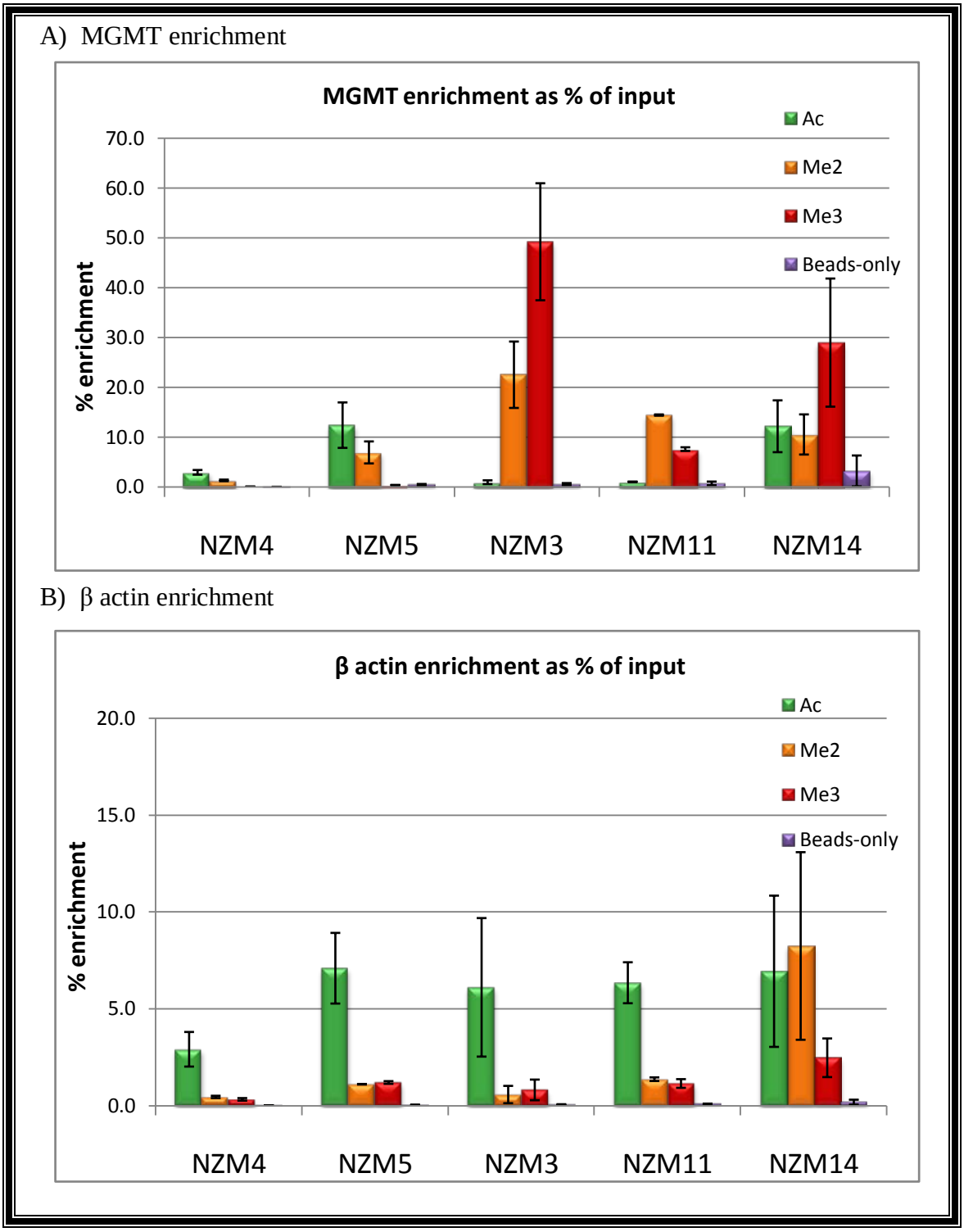

Figure 5-4 A) Relative enrichment of ChIP samples for the MGMT promoter and B) the β actin gene. Error bars shown are standard error. $n = 3$.

Green bars show enrichment of acetylated MGMT/β actin template with respect to input.

Orange bars indicate enrichment of diMe MGMT/β actin template with respect to input.

Red bars show enrichment of triMe MGMT/β actin template with respect to input.

Purple bars indicate enrichment of beads-only MGMT/β actin template with respect to input.

Previously published research using a very similar ChIP method on *xenopus* oocytes using antibodies raised against TBP2 indicate that a signal of between 5-100 % of input is within the expected range for RT-qPCR analysis (Jallow, et al., 2004).

The MGMT expressing cell lines NZM4 and NZM5 were expected to display the active chromatin mark H3K9ac at the MGMT promoter. The absence of the H3K9me2 and H3K9me3 marks was expected. The constitutively active β actin gene was expected to display the H3K9ac mark, but be depleted in H3K9me2 and H3K9me3. In contrast to these predictions the H3K9ac modification was substantially absent at the MGMT promoter in the NZM4 cell line. However, the H3K9ac signal for the NZM4 cell line was reproducibly low compared to input for both MGMT and β actin (Cp's approximately 28 and 26 respectively) suggesting that the true H3K9ac levels may be masked in this cell line. Alternatively, other mechanisms may keep the MGMT promoter and the β actin gene competent for transcription in the NZM4 cell line. Consistent with expectations, H3K9ac was observed at the β actin gene in the NZM5 cell line. Niether H3K9me2 nor H3K9me3 were observed at significant levels.

MGMT silent cell lines NZM3, NZM11, NZM14 and were expected to display an absence of H3K9ac on the MGMT promoter. In addition, these cell lines were expected to display the H3K9me2 or H3K9me3 modifications. NZM3 and NZM11 were observed to display a lack of H3K9ac on the MGMT promoter, however NZM14 displays H3K9ac. Taken together, these results suggest that the H3K9ac mark may not be a strong indicator of active gene expression for the MGMT gene. However, a larger sample size would be necessary to validate this suggestion.

Previously, the Mukai group (Nakagawachi, et al., 2003) used the ChIP technique coupled with semi-quantitative PCR to examine a number of histone modifications present at the MGMT promoter in cancer cell lines. Methylation of H3K9 throughout the CpG island was observed in the MGMT silenced LU65 lung cancer cell line and the H3K9ac mark was observed throughout the CpG island in the MGMT expressing A549 lung cancer cell line. More recently, using five cell lines including LU65 and A549 this group described H3K9me2 along with MeCP2 binding at the MGMT promoter CpG

island in MGMT silenced cell lines. This group also described the presence of H3K9me3 in all cell lines regardless of MGMT expression status (W. Zhao, et al., 2005).

In the current study, all MGMT silenced cell lines were observed to display H3K9me2 modification. This finding is consistent with previous research (Nakagawachi, et al., 2003). All MGMT silenced cell lines were observed to display the H3K9me3 modification. This finding, together with the finding that H3K9me3 was observed to be absent in MGMT expressing cell lines, contradicts a previous report by the Mukai group, who observed that the H3K9me3 modification was present at the MGMT promoter regardless of MGMT expression status (W. Zhao, et al., 2005).

5.4 Chapter summary

ChIP assays were carried out on 5 melanoma cell lines with antibodies against H3K9ac, H3K9me2, H3K9me3 and beads-only control. Enrichment of the MGMT promoter and β actin gene were calculated independently with respect to an input DNA standard curve. Consistent with expectations, the MGMT expressing cell line NZM5 was observed to display the active chromatin mark H3K9ac and an absence of H3K9me2 and H3K9me3. In addition, the MGMT silenced cell lines NZM3, NZM11 and NZM14 were observed to display the silenced chromatin marks H3K9me2 and H3K9me3. MGMT silenced cell lines NZM3 and NZM11 were observed to display an absence of the H3K9ac modification.

In summary, MGMT silenced cell lines were found to display H3K9me2 and H3K9me3 as hypothesised. Results derived from the H3K9ac mark are inconclusive. Given the small sample size used more research would be required before any firm conclusions can be drawn regarding the presence of H3K9ac in MGMT expressing and silenced cell lines.

Overall, ChIP data were authenticated by the observation that the β actin gene was observed to display H3K9ac regardless of MGMT expression status. Overall the H3K9me2 and H3K9me3 marks were low or absent on the β actin gene with the exception of NZM14.

6 Conclusions and future directions

6.1 Overview

Epigenetic processes such as DNA methylation and chromatin modification are increasingly being found to influence a broad range of biological processes. From embryonic development and stem cell differentiation, to drug addiction (Maze et al., 2010) and cancer, epigenetic events has great potential for molecular diagnostics and therapy. Understanding the epigenetic changes which occur in cancer is important not only for prevention and treatment stratagies, but for understanding the underlying molecular mechanisms responsible for the diverse and complex effects of epigenetic signals in normal and diseased states.

Primers were designed to amplify regions with the MGMT promoter and two reference genes. Amplicons were validated by restriction endonuclease digestion. Single products were generated in an RT-qPCR assay indicating that the assay is specific for the desired amplicons. Amplification for each primer pair was consistent, efficient and linear. Taken together, these results indicate a robust and reliable assay.

Two types of epigenetic signal, DNA methylation and chromatin modification were examined in the current study, in comparison to transcription of the MGMT gene. At the beginning of the study, data for TMZ sensitivity and MGMT expression were available for a number of cell lines. Cell lines showing a correlation between TMZ sensitivity and MGMT expression were selected for analysis by the MeDIP technique. A roughly equal number of MGMT negative and MGMT positive cell lines were selected. Similarly, for the ChIP technique, cell lines which showed a correlation between MGMT expression and MGMT promoter methylation were selected. Time constraints at the cell culture stage and the RT-qPCR stage of the study were a major factor that influenced the number of cell lines analysed for each technique.

Conclusions and discussion

Two types of RT-qPCR quantification were used to analyse the output of the MeDIP and ChIP techniques. For the MeDIP technique the relative quantification method was used. Relative quantification provides quantification of target DNA concentration compared to selected reference DNA concentrations. The addition of a calibrator template in each reaction set allows comparison between biological samples. Two reference genes for relative quantification were chosen due to their known methylated or constitutively active state. Using this technique the methylation state of the MGMT gene was estimated relative to each reference.

For the ChIP technique absolute quantification was used. It is well established that chromatin modifications can differ between tissue types and between cancer types therefore selecting reliable reference genes for relative quantification is very difficult. There is currently insufficient evidence in melanoma cells to establish reliable reference loci. Absolute quantification allows comparison between target DNA concentration and input recovery only and therefore does not require multiple reference genes. Input recovery should be equivalent in each cell line unless there is unanticipated copy number variation. Therefore the MGMT gene and β actin gene were analysed as individual targets by absolute quantification as a percentage of input recovery.

6.1.1 MeDIP analysis

The first aim in this study was to correlate the DNA methylation status of the MGMT promoter to MGMT expression levels in melanoma cell lines. The DNA methylation state of the MGMT gene has been linked to MGMT expression in a number of cancer cell lines (Cao et al., 2009), however this link has not yet been demonstrated for melanoma. The MeDIP technique was used to analyse MGMT promoter DNA methylation across seven melanoma cell lines. The MeDIP method, coupled with relative quantification by RT-qPCR, proved to be an effective tool to estimate DNA methylation at the MGMT promoter. It should be noted, however, that primer design and amplicon placement were critical for success and reliability. The experimental strategy included the use of two reference genes, as opposed to a single reference, which improved confidence in the observed results. Table 6-1 shows a summary of MeDIP data in relation to TMZ IC_{50} (B, Baguley, personal communication, Nov, 2007) and MGMT expression (M, Aalderink, personal communication, Nov, 2007).

Table 6-1 Results summary for MeDIP data.

	TMZ IC_{50}	MGMT expression relative to β actin	MGMT promoter DNA methylation
NZM2	>100	1	X
NZM4	>100	1.43 ± 0.12	intermediate
NZM5	>100	0.65 ± 0.11	X
NZM3	29-37	0.00	√
NZM11	1.9-31	0.00	√
NZM14	74-76	0.00	√
NZM58	59	0.02 ± 0.02	√

There was little DNA methylation observed at the MGMT promoter in 3/3 (100%) cell lines expressing MGMT. In addition, in 4/4 (100%) MGMT silenced cell lines there was significant DNA methylation at the MGMT promoter. The observed results indicate a strong association between DNA methylation and gene silencing. These data

support the theory that the DNA methylation state of the MGMT promoter region is inversely correlated with the expression of MGMT mRNA.

6.1.2 ChIP analysis

The second aim in this study was to correlate post-translational histone lysine modifications at the MGMT locus to MGMT expression levels in melanoma cell lines. The chromatin immunoprecipitation method, coupled with absolute quantification by RT-qPCR was used to examine histone modifications at the MGMT promoter. The NZM4 and NZM14 cell lines show inconclusive results with respect to H3K9ac. Data for MGMT and β actin in the NZM4 cell line show a low overall signal, indicating an experimental issue such as an inefficient immunoprecipitation reaction. In addition, data for the NZM14 cell line indicate that the H3K9ac modification is present regardless of MGMT silencing. A much larger sample set would be required before any firm conclusions can be made regarding the H3K9ac modification in relation to MGMT expression state.

In 5/5 (100%) cell lines the presence of both H3K9me2 and H3K9me3 were associated with MGMT silencing. These data support previous research which indicated that the presence of the H3K9me2 modification at the MGMT promoter is associated with silencing (Nakagawachi, et al., 2003). However, these data are in contrast to previous research indicating the presence of the H3K9me3 modification at the MGMT promoter regardless of MGMT expression status (W. Zhao, et al., 2005). Table 6-2 shows a summary of ChIP data for the MGMT promoter amplicon.

Table 6-2 Results summary for MGMT ChIP data.

	TMZ IC_{50}	MGMT expression	MGMT H3K9ac	MGMT H3K9me2	MGMT H3K9me3
NZM4	>100	1.43 ± 0.12	x*	x	x
NZM5	>100	0.65 ± 0.11	↑↑	↑	x
NZM3	29-37	0.00	x	↑↑↑	↑↑↑↑
NZM11	1.9-31	0.00	x	↑↑	↑
NZM14	74-76	0.00	↑↑	↑↑	↑↑↑

* Low enrichment overall for both β actin and MGMT.

Overall, the β actin gene shows acetylation of H3K9 as expected. Data for NZM14 show surprising results for the β actin gene as it appears that this gene contains the H3K9me2 mark. However, given the high variability of data for this cell line, this result might not be seen if the experiment were repeated. Table 6-3 shows a summary of ChIP data for the β actin gene amplicon.

Table 6-3 Results summary for β actin ChIP data.

	TMZ IC_{50}	MGMT expression	β actin H3K9ac	β actin H3K9me2	β actin H3K9me3
NZM4	>100	1.43 ± 0.12	↑	x	x
NZM5	>100	0.65 ± 0.11	↑↑	x	x
NZM3	29-37	0.00	↑↑	x	x
NZM11	1.9-31	0.00	↑↑	x	x
NZM14	74-76	0.00	↑↑	↑↑	↑

Crossing points used to calculate relative expression data were reproducible. Table 6-4 shows Cps used to calculate MGMT mRNA expression in cell lines used in the current study (M, Aalderink, personal communication, Nov, 2007), (K, Stowell, personal communication, Feb, 2010). Notably, for the NZM14 cell line, Cps for β actin mRNA are more than three cycles less than the closest data point, indicating an approximately 10 fold increase in β actin mRNA template over NZM58 and >50 fold over other cell lines. Somewhat surprisingly, there would seem to be no correlation between acetylation levels of the β actin gene from the current study and β actin Cps.

Table 6-4 MGMT expression crossing points.

	MGMT expression	MGMT expression Cp average	β actin Cp average
NZM2	1	27.42 ± 0.09	24.96 ± 0.17
NZM4	1.43 ± 0.12	27.95 ± 0.06	21.15 ± 0.02
NZM5	0.65 ± 0.11	28.35 ± 0.22	24.65 ± 0.58
NZM3	0.00	>35	27.16 ± 0.14
NZM11	0.00	>35	21.09 ± 0.06
NZM14	0.00	>35	16.33 ± 0.25
NZM58	0.02 ± 0.02	>35	19.80 ± 0.13

Summary

In the current study, the DNA methylation state of seven melanoma cell lines was estimated using the MeDIP technique coupled with relative quantification by RT-qPCR. Histone modifications were examined using the ChIP technique coupled with absolute quantification by RT-qPCR. These data were compared with MGMT expression levels. It was earlier hypothesised that MGMT promoter DNA methylation, H3K9 de-acetylation and H3K9 dimethylation at the MGMT promoter could be directly correlated with MGMT silencing.

DNA methylation at the MGMT promoter was found to be closely correlated with low MGMT expression. Current literature suggests that DNA methylation at gene promoters is a strong indication of epigenetic silencing. These data support the current literature in this regard. H3K9 de-acetylation at the MGMT promoter was observed to some extent in MGMT silenced cell lines however a much larger sample number would provide clearer results and may show a significant correlation. The presence of H3K9me2 was closely correlated with MGMT silencing. These data support previous findings (Nakagawachi, et al., 2003). In addition a third histone modification (H3K9me3) was examined. It was hypothesised that this modification would also be associated with MGMT silencing. These data support this hypothesis and support previous theories on histone modification mechanisms (Kouzarides & Berger, 2007) however, these data contradict a previous report (W. Zhao, et al., 2005).

Overall, the current study provides evidence supporting current literature regarding the function of DNA methylation and the H3K9me2 modification. More research is required to clarify the presence or absence of H3K9ac at the MGMT promoter and to elucidate the order of events during the transition from an active euchromatic state to a silenced state. These data are in concordance with previous findings regarding epigenetic MGMT silencing in glioblastoma (Cao, et al., 2009). In glioblastoma the prognostic value of MGMT promoter methylation is well recognised (M. E. Hegi et al., 2005; Spiegl-Kreinecker et al., 2010), therefore these findings support the prognostic significance of MGMT promoter methylation in melanoma. However, the use of a much larger sample number is required to validate such a correlation.

6.1.3 Possible sources of bias

6.1.3.1 Nucleosome reshuffling

One possibility to explain inconsistency of the H3K9ac ChIP data is that nucleosome reshuffling has altered the nucleosomal state of the MGMT promoter in some melanoma cell lines. It is now well established that nucleosome reshuffling plays a role in silent chromatin formation (Corona et al., 2007; Sun, Cuaycong, & Elgin, 2001). Typically, transcriptionally competent promoters are nucleosome poor over the transcription start site (Figure 6-1), whereas silenced promoters contain regularly spaced nucleosomes (Sun, et al., 2001). Nucleosome reshuffling could decrease the ChIP signal for euchromatic marks such as H3K9ac and increase the signal for heterochromatic marks such as H3K9me2 and H3K9me3. This could explain why a low H3K9ac signal was observed in the NZM4 cell line which expresses MGMT, and high H3K9me2 and H3K9me3 signals were observed in the NZM3 cell line which does not.

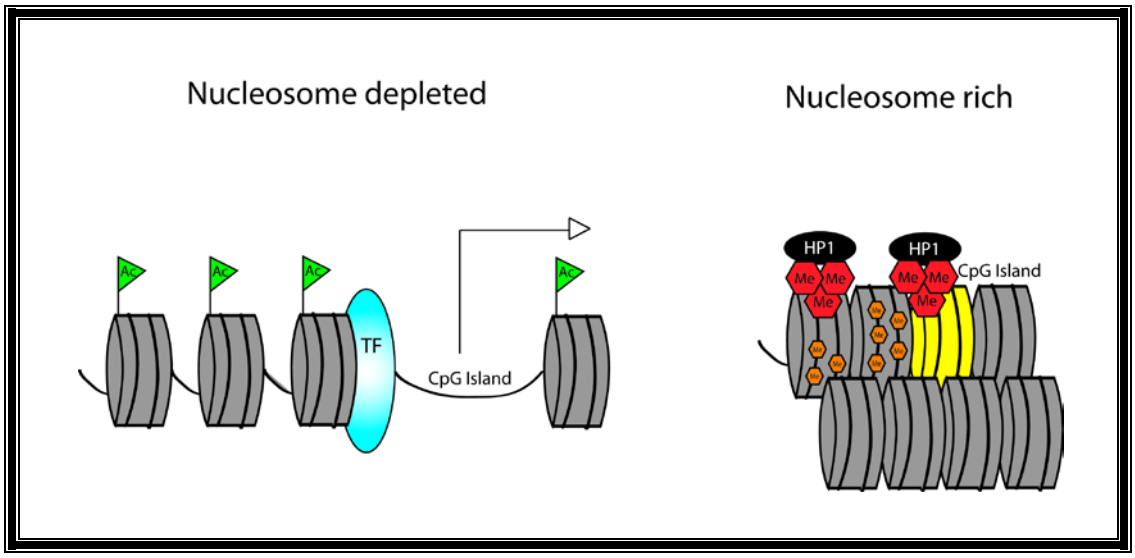

Figure 6-1 Possible bias due to nucleosome reshuffling

6.1.3.2 Primer placement

Primer design and amplicon placement present bias issues for both the MeDIP and ChIP techniques. For any assay in which two or more primer pairs are amplified on the same 96-well plate sequences must have similar properties in order to maintain an efficient PCR reaction. However, the MGMT gene promoter contains a CpG island rich in

cytosine and guanine nucleotides covering the promoter. To design primer sets with similar annealing temperature to both the MGMT promoter and the β actin gene requires that MGMT primers be designed to an area upstream or downstream of the promoter. This could result in bias due to the nature of the MeDIP or ChIP procedure. In theory, an MeDIP assay could be more sensitive to methylation nearer to the primer binding region. This could lead to a higher signal where the methylation is closer to the primer binding site. This could possibly affect the MeDIP results in the current study. Bisulfate sequencing or methylation sensitive PCR could allow quantification of such bias.

6.2 Future directions

In normal cells active genes are kept active by a lack of DNA methylation at promoter CpG islands and covalent marks such as lysine acetylation and H3K4 methylation (Kouzarides & Berger, 2007). Regions at the 5' and 3' boarders outside active genes tend to show DNA methylation of less frequent CpG dinucleotides. In addition, these outer regions recruit MBD proteins and associated HDACs (Li & Bird, 2007) and disply repressive histone modifications, especially H3K9me2 (Nguyen, Gonzales, & Jones, 2001). It would seem that boundary elements exist which protect active genes from epigenetic silencing in normal cells. One important theme for cancer epigenetics in the future will be characterisation of the nature and position of these boundaries and how they are altered in cancerous cells.

6.2.1 Future experiments

There is great potential for future studies into the epigenetic regulation of the MGMT gene. Firstly, only the promoter region of MGMT was examined in the present study. It is well established that epigenetic modifications at the 1st intron, the coding region and 5' un-translated region are involved in transcriptional regulation, however, this has not yet been demonstrated for MGMT. Examination of active and silent epigenetic modifications in these regions could provide further information regarding the epigenetic state of the MGMT gene.

Deregulation of modification enzymes such as EZH2, MLL and G9a (Nagano et al., 2008) has been implicated in cancer. ChIP experiments could be used to examine histone-modifying complexes responsible for altering the epigenetic state of MGMT.

Recently researchers demonstrated that the activity of EZH2, a histone methyltransferase that modifies the H3K27 residue, is commonly down-regulated as a result of somatic mutation in large B-cell lymphoma (Morin et al., 2010). A supporting commentary noted that although this mutation would seem to show specificity for large B-cell lymphoma, EZH2 over-expression is common in other types of cancer. However, niether melanoma or glioblastoma were represented in the cited study (Simon & Lange, 2008).

The G9a and EZH2 enzymes and their corresponding targets, H3k9 and H3K27 respectively are of particular interest. These marks have the uncommon ability to display bivalent (active or repressive) histone marks. In cells derived from colorectal cancer, both G9a and EZH2, as well as the HP1 protein, were shown by ChIP to be present at the epigenetically silenced hMLH gene. In addition, the H3K9me2, H3K9me3 and H3K27me3 marks were present (McGarvey et al., 2006). Notably, upon gene re-expression by the DNA methylation inhibitor 5-aza-deoxycytidine (5-aza-dC), the H3K9me2 modification was shown to dcrease over time, concomitant with increased gene expression. However, neither the H3K9me3 modification, nor any of the H3K27me forms showed a significant change (McGarvey, et al., 2006) indicating that these marks may be more stable than previously thought.

DNA methylation and histone modifications may not be the only factors influencing MGMT expression. It is possible that nucleosome positioning is important for the regulation of MGMT as differences in position have been reported to have a large impact on promoter access (Corona, et al., 2007). The *In vivo* nucleosome positioning technique would allow further examination of this effect (Steward & Sano, 2004).

There is currently evidence showing correlations between active or silent chromatin conformation and nuclear territory localization (Akhtar & Gasser, 2007). In the control of lymphopoiesis, epigenetically silenced alleles of the immunoglobulin cluster are re-located to the nuclear periphery (Busslinger & Tarakhovsky, 2007). Two modifications thought to be involved in this process are H3K9 and H3K27. One direction of research could be to examine the relationship between the chromatin state of the MGMT promoter and nuclear localization. The fluorescence in situ hybridisation (FISH)

technique could be used to examine nuclear localisation. It is possible that MGMT silencing is associated with nuclear membrane localisation, or that in MGMT-silenced cell lines, the MGMT gene co-localises with other down-regulated or silenced genes (Akhtar & Gasser, 2007).

The current study represents a small number of samples from over 50 melanoma and glioblastoma cell lines for which MGMT expression and TMZ IC_{50} data is available. One ambitious line of research could be to analyse H3K4me2 (active) H3K9me2, H3K9me3 and H3K27me3 states and G9a, HP1-α and EZH2 occupancy by chromatin immunoprecipitation at the MGMT gene in these cell lines. By using primers designed to 5', promoter, 1st intron and 3' regions of the MGMT gene, the boarders of active chromatin could be established. In addition, the presence or absence of HP1 would provide insight into the relative importance of the H3K9me3 and H3K27me3 modifications as HP1 is classically considered to be targeted by H3K9me3 (Maison & Almouzni, 2004). A less ambitious line of research could be to carry out FISH analysis of the MGMT gene combined with immunofluorescence of each cell line with antibodies rasied against some or all of the modifications or enzymes mentioned above.

Next-generation sequencing has great potential for genome-wide studies which can be coupled to the MeDIP or ChIP techniques (Barski et al., 2007). Chromosome conformation capture (Dekker, Rippe, Dekker, & Kleckner, 2002) combined with the ChIP seq technique may also provide an extremely powerful tool for the comparative analysis of nuclear localization, and histone modification profiles in future studies. However, the tools to analyse such data remain limiting at the current time.

6.2.2 Clinical aspects

Research into epigenetic events commonly occurring in cancer has highlighted a number of possible intervention strategies. Two of these include the use of DNA methylation inhibitors or histone modifier inhibitors.

One example of a DNA methylation inhibitor is 5-aza-dC, a drug which is incorporated into the DNA of replicating S-phase cells (P. A. Jones & Taylor, 1980) where it then forms covalent intermediates with DNMTs. This interaction results in the disruption of

de novo CpG methylation and blockage of further methylation (Baylin & Jones, 2007). The drug 5-aza-dC has been trialled *in vitro* and has undergone a number of human clinical trials with positive results. It is thought that by blocking DNA methylation, 5-aza-dC may counteract the adverse effects of the de-regulation of DNA methylation, a hallmark of cancer (Baylin & Jones, 2007; Klose & Bird, 2006). Some possible side effects may include up-regulation of normally silenced genes and instability of the genome due to re-activation of previously methylated mobile DNA elements.

There are now a number of HDAC and HAT inhibitors in development by major drug companies (Baylin & Jones, 2007). Each of these enzymes and inhibitors has varying degrees of specificity. Recently, for the first time, the reversal of the H3K9me2 mark was demonstrated *in vitro* using a histone methltransferase inhibitor showing specificity for G9a (Kubicek et al., 2007). In the future, drugs like 5-aza-dC and histone modifier inhibitors could be tested in animal models to examine the effects of a reduction in DNA methylation and altered histone marks on MGMT expression *in vivo*. Manipulation of histone modification and DNA methylation could result in partial or complete re-expression of the MGMT gene in cancer. In patients, MGMT expression counteracts the effects of TMZ however, as MGMT is a tumour suppressor, these patients can often expect an improved prognosis. Therefore, targeted histone modifier inhibition and DNMT inhibition is an exciting possibility for epigenetic therapy.

Knowing whether MGMT is expressed in a tumour is of great importance to physicians as this knowledge can allow tailored treatment and improved drug efficacy. An assay to detect DNA methylation or specific histone modification at the MGMT promoter could give valuable insight into the MGMT expression state of a tumour. In the present study a distinct pattern of DNA methylation and H3K9me2 and H3K9me3 histone modifications were found to correlate with MGMT silencing in melanoma derived cell lines. These marks represent potential biomarkers to predict patient response to the drug TMZ. Future validation of these biomarkers and others for the expression of MGMT in melanoma could potentially lead to an increase in the efficacy of treatment and an increase in the quality of life for patients in New Zealand.

Bibliography

Aagaard, L., Schmid, M., Warburton, P., & Jenuwein, T. (2000). Mitotic phosphorylation of SUV39H1, a novel component of active centromeres, coincides with transient accumulation at mammalian centromeres. *J Cell Sci, 113*(5), 817-829.

Ahringer, J. (2000). NuRD and SIN3 - histone deacetylase complexes in development. *Trends in Genetics, 16*(8), 351-356.

Akhtar, A., & Gasser, S. M. (2007). The nuclear envelope and transcriptional control. *Nature Reviews Genetics, 8*(7), 507-517.

Allis, C. D., Jenuwein, T., & Reinberg, D. (2007). Overview and concepts. In C. D. Allis (Ed.), *Epigenetics*. New York: Cold Spring Harbour Laboratory Press.

An, W., Kim, J., & Roeder, R. G. (2004). Ordered cooperative functions of PRMT1, p300, and CARM1 in transcriptional activation by p53. [Article]. *Cell, 117*(6), 735-748.

Barski, A., Cuddapah, S., Cui, K. R., Roh, T. Y., Schones, D. E., Wang, Z. B., et al. (2007). High-resolution profiling of histone methylations in the human genome. *Cell, 129*(4), 823-837.

Baylin, B. S., & Jones, P. A. (2007). Epigenetic Determinants of Cancer. In C. D. Allis (Ed.), *Epigenetics*. New York: Cold Spring Harbour Laboratory Press.

Bird, A. P., & Wolffe, A. P. (1999). Methylation-induced repression - Belts, braces, and chromatin. *Cell, 99*(5), 451-454.

Biswas, T., Ramana, C. V., Srinivasan, G., Boldogh, I., Hazra, T. K., Chen, Z. P., et al. (1999). Activation of human O-6-methylguanine-DNA methyltransferase gene by glucocorticoid hormone. *Oncogene, 18*(2), 525-532.

Bittner, M., Meitzer, P., Chen, Y., Jiang, Y., Seftor, E., Hendrix, M., et al. (2000). Molecular classification of cutaneous malignant melanoma by gene expression profiling. *Nature, 406*(6795), 536-540.

Bliss, J. M., Ford, D., Swerdlow, A. J., Armstrong, B. K., Cristofolini, M., Elwood, J. M., et al. (1995). Risk of cutaneous melanoma-associated with pigmentation characteristics and freckling - systematic overview of 10 case-control studies. *International Journal of Cancer, 62*(4), 367-376.

Boldogh, I., Ramana, C. V., Chen, Z. P., Biswas, T., Hazra, T. K., Grosch, S., et al. (1998). Regulation of expression of the DNA repair gene O-6-methylguanine-DNA methyltransferase via protein kinase C-mediated signaling. *Cancer Research, 58*(17), 3950-3956.

Bonfanti, M., Broggini, M., Prontera, C., & Dincalci, M. (1991). O6-methylguanine inhibits the binding of transcription factors to DNA. *Nucleic Acids Research, 19*(20), 5739-5742.

Busslinger, M., & Tarakhovsky, A. (2007). Epigenetic control of lymphopoiesis. In C. D. Allis (Ed.), *Epigenetics*. Cold Spring Harbor: Cold Spring Harbor Laboratory Press.

Cairns, B. R. (2009). The logic of chromatin architecture and remodelling at promoters. [Review]. *Nature, 461*(7261), 193-198.

Candau, R., Zhou, J. X., Allis, C. D., & Berger, S. L. (1997). Histone acetyltransferase activity and interaction with ADA2 are critical for GCN5 function in vivo. *Embo Journal, 16*(3), 555-565.

Cao, V. T., Lung, T. Y., Jung, S., Jin, S. G., Moon, K. S., Kim, I. Y., et al. (2009). The Correlation and Prognostic Significance of MGMT Promoter Methylation and MGMT Protein in Glioblastomas. [Article]. *Neurosurgery, 65*(5), 866-875.

Corona, D. F. V., Siriaco, G., Armstrong, J. A., Snarskaya, N., McClymont, S. A., Scott, M. P., et al. (2007). ISWI Regulates Higher-Order Chromatin Structure and Histone H1 Assembly In Vivo. *PLoS Biol, 5*(9), e232.

Costello, J. F., Futscher, B. W., Tano, K., Graunke, D. M., & Pieper, R. O. (1994). Graded methylation in the promoter and body of 06-methylguanine DNA methyltransferase (MGMT) gene correlates with MGMT expression in human glioma-cells. *Journal of Biological Chemistry, 269*(25), 17228-17237.

D'Atri, S., Tentori, L., Lacal, P. M., Graziani, G., Pagani, E., Benincasa, E., et al. (1998). Involvement of the mismatch repair system in temozolomide-induced apoptosis. *Molecular Pharmacology, 54*(2), 334-341.

Danam, R. P., Howell, S. R., Brent, T. P., & Harris, L. C. (2005). Epigenetic regulation of O-6-methylguanine-DNA methyltransferase gene expression by histone acetylation and methyl-CpG binding proteins. *Molecular Cancer Therapeutics, 4*(1), 61-69.

Davis, T. L., Yang, G. J., McCarrey, J. R., & Bartolomei, M. S. (2000). The H19 methylation imprint is erased and re-established differentially on the parental alleles during male germ cell development. *Human Molecular Genetics, 9*(19), 2885-2894.

Dekker, J., Rippe, K., Dekker, M., & Kleckner, N. (2002). Capturing Chromosome Conformation. *Science, 295*(5558), 1306-1311.

Delmas, V., Stokes, D. G., & Perry, R. P. (1993). A mammalian DNA-binding protein that contains a chromodomain and an SNF2 SWI2-like helicase domain. *Proceedings of the National Academy of Sciences of the United States of America, 90*(6), 2414-2418.

Denny, B. J., Wheelhouse, R. T., Stevens, M. F. G., Tsang, L. L. H., & Slack, J. A. (1994). NMR and molecular modeling investigation of the mechanism of activation of the antitumor drug temozolomide and its interaction with DNA. *Biochemistry, 33*(31), 9045-9051.

Dingwall, A. K., Beek, S. J., McCallum, C. M., Tamkun, J. W., Kalpana, G. V., Goff, S. P., et al. (1995). The *drosophila* SNR1 and BRM proteins are related to yeast SWI/SNF proteins and are components of a large protein complex. *Molecular Biology of the Cell, 6*(7), 777-791.

Esteller, M., Corn, P. G., Baylin, S. B., & Herman, J. G. (2001). A gene hypermethylation profile of human cancer. *Cancer Research, 61*(8), 3225-3229.

Esteller, M., Hamilton, S. R., Burger, P. C., Baylin, S. B., & Herman, J. G. (1999). Inactivation of the DNA repair gene O-6-methylguanine-DNA methyltransferase by promoter hypermethylation is a common event in primary human neoplasia. *Cancer Research, 59*(4), 793-797.

Fornace, A. J., Papathanasiou, M. A., Hollander, M. C., & Yarosh, D. B. (1990). Expression of the O-6-methylguanine-DNA methyltransferase gene MGMT in MER+ and MER- human tumor-cells. *Cancer Research, 50*(24), 7908-7911.

Friedman, H., Kerby, T., & Calvert, H. (2000). Temozolomide and Treatment of Malignant Glioma. *Clinical Cancer Research, 6*, 2585-2597.

Furie, B., Cassileth, P. A., Atkins, M. B., & Mayer, R. J. (2003). *Clinical Hematology and Oncology: Presentation, Diagnosis and Treatment*. Philadelphia: Chruchill Livingstone.

Grafstrom, R. C., Pegg, A. E., Trump, B. F., & Harris, C. C. (1984). O-6-alkylguanine-DNA alkyltransferase activity in normal human-tissues and cells. *Cancer Research, 44*(7), 2855-2857.

Grant, P. A., Duggan, L., Cote, J., Roberts, S. M., Brownell, J. E., Candau, R., et al. (1997). Yeast Gcn5 functions in two multisubunit complexes to acetylate nucleosomal histones: Characterization of an Ada complex and the SAGA (Spt/Ada) complex. *Genes & Development, 11*(13), 1640-1650.

Haynes, S. R., Dollard, C., Winston, F., Beck, S., Trowsdale, J., & Dawid, I. B. (1992). The bromodomain - a conserved sequence found in human, *drosophila* and yeast proteins. *Nucleic Acids Research, 20*(10), 2603-2603.

Hegi, M. E., Diserens, A.-C., Godard, S., Dietrich, P.-Y., Regli, L., Ostermann, S., et al. (2004). Clinical trial substantiates the predictive value of O-6-methylguanine-DNA methyltransferase promoter methylation in glioblastoma patients treated with temozolomide. *Clinical Cancer Research, 10*, 1871-1874.

Hegi, M. E., Diserens, A., Gorlia, T., Hamou, M., de Tribolet, N., Weller, M., et al. (2005). MGMT gene silencing and benefit from temozolomide in glioblastoma. *New England Journal of Medicine, 352*(10), 997-1003.

Hendrich, B., Guy, J., Ramsahoye, B., Wilson, V. A., & Bird, A. (2001). Closely related proteins MBD2 and MBD3 play distinctive but interacting roles in mouse development. *Genes & Development, 15*(6), 710-723.

Hepburn, P. A., Margison, G. P., & Tisdale, M. J. (1991). Enzymatic methylation of cytosine in DNA is prevented by adjacent O6-methylguanine residues. *Journal of Biological Chemistry, 266*(13), 7985-7987.

Herman, J. G., Graff, J. R., Myohanen, S., Nelkin, B. D., & Baylin, S. B. (1996). Methylation-Specific PCR: A Novel PCR Assay for Methylation Status of CpG Islands. *Proceedings of the National Academy of Sciences of the United States of America, 93*(18), 9821-9826.

Hoeijmakers, J. H. J. (2001). Genome maintenance mechanisms for preventing cancer. *Nature, 411*(6835), 366-374.

Hussussian, C. J., Struewing, J. P., Goldstein, A. M., Higgins, P. A. T., Ally, D. S., Sheahan, M. D., et al. (1994). Germline p16 mutations in familial melanoma. *Nature Genetics, 8*(1), 15-21.

Hutchins, A. S., Mullen, A. C., Lee, H. W., Sykes, K. J., High, F. A., Hendrich, B. D., et al. (2002). Gene silencing quantitatively controls the function of a developmental trans-activator. *Molecular Cell, 10*(1), 81-91.

Irvine, R. A., & Hsieh, C.-L. (2004). Q-PCR in Combination with ChIP Assays to Detect Changes in Chromatin Acetylation. In T. O. Tollefsbol (Ed.), *Epigenetics Protocols* (Vol. 287). Totowa, New Jersey: Humana Press Inc.

Jallow, Z., Jacobi, U. G., Weeks, D. L., Dawid, I. B., & Veenstra, G. J. C. (2004). Specialized and redundant roles of TBP and a vertebrate-specific TBP paralog in embryonic gene regulation in Xenopus. [Article]. *Proceedings of the National Academy of Sciences of the United States of America, 101*(37), 13525-13530.

Jenuwein, T., & Allis, C. D. (2001). Translating the histone code. *Science, 293*(5532), 1074-1080.

Jones, P. A., & Taylor, S. M. (1980). Cellular-differentiation, cytidine analogs and DNA methylation. *Cell, 20*(1), 85-93.

Jones, P. L., Veenstra, G. J. C., Wade, P. A., Vermaak, D., Kass, S. U., Landsberger, N., et al. (1998). Methylated DNA and MeCP2 recruit histone deacetylase to repress transcription. *Nature Genetics, 19*(2), 187-191.

Jones, W. O., Harman, C. R., Ng, A. K. T., & Shaw, J. H. F. (1999). Incidence of malignant melanoma in Auckland, New Zealand: Highest rates in the world. *World Journal of Surgery, 23*(7), 732-735.

Kadam, S., & Emerson, B. M. (2003). Transcriptional specificity of human SWI/SNF BRG1 and BRM chromatin remodeling complexes. *Molecular Cell, 11*(2), 377-389.

Kangaspeska, S., Stride, B., Metivier, R., Polycarpou-Schwarz, M., Ibberson, D., Carmouche, R. P., et al. (2008). Transient cyclical methylation of promoter DNA. [Article]. *Nature, 452*(7183), 112-U114.

Keshet, I., Liemanhurwitz, J., & Cedar, H. (1986). DNA methylation affects the formation of active chromatin. *Cell, 44*(4), 535-543.

Ketting, R. F., Fischer, S. E. J., Bernstein, E., Sijen, T., Hannon, G. J., & Plasterk, R. H. A. (2001). Dicer functions in RNA interference and in synthesis of small RNA involved in developmental timing in C-elegans. *Genes & Development, 15*(20), 2654-2659.

Klose, R. J., & Bird, A. P. (2006). Genomic DNA methylation: the mark and its mediators. *Trends in Biochemical Sciences, 31*(2), 89-97.

Klose, R. J., Sarraf, S. A., Schmiedeberg, L., McDermott, S. M., Stancheva, I., & Bird, A. P. (2005). DNA binding selectivity of MeCP2 due to a requirement for A/T sequences adjacent to methyl-CpG. *Molecular Cell, 19*(5), 667-678.

Kouzarides, T., & Berger, S. L. (2007). Chromatin modifications and thier mechanism of action. In C. D. Allis (Ed.), *Epigenetics*. New York: Cold Spring Harbour Laboratory Press.

Kubicek, S., O'Sullivan, R. J., August, E. M., Hickey, E. R., Zhan, Q., Teodoro, M. L., et al. (2007). Reversal of H3K9me2 by a small-molecule inhibitor for the G9a histone methyltransferase. *Molecular Cell, 25*(3), 473-481.

Lane, D. P. (1992). Cancer - p53, guardian of the genome. *Nature, 358*(6381), 15-16.

Lehnertz, B., Ueda, Y., Derijck, A., Braunschweig, U., Perez-Burgos, L., Kubicek, S., et al. (2003). Suv39h-mediated histone H3 lysine 9 methylation directs DNA methylation to major satellite repeats at pericentric heterochromatin. *Current Biology, 13*(14), 1192-1200.

Lens, M. B., & Dawes, M. (2004). Global perspectives of contemporary epidemiological trends of cutaneous malignant melanoma. *British Journal of Dermatology, 150*(2), 179-185.

Li, E., Bestor, T. H., & Jaenisch, R. (1992). Targeted mutation of the DNA methyltransferase gene results in embryonic lethality. *Cell, 69*(6), 915-926.

Li, E., & Bird, A. (2007). DNA methylation in Mammals. In C. D. Allis (Ed.), *Epigenetics*. New York: Cold Spring Harbour Laboratory Press.

Liang, G. N., Lin, J. C. Y., Wei, V. V., Yoo, C., Cheng, J. C., Nguyen, C. T., et al. (2004). Distinct localization of histone H3 acetylation and H3-K4 methylation to the transcription start sites in the human genome. *Proceedings of the National Academy of Sciences of the United States of America, 101*(19), 7357-7362.

Liu, L. L., Markowitz, S., & Gerson, S. L. (1996). Mismatch repair mutations override alkyltransferase in conferring resistance to temozolomide but not to 1,3-bis(2-chloroethyl)nitrosourea. *Cancer Research, 56*(23), 5375-5379.

Luger, K., Mader, A. W., Richmond, R. K., Sargent, D. F., & Richmond, T. J. (1997). Crystal structure of the nucleosome core particle at 2.8 angstrom resolution. *Nature, 389*(6648), 251-260.

Mahadevan, L. C., Willis, A. C., & Barratt, M. J. (1991). Rapid histone H3 phosphorylation in response to growth-factors, phorbol esters, okadaic acid, and protein synthesis inhibitors. *Cell, 65*(5), 775-783.

Maison, C., & Almouzni, G. (2004). HP1 and the dynamics of heterochromatin maintenance. *Nature Reviews Molecular Cell Biology, 5*(4), 296-304.

Martiensen, R., & Moazed, D. (2007). RNAi and heterochromatin assembly. In C. D. ALLIS (Ed.), *Epigenetics*. New York: Cold Spring Harbour Laboratory Press.

Martin, C., & Zhang, Y. (2005). The diverse functions of histone lysine methylation. *Nature Reviews Molecular Cell Biology, 6*(11), 838-849.

Martinez, R., Schackert, G., Yaya-Tur, R., Rojas-Marcos, I., Herman, J. G., & Esteller, M. (2007). Frequent hypermethylation of the DNA repair gene MGMT in long-term survivors of glioblastoma multiforme. *Journal of Neuro-Oncology, 83*(1), 91-93.

Maze, I., Covington, H. E., III, Dietz, D. M., LaPlant, Q., Renthal, W., Russo, S. J., et al. (2010). Essential Role of the Histone Methyltransferase G9a in Cocaine-Induced Plasticity. *Science, 327*(5962), 213-216.

McGarvey, K. M., Fahrner, J. A., Greene, E., Martens, J., Jenuwein, T., & Baylin, S. B. (2006). Silenced tumor suppressor genes reactivated by DNA demethylation do not return to a fully euchromatic chromatin state. *Cancer Research, 66*(7), 3541-3549.

Miller, A. J., & Mihm, M. C. (2006). Mechanisms of disease - Melanoma. *New England Journal of Medicine, 355*(1), 51-65.

Morin, R. D., Johnson, N. A., Severson, T. M., Mungall, A. J., An, J., Goya, R., et al. (2010). Somatic mutations altering EZH2 (Tyr641) in follicular and diffuse large B-cell lymphomas of germinal-center origin. [10.1038/ng.518]. *Nat Genet, 42*(2), 181-185.

Nagano, T., Mitchell, J. A., Sanz, L. A., Pauler, F. M., Ferguson-Smith, A. C., Feil, R., et al. (2008). The Air Noncoding RNA Epigenetically Silences Transcription by Targeting G9a to Chromatin. *Science, 322*(5908), 1717-1720.

Nakagawachi, T., Soejima, H., Urano, T., Zhao, W., Higashimoto, K., Satoh, Y., et al. (2003). Silencing effect of CpG island hypermethylation and histone modifications on O6-methylguanine-DNA methyltransferase (MGMT) gene expression in human cancer. [Article]. *Oncogene, 22*(55), 8835-8844.

Nguyen, C. T., Gonzales, F. A., & Jones, P. A. (2001). Altered chromatin structure associated with methylation-induced gene silencing in cancer cells: correlation of accessibility, methylation, MeCP2 binding and acetylation. *Nucleic Acids Research, 29*(22), 4598-4606.

Orphanides, G., LeRoy, G., Chang, C. H., Luse, D. S., & Reinberg, D. (1998). FACT, a factor that facilitates transcript elongation through nucleosomes. *Cell, 92*(1), 105-116.

Ostrowski, L. E., Vonwronski, M. A., Bigner, S. H., Rasheed, A., Schold, S. C., Brent, T. P., et al. (1991). Expression of O6-methylguanine-DNA methyltransferase in malignant human glioma cell-lines. *Carcinogenesis, 12*(9), 1739-1744.

Pegg, A. E. (1990). Mammalian O-6-alkylguanine-DNA alkyltransferase - regulation and importance in response to alkylating carcinogenic and therapeutic agents. *Cancer Research, 50*(19), 6119-6129.

Pieper, R. O., Costello, J. F., Kroes, R. A., Futscher, B. W., Marathi, U., & Erickson, L. C. (1991). Direct correlation between methylation status and expression of the human O-6-methylguanine DNA methyltransferase gene. *Cancer Communications, 3*(8), 241-253.

Price, S. A., & Wilson, L. M. (2003). *Pathophysiology: Clinical concepts of Disease Processes* (6th ed.). St. Louis, Missouri: Mosby.

Quirt, I., Verma, S., Petrella, T., Bak, K., & Charette, M. (2007). Temozolomide for the treatment of metastatic melanoma: A systematic review. *Oncologist, 12*(9), 1114-1123.

Rea, S., Eisenhaber, F., O'Carroll, N., Strahl, B. D., Sun, Z. W., Schmid, M., et al. (2000). Regulation of chromatin structure by site-specific histone H3 methyltransferases. *Nature, 406*(6796), 593-599.

Rice, J. C., Briggs, S. D., Ueberheide, B., Barber, C. M., Shabanowitz, J., Hunt, D. F., et al. (2003). Histone methyltransferases direct different degrees of methylation to define distinct chromatin domains. *Molecular Cell, 12*(6), 1591-1598.

Ruthenburg, A. J., Allis, C. D., & Wysocka, J. (2007). Methylation of lysine 4 on histone H3: Intricacy of writing and reading a single epigenetic mark. [Review]. *Molecular Cell, 25*(1), 15-30.

Schlesinger, Y., Straussman, R., Keshet, I., Farkash, S., Hecht, M., Zimmerman, J., et al. (2007). Polycomb-mediated methylation on Lys27 of histone H3 pre-marks genes for de novo methylation in cancer. [Article]. *Nature Genetics, 39*(2), 232-236.

Shogren-Knaak, M., Ishii, H., Sun, J. M., Pazin, M. J., Davie, J. R., & Peterson, C. L. (2006). Histone H4-K16 acetylation controls chromatin structure and protein interactions. *Science, 311*(5762), 844-847.

Shogren-Knaak, M. A., Fry, C. J., & Peterson, C. L. (2003). A Native Peptide Ligation Strategy for Deciphering Nucleosomal Histone Modifications. *Journal of Biological Chemistry, 278*(18), 15744-15748.

Simon, J. A., & Lange, C. A. (2008). Roles of the EZH2 histone methyltransferase in cancer epigenetics. *Mutation Research-Fundamental and Molecular Mechanisms of Mutagenesis, 647*(1-2), 21-29.

Spiegl-Kreinecker, S., Pirker, C., Filipits, M., Lotsch, D., Buchroithner, J., Pichler, J., et al. (2010). O-6-Methylguanine DNA methyltransferase protein expression in tumor cells predicts outcome of temozolomide therapy in glioblastoma patients. *Neuro-Oncology, 12*(1), 28-36.

Spratt, T. E., & Levy, D. E. (1997). Structure of the hydrogen bonding complex of O-6-methylguanine with cytosine and thymine during DNA replication. *Nucleic Acids Research, 25*(16), 3354-3361.

Srivenugopal, K. S., Mullapudi, S. R. S., Shou, J. A., Hazra, T. K., & Ali-Osman, F. (2000). Protein phosphorylation is a regulatory mechanism for O-6-alkylguanine-DNA alkyltransferase in human brain tumor cells. *Cancer Research, 60*(2), 282-287.

Steward, N., & Sano, H. (2004). Measuring Changes in Chromatin Using Micrococcal Nuclease. In T. O. Tollefsbol (Ed.), *Epigenetics Protocols* (Vol. 287). Totowa: Humana Press Inc.

Struhl, K. (1985). Naturally-occurring poly (dA-dT) sequences are upstream promoter elements for constitutive transcription in yeast. *Proceedings of the National Academy of Sciences of the United States of America, 82*(24), 8419-8423.

Sun, F.-L., Cuaycong, M. H., & Elgin, S. C. R. (2001). Long-Range Nucleosome Ordering Is Associated with Gene Silencing in Drosophila melanogaster Pericentric Heterochromatin. *Mol. Cell. Biol., 21*(8), 2867-2879.

Tachibana, M., Sugimoto, K., Fukushima, T., & Shinkai, Y. (2001). SET Domain-containing Protein, G9a, Is a Novel Lysine-preferring Mammalian Histone Methyltransferase with Hyperactivity and Specific Selectivity to Lysines 9 and 27 of Histone H3. *Journal of Biological Chemistry, 276*(27), 25309-25317.

Tamaru, H., & Selker, E. U. (2001). A histone H3 methyltransferase controls DNA methylation in Neurospora crassa. *Nature, 414*(6861), 277-283.

Tentori, L., Graziani, G., Gilberti, S., Lacal, P. M., Bonmassar, E., & Datri, S. (1995). Triazene compounds induce apoptosis in O-6-alkylguanine-DNA alkyltransferase deficient leukemia-cell lines. *Leukemia, 9*(11), 1888-1895.

Tsukada, Y., Fang, J., Erdjument-Bromage, H., Warren, M. E., Borchers, C. H., Tempst, P., et al. (2006). Histone demethylation by a family of JmjC domain-containing proteins. *Nature, 439*(7078), 811-816.

Tsukiyama, T. (2002). The in vivo functions of ATP-dependent chromatin-remodelling factors. [Review]. *Nature Reviews Molecular Cell Biology, 3*(6), 422-429.

Tufarelli, C., Stanley, J. A. S., Garrick, D., Sharpe, J. A., Ayyub, H., Wood, W. G., et al. (2003). Transcription of antisense RNA leading to gene silencing and methylation as a novel cause of human genetic disease. *Nature Genetics, 34*(2), 157-165.

Verdel, A., Jia, S. T., Gerber, S., Sugiyama, T., Gygi, S., Grewal, S. I. S., et al. (2004). RNAi-mediated targeting of heterochromatin by the RITS complex. *Science, 303*(5658), 672-676.

Wade, P. A., Gegonne, A., Jones, P. L., Ballestar, E., Aubry, F., & Wolffe, A. P. (1999). Mi-2 complex couples DNA methylation to chromatin remodelling and histone deacetylation. *Nature Genetics, 23*(1), 62-66.

Wang, Y., Kato, T., Ayaki, H., Ishizaki, K., Tano, K., Mitra, S., et al. (1992). Correlation between DNA methylation and expression of O6-methylguanine-DNA methyltransferase gene in cultured human tumor-cells. *Mutation Research, 273*(2), 221-230.

Watt, F., & Molloy, P. L. (1988). Cytosine methylation prevents binding to DNA of a Hela-cell transcription factor required for optimal expression of the adenovirus major late promoter. *Genes & Development, 2*(9), 1136-1143.

Watts, G. S., Pieper, R. O., Costello, J. F., Peng, Y. M., Dalton, W. S., & Futscher, B. W. (1997). Methylation of discrete regions of the O-6-methylguanine DNA methyltransferase (MGMT) CpG island is associated with heterochromatinization of the MGMT transcription start site and silencing of the gene. *Molecular and Cellular Biology, 17*(9), 5612-5619.

Weber, M., Davies, J. J., Wittig, D., Oakeley, E. J., Haase, M., Lam, W. L., et al. (2005). Chromosome-wide and promoter-specific analyses identify sites of differential DNA methylation in normal and transformed human cells. *Nature Genetics, 37*(8), 853-862.

Wei, Y., Yu, L. L., Bowen, J., Gorovsky, M. A., & Allis, C. D. (1999). Phosphorylation of histone H3 is required for proper chromosome condensation and segregation. *Cell, 97*(1), 99-109.

Winston, F., & Allis, C. D. (1999). The bromodomain: a chromatin-targeting module? *Nature Structural Biology, 6*(7), 601-604.

Wysocka, J., Swigut, T., Xiao, H., Milne, T. A., Kwon, S. Y., Landry, J., et al. (2006). A PHD finger of NURF couples histone H3 lysine 4 trimethylation with chromatin remodelling. *Nature, 442*(7098), 86-90.

Yan, Y., Chen, H., & Costa, M. (2004). Chromatin Immunoprecipitation Assays. In T. O. Tollefsbol (Ed.), *Epigenetics Protocols* (Vol. 287). Totowa, New Jersey: Humana Press Inc.

Yegnasubramanian, S., Lin, X. H., Haffner, M. C., DeMarzo, A. M., & Nelson, W. G. (2006). Combination of methylated-DNA precipitation and methylation-sensitive restriction enzymes (COMPARE-MS) for the rapid, sensitive and quantitative detection of DNA methylation. *Nucleic Acids Research, 34*(3).

Zhang, Y., & Reinberg, D. (2001). Transcription regulation by histone methylation: interplay between different covalent modifications of the core histone tails. *Genes & Development, 15*(18), 2343-2360.

Zhao, Q., Rank, G., Tan, Y. T., Li, H. T., Moritz, R. L., Simpson, R. J., et al. (2009). PRMT5-mediated methylation of histone H4R3 recruits DNMT3A, coupling histone and DNA methylation in gene silencing. [Article]. *Nature Structural & Molecular Biology, 16*(3), 304-311.

Zhao, W., Soejima, H., Higashimoto, K., Nakagawachi, T., Urano, T., Kudo, S., et al. (2005). The essential role of histone H3 Lys9 di-methylation and MeCP2 binding in MGMT silencing with poor DNA methylation of the promoter CpG island. *Journal of Biochemistry, 137*(3), 431-440.

Zipper, H., Brunner, H., Bernhagen, J., & Vitzthum, F. (2004). Investigations on DNA intercalation and surface binding by SYBR Green I, its structure determination and methodological implications. *Nucleic Acids Research, 32*(12).

Appendices

Appendix I MGMT promoter sequence

The sequence of the MGMT gene and promoter was obtained from the National Centres for Biotechnology Information (NCBI) website.

ACCESSION : NT_008818, REGION: 2499384..2799713

GPS_000125285, VERSION : NT_008818.16, GI:224514688

```
2493661 tcacctgcat cgtgaggagc accagcaaag gccgcctgac actgccctca ccaagaaatg
2493721 agcaccccca gcttcacaac tttcccctac ccctgccagg aatgaaggtg ctgtcctatt
2493781 cctgtccagc gggctcctgg acaaagaagg gagagtctct gatctccagg cgctgctgat
2493841 cagacagatg gagggatcat tctgaggacc tcagtgtctg tcattcccca ctcctagatt
2493901 gagtggggtt atctcaggca aagagacaat gggacagacg gccaccggca ccagccccag
2493961 ctccaattct gccgctcagg tggtgatcac tctcccacat ctgcctcctg ttaccttaaa
2494021 gcagtggttc aatgtgctag gctggtttga agcagttacc ctgggaggaa atgcagccac
2494081 ttttccttte taaatttgta ttttggtgac tgagacagaa cccttagtgt ggctgttttt
2494141 cttgtcttaa tttcattcgt ggtttcccag tcagaagcaa atgacagcaa atcacaatct
2494201 cagcatcgaa atccccacgt ctcttgcttt aatttccaag tcacaaaagc atgggcactt
2494261 ctggttcatc ccagtggggc aggggagggg ggggacccac ttccttctag tgacccaggt
2494321 gcacactccc cagctcttca caccatttaa aggattctgc ccaaactgcc aaccatgtgt
2494381 tacaaataaa gcccttcccg aaaatggatc aaaaacactt tgtaatgagt gaaggagctg
2494441 gtttaaaaag ggccaacatc aaacaaaatc ccagtcctga gtcacagaca ctcaaatagc
2494501 cccttccagg gtgggaatgt cctccaaagc acttccattt gtgtgagtag ttcttcaagc
2494561 caacgtatcc aaatacatac atctgatgag cggactttgc ttgtttacat acattatgta
2494621 cattcctttg atagtcaatt gtctaaagtt ggaacagttc ggagggaaga gctatataag
2494681 gtttgcaatg atctttgtcc accagttact ggacaactgg atccaaattc cacaaatagc
2494741 tgtggttctt tacctgcatg gttctcctcc cctgagacat ccagtgccat gcattttctc
2494801 ttgcaggtct ttccttgcat caccctcca accccagcag atatcctggc tgagcctgtt
2494861 ttctctgtga ggggctacac tgcacactgg ggctcttgaa aagggcttgc tgggctgggc
2494921 acggtggctc acgcctgtaa tcctgacact ttggtaggcc gaggtgggtg gatcacctga
2494981 ggtcaggtgt tcaagatcag cctggccaat atggtgaaac cccgtctcta ctaaaaatac
2495041 agaaaaatta gctgggcatg gtggtgtgca cctgtaatcc cagctactca ggaggctgag
2495101 gcaggagaat cacttgaacc cgggaggcag aggttccagt gagccaagat ggcaccattg
2495161 tacttcagcc taggcgacag agagagactc caattcaaaa aaagaaaaag agaaaaaaaa
2495221 aaaaaagaaa aaaaagaaag ggcttcctgc agggacagtc agtgcaggaa agggcctctt
2495281 tcgtactccc actgccccta cgcatctcct gggtagaggt cgctgctcca gagagcaaac
2495341 tatttcctca tctgtgtgcc attccactac aagccccaca ggggcctgca acgagtccca
2495401 taaatccatc tccaggccct gcacccacaa actggcaaag gaagtttcag gaaaagtctt
2495461 tctaatagga gtctgtgggc tgcctctggt tcgtttcttt aggaattctc ctccatgccc
2495521 ttcttgacac aaaagggcct gaagggttcc agttctcaac aggagctccc aggggctcct
2495581 ggcaggagga tgttctgcct ctttggagga aagcaagagc taaggagccc ctcctgtttt
2495641 agttgcacct ccatcccctt tctccaccct gcaccattcc cttaccctct atgtgaggca
2495701 aagcctgaag tccctccttc ccgccctctc tcctgcccac tagtagatta cactccctgc
2495761 tgcagttaca ccatgatgcc tctgccatgc tgacaactag tgtcacacag gagcgtaatc
2495821 agaagcacct ggcattcaac cccggtaccg atggcccca ccttttcatt tcaggcttct
2495881 tcctccagag tgcttgaggc tccctggcct cctggcctct cccaggtcca aggcgctgac
2495941 tccagctctt ggctccaaca tttacaggaa cactgggact aagaaaatca attgtgttaa
2496001 tcagcaaaac cctccacttg agatgctatc ctaaaagcaa actatatgta aaacacttaa
2496061 cgtggggagc tctgtaatat gtttcttttg ttacacgacc atcacacatt tgtccggagt
2496121 ttggggcttt caaaccacat aaggttttat gtgatcgtta taaaatccct tcatttccca
2496181 aaggtagggt agtaaggatt aagtttgact actgaaggca gctttgttgt aagtggtctc
2496241 taatgtcaca aaagtagctt gggaagacag gcttattaaa caaatttctt gggttgcaaa
2496301 tcattagaag caatcgcatg tcatgttcat ttgcttaacc cgaaaggtat ccatttggat
2496361 gtttaaagaa actatgcaga ttaacattgt tcccagtgcc cacaagaaag ctggctgatc
2496421 ttaaaggaaa tccagggagc tccttgagga agtcggactg cagttgagca tacccttttg
2496481 tggttttccc acctcttttg taaaaagttc ttcataggaa tctgtgtctg gaggaaaagg
```

2496541 ggttgtgatt tgttaatctg aagatgggag acctcaaagg aatctcaccc aaccagtcct
2496601 gcactgtcat cctatgaaca gagaagtcag gtggttgctc agtgaggggc agggctggca
2496661 ccacatccga gcctccctgt cctgtgttcc ttactcttca gtggacccgg cgacctcccg
2496721 gctttggagc catcctgtgt tcctttaaca gtaggacgaa cacacaggcg atgatgagat
2496781 tgtaatggga caagggggag aggcgtgggg agctcttgat gaaaacttgg gtttttgaaa
2496841 ttaccatgat gaagggagga gcttgcacca gcaggtgtaa ggagtgtgag tttgagttct
2496901 gctcatcaga cagcctaagc agtcacatcc ttgaatcctg gtcttttgca ggccagtcct
2496961 tggtcaggtg gtggcctttt tcctctttcc cctctgcact gagaccctta tttggctcct
2497021 gatcctggag cccctgacac agtccttacc actgaagtag ctgtggccct tcacatagtt
2497081 cttcccacca cgccagcaag gggactgagt tctttcagta cagccagggc caggtccaca
2497141 catctccctg ggaagccagc actttctctc gtggaccgcc tccccattcc cacagggccc
2497201 tcctaaaggg cctttggatg accacattgg cctttctttc ctagggtggg gaattagaga
2497261 tgctaagact ggccagtctc tttttcttaa gagtttaggg attcgtctta aaatattatt
2497321 cagataaacg tatgagtcat gtgttaactg caaaactact taacagcaca cttgttagaa
2497381 tatcagtcgg cactctgatt ccatttcggc attgtttttc ctttggttct attaagatcc
2497441 cggttctaac tgggtcctgg tagtaacagg ctgtaagtgg ccaggtgtat agcattattt
2497501 cttagtagtg tggtgtggtg ctggtggttt attttcccta tgcacacatg ccctaatatg
2497561 gaaggatagt ttgtacacac gtagggtacg ttatcatgag actcctttac agagtatgaa
2497621 actgaggatt agagaagtca gacgagtttc ccgaagtctt atagaaggct aatggaaaaa
2497681 accagagcca agggcaaaca tgtttcatct gtccttccac attagtttaa atgtgaatgg
2497741 ctgcttggaa cacagtgttg agaaggattc cgaggctgtg tccaggttca gtggggaaaa
2497801 agtgccttga tttgaccatt atatcgtgta ctcagggcct agtttatttc ccacaagcag
2497861 ctatttaaaa catgtctcat ccaaggcagg gtcggggtgg ggaacctcag aggatcaatg
2497921 atgcagcctg tattgtcacc agggctcatc ccaaagcaaa tcctgctgaa gttctcctct
2497981 gaacaaccct tatcactcat gctaatatgt tggatcctgc aagtcacaaa tacgaaggta
2498041 tgagcattgg ccgaatccca acagggaaac ttcaccggga aggtgaagac ccctttccat
2498101 taagataaca aacagaacct agaaggcccg tagcatggtg gcttagaaca tgtgggcctt
2498161 ggatgggatc ctgccaaggg gtgtgtgacc tctccgaagc ctccagggat gatactactc
2498221 cctggggtgc ttatgccaac cacgttagag acaatggttt ctgtacccat tgcctggggc
2498281 tgccataata aagtgccaca cactgagtgg cttaaaacaa cagaaaccta ttgtctcaca
2498341 cttccggggg ccagaagttt gaaacccagg tgtgttagga tcctgctccc tctgaaggct
2498401 ccagggaaga gtgtcctctg ctccctccga aggctccagg gaagggtctg tcctcttagg
2498461 cttctggtgg cttgcaggtg cagccctcca atcctcctcc ccaagcggcc ttctgcctat
2498521 aaggacacga gtcatactgg atgaggggcc cactaattga tggcttctgt aaagtcccca
2498581 tctccaaata aggtcacatt gtgaggtact gggagttagg actccaacat agcttctctg
2498641 gtggacacaa ttcaactcct aataacgtcc acacaacccc aagcagggcc tggcaccctg
2498701 tgtgctctct ggagagcggc tgagtcaggc tctggcagtg tctaggccat cggtgactgc
2498761 agcccctgga cggcatcgcc caccacaggc cctggaggct gcccccacgg ccccctgaca
2498821 gggtctctgc tggtctgggg gtccctgact aggggagcgg caccaggagg ggagagactc
2498881 gcgctccggg ctcagcgtag ccgccccgag caggaccggg attctcacta agcgggcgcc
2498941 gtcctacgac ccccgcgcgc tttcaggacc actcgggcac gtggcaggtc gcttgcacgc
2499001 ccgcggacta tccctgtgac aggaaaaggt acgggccatt tggcaaacta aggcacagag
2499061 cctcaggcgg aagctgggaa ggcgccgccc ggcttgtacc ggccgaaggg ccatccgggt
2499121 caggcgcaca gggcagcggc gctgccggag gaccagggcc ggcgtgccgg cgtccagcga
2499181 ggatgcgcag actgcctcag gcccggcgcc gccgcacagg gcatgcgccg acccggtcgg
2499241 gcgggaacac cccgcccctc ccgggctccg ccccagctcc gcccccgcgc gccccggccc
2499301 cgccccccgcg cgctctcttg cttttctcag gtcctcggct ccgccccgct ctagaccccg
2499361 ccccacgccg ccatccccgt gcccctcggc cccgcccccg cgccccggat atgctgggac
2499421 agcccgcgcc cctagaacgc tttgcgtccc gacgcccgca ggtcctcgcg gtgcgcaccg
2499481 tttgcgactt ggtgagtgtc tgggtcgcct cgctcccgga agagtgcgga gctctccctc
2499541 gggacggtgg cagcctcgag tggtcctgca ggcgccctca cttcgccgtc gggtgtgggg
2499601 ccgccctgac ccccacccat cccgggcgag ctccaggtgc gccccaagtg cctcccaggt
2499661 gttgcccagc ctttccccgg gcctggggtt cctggactag gctgcgctgc agtgactgtg
2499721 gactggcgtg tggcgggggt cgtggcagcc cctgccttac ctctaggtgc cagccccagg
2499781 cccgggcccc gggttcttcc tacccttcca tgctgccagc tttccctccg ccagctgctc
2499841 caggaagctt ccagaagccc ctgcgcgggc cttggcttgc agcaaccctt tagcatactt
2499901 aggcagagtc ccatatttcc ttcctgctgg aggccaagtt ctaggggcct tctggttact
2499961 atggctggtg tttgtgtaca tcataccta actgtattca tcaacactta gagtaagcaa
2500021 ggctcgctgg agagccacac acactgggca ccgtaatgtc ggttataaca ccgcagagga
2500081 gttctgaact atgtatttcg cactcctggg ttcatcatct cctgaaatct cagggtggtg
2500141 tttgctctca gttgcttcag ctgagtagct ggctttctgt cctggaaagc agactttgta
2500201 catgtgtgtg caacctatgc ctgctgagat catcatcaga cagggaagcg gcttggtcca
2500261 gagagctgtt ctcagtagaa tgttaagcac agagagctga gaattagact ggttatttac
2500321 atagacatcc aaatagaaac ctatagagta tctgttaagt caggctctcc cgtcatctcc
2500381 cccatccctg ggcaggtgtc taggagatgg ttttgttatt ttcagggccc tctcaatggc
2500441 taaaacactc tgggagatga acaagatttt aaaaacccaa agcttagcgc acctggtggg
2500501 tgggggtgtg aaaactttga aggaaaccgc gtcaagagcc tggctgattg ttaatatcac
2500561 gttaactcag agggccagga tacttgccca gacccggagt ctgcctgcaa gtagcagagg

2500621 agagctggcc ttgctctgcc gcgtgtcttt cttcctgggc cctctgtctc gggttggaat
2500681 ttgaatagtg gagtagtgtc tgccacagtc aggggcctgg atgaagtaga ccaccagtac
2500741 ggagctatac tcaggtactt ttcaatgtat atatcttcat taaaaaaaaa aaatctgggc
2500801 caggcacagt gggtcacgcc tgtaatctca gcactttggg aggccgaggt gggtggatca
2500861 cctgaagtca ggagtttgag accagcctgg ccaacatggt gaaacccagt ttctactaaa
2500921 aacacaaaaa ttatccaggc gtggtggtgc atgctggtaa tcccagttac ttgggagact
2500981 gaggcaggag aattgcttga acctgggagg cggaggttgc agtgagccga gattgcgcca
2501041 ttgcactcca acctgggcga cgagagtgaa actgtcctga aggggaaaca aaaaaatctg
2501101 tatcaaaata aggatttaac taatagtatt aggcactact ttaaaaaggc tttgctgtta
2501161 gtaaggttga aagaaataga gccctaggta tacattgggt agcaccttgt tcagctgctc
2501221 agattcttga accttgttga ggtcttactt tgatatcacc tgggccttac ttttcgttgt
2501281 ttgggtttcc tccccaggtg tctcaatcag ggcctcctct gtccttttgc agggaagaag
2501341 ggggtaggaa gggcctgaaa aagaacttgc cttccccatt gccccctcag agtttgttcc
2501401 tctccagtcc tcttcccacc ctttcttagg acaccaaaac cctgactctt tcagtatttt
2501461 ataataaaat aaagttacta aattgtctgt tctgttttgc agaggacaca catttaggag
2501521 ccagtgattc agaccttcca tttttctttt tggtgctaat gctcttttca gtatattctc
2501581 tttgatagaa aaaaaatgga ggcaaaactg aattttctgc attatctttt cctttagcat
2501641 tattcttgtt tctgcacttc attctgaccc ccttccccag cataaagttc catgtccaga
2501701 tccacttgcc ctgagatttt tgacttccgt ttgggactct agtccctcca ggggacacat
2501761 tgagcctccc agaccctgca gggccctgtg ctcattcggc tcttgggctg ttgctacggt
2501821 ccttcctgac cctctgtttc ctgggacaag tagtttttaa tgcagctact ttctgaaaga
2501881 gctggggtct taccgcagaa tattatttta ttatttttag agacaaggtc ttggtctttc
2501941 gcccaggctg gagtgcagtg gtgagatcat agctccctgc agcctcaagc tcctgggctc
2502001 aagcgaacct cctgctttga cctcccaagt accagggact acaggtgtgc gccaccatac
2502061 ctggctaatt gttgttgttg ttgtttttag aggccagggt ctccgtatgt tgcctagggt
2502121 ggtctcgaac tcctggactc aagtgatctt ccctcctagg cctcccaaag tgctggaatt
2502181 ataggcatga gccaccatgc ctggcctcgc aggatattat ttaaacgaaa cctgaaggat
2502241 ttaaaatcag agaagacaca taaaccatca cctgactgtg gggtgagagt ggtctttata
2502301 tagacactca tgatgcacaa gccagccctt cgccccactc ttgttttgaa gtgaaaggat
2502361 ttatatggga gggaggaggt ttgagctgtg caggagggtc cttggttggc atgaggattt
2502421 tgtgaaccta cgctgttagc tctgcaggcc tgtcttggac ataggtaagt agaagttgga
2502481 gaccttgtgt tgtggaccaa atgttgcaag atgtgtgttc tgtggctttt cattaactgc
2502541 tgcatatctg ctggttggtg gacatagtct agttttcttt tgacttaaaa aaattaacag
2502601 tacagcttat atcggagggc tgcatagttt gggggaaact aatgaatata gtatggaatg
2502661 taatgaatga ctgacttctt catagagcta ttgaagtgat ttatgaagag gaagaaatca
2502721 tttttgtgac tttgttgatc tttgaagtat tagagtggct ttggcaggtg tggatcaccc
2502781 ggaaaggaat caaacactga gtcctgccaa ggtgctcggt cccggcagca aagccagtcc
2502841 tcagcagcct gcgctcccga agctcctcca gctaagtaac tgaataggcc gccctgggag
2502901 ctgcccatgc ggatgctctg aatggtgaaa cttggttttg acaccacaag ttgttttcag
2502961 ttaaatcagt ggctcagcag cagagcaggg ttctccaagg aggcctcgtg tccccttcac
2503021 cccacctgga ggtagctgtt ctaaaaccag taaaaaattc tacaaaaaca ttttcttagg
2503081 gttgttaaat tagtcatagt gtgtgtaacc atgaaaggaa tggtgagagt gcaataaatg
2503141 cctggtgtgt tcactctcct actcctaaaa gtttcttggt agaataattt cctacctgtg

Appendix II β-actin gene sequence

The sequence of the β-actin gene and promoter was obtained from the National Centres for Biotechnology Information (NCBI) website.

ACCESSION : NC_000007, REGION: complement(5566778..5570231)
GPC_00000003, VERSION: NC_000007.13, GI:224589819

```
0001 ccgccgagac cgcgtccgcc ccgcgagcac agagcctcgc ctttgccgat ccgccgcccg
0061 tccacacccg ccgccaggta agcccggcca gccgaccggg gcaggcggct cacggcccgg
0121 ccgcaggcgg ccgcggcccc ttcgcccgtg cagagccgcc gtctgggccg cagcgggggg
0181 cgcatggggg gggaaccgga ccgccgtggg gggcgcggga gaagcccctg ggcctccgga
0241 gatgggggac accccacgcc agttcggagg cgcgaggccg cgctcgggag gcgcgctccg
0301 ggggtgccgc tctcggggcg ggggcaaccg gcggggtctt tgtctgagcc gggctcttgc
0361 caatggggat cgcagggtgg gcgcggcgga gcccccgcca ggcccggtgg gggctggggc
0421 gccattgcgc gtgcgcgctg gtcctttggg cgctaactgc gtgcgcgctg ggaattggcg
0481 ctaattgcgc gtgcgcgctg ggactcaagg cgctaactgc gcgtgcgttc tggggcccgg
0541 ggtgccgcgg cctgggctgg ggcgaaggcg ggctcggccg gaaggggtgg ggtcgccgcg
0601 gctcccgggc gcttgcgcgc acttcctgcc cgagccgctg gccgcccgag ggtgtggccg
0661 ctgcgtgcgc gcgcgccgac ccggcgctgt ttgaaccggg cggaggcggg gctggcgccc
0721 ggttgggagg gggttggggc ctggcttcct gccgcgcgcc gcggggacgc ctccgaccag
0781 tgtttgcctt ttatggtaat aacgcggccg gcccggcttc ctttgtcccc aatctgggcg
0841 cgcgccggcg ccccctggcg gcctaaggac tcggcgcgcc ggaagtggcc agggcggggg
0901 cgacctcggc tcacagcgcg cccggctatt ctcgcagctc accatggatg atgatatcgc
0961 cgcgctcgtc gtcgacaacg gctccggcat gtgcaaggcc ggcttcgcgg gcgacgatgc
1021 cccccgggcc gtcttcccct ccatcgtggg gcgccccagg caccaggtag gggagctggc
1081 tgggtggggc agccccggga gcgggcggga ggcaagggcg ctttctctgc acaggagcct
1141 cccggtttcc ggggtggggg ctgcgcccgt gctcagggct tcttgtcctt tccttcccag
1201 ggcgtgatgg tgggcatggg tcagaaggat tcctatgtgg gcgacgaggc ccagagcaag
1261 agaggcatcc tcaccctgaa gtaccccatc gagcacggca tcgtcaccaa ctgggacgac
1321 atggagaaaa tctggcacca caccttctac aatgagctgc gtgtggctcc cgaggagcac
1381 cccgtgctgc tgaccgaggc ccccctgaac cccaaggcca accgcgagaa gatgacccag
1441 gtgagtggcc cgctacctct tctggtggcc gcctccctcc ttcctggcct cccggagctg
1501 cgccctttct cactggttct ctcttctgcc gttttccgta ggactctctt ctctgacctg
1561 agtctccttt ggaactctgc aggttctatt tgctttttcc cagatgagct ctttttctgg
1621 tgtttgtctc tctgactagg tgtctaagac agtgttgtgg gtgtaggtac taacactggc
1681 tcgtgtgaca aggccatgag gctggtgtaa agcggccttg gagtgtgtat taagtaggtg
1741 cacagtaggt ctgaacagac tccccatccc aagaccccag cacacttagc cgtgttcttt
1801 gcactttctg catgtccccc gtctggcctg gctgtcccca gtggcttccc cagtgtgaca
1861 tggtgtatct ctgccttaca gatcatgttt gagaccttca acaccccagc catgtacgtt
1921 gctatccagg ctgtgctatc cctgtacgcc tctggccgta ccactggcat cgtgatggac
1981 tccggtgacg gggtcaccca cactgtgccc atctacgagg ggtatgccct cccccatgcc
2041 atcctgcgtc tggacctggc tggccgggac ctgactgact acctcatgaa gatcctcacc
2101 gagcgcggct acagcttcac caccacggcc gagcgggaaa tcgtgcgtga cattaaggag
2161 aagctgtgct acgtcgccct ggacttcgag caagagatgg ccacggctgc ttccagctcc
2221 tccctggaga agagctacga gctgcctgac ggccaggtca tcaccattgg caatgagcgg
2281 ttccgctgcc ctgaggcact cttccagcct tccttcctgg gtgagtggag actgtctccc
2341 ggctctgcct gacatgaggg ttacccctcg gggctgtgct gtggaagcta agtcctgccc
2401 tcatttccct ctcaggcatg gagtcctgtg gcatccacga aactaccttc aactccatca
2461 tgaagtgtga cgtggacatc cgcaaagacc tgtacgccaa cacagtgctg tctggcggca
2521 ccaccatgta ccctggcatt gccgacagga tgcagaagga gatcactgcc ctggcaccca
2581 gcacaatgaa gatcaaggtg ggtgtctttc ctgcctgagc tgacctgggc aggtcggctg
2641 tggggtcctg tggtgtgtgg ggagctgtca catccagggt cctcactgcc tgtccccttc
2701 cctcctcaga tcattgctcc tcctgagcgc aagtactccg tgtggatcgg cggctccatc
2761 ctggcctcgc tgtccacctt ccagcagatg tggatcagca agcaggagta tgacgagtcc
2821 ggcccctcca tcgtccaccg caaatgcttc taggcggact atgacttagt tgcgttacac
2881 cctttcttga caaaacctaa cttgcgcaga aaacaagatg agattggcat ggctttattt
2941 gttttttttg ttttgttttg gttttttttt ttttttggc ttgactcagg atttaaaaac
3001 tggaacggtg aaggtgacag cagtcggttg gagcgagcat cccccaaagt tcacaatgtg
3061 gccgaggact ttgattgcac attgttgttt ttttaatagt cattccaaat atgagatgcg
```

```
3121 ttgttacagg aagtcccttg ccatcctaaa agccacccca cttctctcta aggagaatgg
3181 cccagtcctc tcccaagtcc acacagggga ggtgatagca ttgctttcgt gtaaattatg
3241 taatgcaaaa tttttttaat cttcgcctta atacttttt attttgtttt attttgaatg
3301 atgagccttc gtgccccccc ttcccccttt tttgtccccc aacttgagat gtatgaaggc
3361 ttttggtctc cctgggagtg ggtggaggca gccagggctt acctgtacac tgacttgaga
3421 ccagttgaat aaaagtgcac accttaaaaa tgag
```

Appendix III H19 gene sequence

The sequence of the H19 gene and promoter was obtained from the National Centres for Biotechnology Information (NCBI) website.

ACCESSION : NC_000011, REGION: complement(2016405..2019064)

GPC_000000035, VERSION: NC_000011.9, GI:224589802

```
0001 ggaggggtg ggatgggtgg ggggtaacgg gggaaactgg ggaagtgggg aaccgagggg
0061 caaccagggg aagatggggt gctggaggag agcttgtggg agccaaggag caccttggac
0121 atctggagtc tggcaggagt gatgacgggt ggaggggcta gctcgaggca gggctggtgg
0181 ggcctgaggc cagtgaggag tgtggagtag gcgcccaggc atcgtgcaga cagggcgaca
0241 tcagctgggg acgatgggcc tgagctaggg ctggaaagaa gggggagcca ggcattcatc
0301 ccggtcactt ttggttacag gacgtggcag ctggttggac gaggggagct ggtgggcagg
0361 gtttgatccc agggcctggg caacggaggt gtagctggca gcagcgggca ggtgaggacc
0421 ccatctgccg ggcaggtgag tcccttccct ccccaggcct cgcttcccca gccttctgaa
0481 agaaggaggt ttaggggatc gagggctggc ggggagaagc agacaccctc ccagcagagg
0541 ggcaggatgg gggcaggaga gttagcaaag gtgacatctt ctcgggggga gccgagactg
0601 cgcaaggctg gggggttatg ggcccgttcc aggcagaaag agcaagaggg cagggaggga
0661 gcacaggggt ggccagcgta gggtccagca cgtggggtgg taccccaggc ctgggtcaga
0721 cagggacatg gcaggggaca caggacagag gggtccccag ctgccacctc acccaccgca
0781 attcatttag tagcaggcac aggggcagct ccggcacggc tttctcaggc ctatgccgga
0841 gcctcgaggg ctggagagcg ggaagacagg cagtgctcgg ggagttgcag caggacgtca
0901 ccaggagggc gaagcggcca cgggaggggg gccccgggac attgcgcagc aaggaggctg
0961 caggggctcg gcctgcgggc gccggtccca cgaggcactg cggcccaggg tctggtgcgg
1021 agagggccca cagtggactt ggtgacgctg tatgccctca ccgctcagcc cctggggctg
1081 gcttggcaga cagtacagca tccaggggag tcaagggcat ggggcgagac cagactaggc
1141 gaggcgggcg gggcggagtg aatgagctct caggagggag gatggtgcag gcaggggtga
1201 ggagcgcagc gggcggcgag cgggaggcac tggcctccag agcccgtggc caaggcgggc
1261 ctcgcgggcg gcgacggagc cgggatcggt gcctcagcgt tcgggctgga gacgagggtg
1321 agtttttccc cctctgccac cctcagcccc cacccgcccc tccccacaca accaacacgt
1381 tctccccaca cgactctctc gttctcccca cagccaggtc tccagctggg gtggacgtgc
1441 ccaccagctg ccgaaggcca agacgccagg tccggtggac gtgacaagca ggacatgaca
1501 tggtccggtg tgacggcgag gacagaggag gcgcgtccgg ccttcctggt gagcgtgtct
1561 gccctccctg cgtcaggacg cggccctgcc cagaccgccc cgccgggcca ccatctcact
1621 gccccgacct ctgtcttcta cagaacacct taggctggtg gggctgcggc aagaagcggg
1681 tctgtttctt tacttcctcc acggagtcgg cacactatgg ctgccctctg ggctcccaga
1741 acccacaaca tgaaaggtga ggggcttcct gccacacttg gggtgggggg cacgcgagag
1801 gagctgagtg ggacctcact ccttccccat ccacagaaat ggtgctaccc agctcaagcc
1861 tgggcctttg aatccggaca caaaaccctc tagcttggaa atgaatatgc tgcactttac
1921 aaccactgca ctacctgact caggaatcgg ctctggaagg tgagcaccag cgctccttcc
1981 ggaagcctcc aggcccccga gcaccctgcc cccatcccac ccacgtgtcg ctatctctag
2041 gtgaagctag aggaaccaga cctcatcagc ccaacatcaa agacaccatc ggaacagcag
2101 cgcccgcagc acccaccccg caccggcgac tccatcttca tggccacccc ctgcggcgga
2161 cggttgacca ccagccacca catcatccca gagctgagct cctccagcgg gatgacgccg
2221 tccccaccac ctccctcttc ttctttttca tccttctgtc tctttgtttc tgagctttcc
2281 tgtctttcct tttttctgag agattcaaag cctccacgac tctgtttccc ccgtcccttc
2341 tgaatttaat ttgcactaag tcatttgcac tggttggagt tgtggagacg gccttgagtc
2401 tcagtacgag tgtgcgtgag tgtgagccac cttggcaagt gcctgtgcag ggcccggccg
2461 ccctccatct gggccgggtg actgggcgcc ggctgtgtgc ccgaggcctc accctgccct
2521 cgcctagtct ggaagctccg accgacatca cggagcagcc ttcaagcatt ccattacgcc
2581 ccatctcgct ctgtgcccct ccccaccagg gcttcagcag gagccctgga ctcatcatca
2641 ataaacactg ttacagcaat
```

Appendix IV MeDIP plate setup for relative quantification

	1	2	3	4	5	6	7	8	9	10	11	12
A												
B	Primers: Sample:	H19155 Blank			Bact114 Blank			MGMT101 Blank				
C		H19155 Input	H19155 Input	H19155 Input	Bact114 Input	Bact114 Input	Bact114 Input	MGMT101 Input	MGMT101 Input	MGMT101 Input		
D		H19155 Beads- only	H19155 Beads- only	H19155 Beads- only	Bact114 Beads- only	Bact114 Beads- only	Bact114 Beads- only	MGMT101 Beads-only	MGMT101 Beads-only	MGMT101 Beads-only		
E		H19155 α - 5mC	H19155 α - 5mC	H19155 α - 5mC	Bact114 α - 5mC	Bact114 α - 5mC	Bact114 α - 5mC	MGMT101 α - 5mC	MGMT101 α - 5mC	MGMT101 α - 5mC		
F		H19155 Calibrator	H19155 Calibrator	H19155 Calibrator	Bact114 Calibrator	Bact114 Calibrator	Bact114 Calibrator	MGMT101 Calibrator	MGMT101 Calibrator	MGMT101 Calibrator		
G												
H												

Appendix V MeDIP plate setup for standard curves

	1	2	3	4	5	6	7	8	9	10	11	12
A												
B	Primers: Dilution:	H19155 Blank			Bact114 Blank			MGMT101 Blank				
C		H19155 1/10	H19155 1/10	H19155 1/10	Bact114 1/10	Bact114 1/10	Bact114 1/10	MGMT101 1/10	MGMT101 1/10	MGMT101 1/10		
D		H19155 1/100	H19155 1/100	H19155 1/100	Bact114 1/100	Bact114 1/100	Bact114 1/100	MGMT101 1/100	MGMT101 1/100	MGMT101 1/100		
E		H19155 1/1000	H19155 1/1000	H19155 1/1000	Bact114 1/1000	Bact114 1/1000	Bact114 1/1000	MGMT101 1/1000	MGMT101 1/1000	MGMT101 1/1000		
F		H19155 1/10000	H19155 1/10000	H19155 1/10000	Bact114 1/10000	Bact114 1/10000	Bact114 1/10000	MGMT101 1/10000	MGMT101 1/10000	MGMT101 1/10000		
G												
H												

Appendix VI ChIP plate setup for absolute quantification

	1	2	3	4	5	6	7	8	9	10	11	12
A												
B Primers: Sample:	MGMT101 Blank						Bact114 Blank					
C	MGMT101 1/10	MGMT101 1/10	MGMT101 1/10	MGMT101 Anti-Ac	MGMT101 Anti-Ac	MGMT101 Anti-Ac	Bact114 1/10	Bact114 1/10	Bact114 1/10	Bact114 Anti-Ac	Bact114 Anti-Ac	Bact114 Anti-Ac
D	MGMT101 1/100	MGMT101 1/100	MGMT101 1/100	MGMT101 Anti-Me2	MGMT101 Anti-Me2	MGMT101 Anti-Me2	Bact114 1/100	Bact114 1/100	Bact114 1/100	Bact114 Anti-Me2	Bact114 Anti-Me2	Bact114 Anti-Me2
E	MGMT101 1/1000	MGMT101 1/1000	MGMT101 1/1000	MGMT101 Anti-Me3	MGMT101 Anti-Me3	MGMT101 Anti-Me3	Bact114 1/1000	Bact114 1/1000	Bact114 1/1000	Bact114 Anti-Me3	Bact114 Anti-Me3	Bact114 Anti-Me3
F	MGMT101 1/10000	MGMT101 1/10000	MGMT101 1/10000	MGMT101 Beads-only	MGMT101 Beads-only	MGMT101 Beads-only	Bact114 1/10000	Bact114 1/10000	Bact114 1/10000	Bact114 Beads-only	Bact114 Beads-only	Bact114 Beads-only
G												
H												

Appendix VII MeDIP data

Sample data for one LC480 MeDIP assay

Pos	Type	Target Name	Cp		mean	SD		Input	LOG
C2	Ref Unknown	H19155	27.801265					Bact vs MGMT	
C3	Ref Unknown	H19155	27.760665					0.76264232	-0.12
C4	Ref Unknown	H19155	27.707669		27.756533	0.04693427			
C5	Ref Unknown	Bact114	24.653450					MeDNA	
C6	Ref Unknown	Bact114	24.572505					Bact vs MGMT	
C7	Ref Unknown	Bact114	24.344382		24.5234456	0.16026805		16.512184	1.22
C8	Target Unknown	MGMT101	28.682530						
C9	Target Unknown	MGMT101	28.638384					Input	
C10	Target Unknown	MGMT101	28.66817		28.6630286	0.02251806		H19 vs MGMT	
D2	Ref Unknown	H19155	37.431390					1.07430673	0.03
D3	Ref Unknown	H19155	34.502738						
D4	Ref Unknown	H19155	Excluded		35.9670641	2.07086964		MeDNA	
D5	Ref Unknown	Bact114	34.153292					H19 vs MGMT	
D6	Ref Unknown	Bact114	34.986970					0.96243618	-0.02
D7	Ref Unknown	Bact114	35.950869		35.030377	0.89957408			
D8	Target Unknown	MGMT101	38						
D9	Target Unknown	MGMT101	38						
D10	Target Unknown	MGMT101	38		38	0			
E2	Ref Unknown	H19155	25.813488						
E3	Ref Unknown	H19155	25.788352						
E4	Ref Unknown	H19155	25.810867		25.8042355	0.01381795			
E5	Ref Unknown	Bact114	27.433455						
E6	Ref Unknown	Bact114	27.457059						
E7	Ref Unknown	Bact114	27.422409		27.4376406	0.01770025			
E8	Target Unknown	MGMT101	26.717457						
E9	Target Unknown	MGMT101	Excluded						
E10	Target Unknown	MGMT101	26.794986		26.7562214	0.05482119			
F2	Ref Calibrator	H19155	30.140595						
F3	Ref Calibrator	H19155	30.245387						
F4	Ref Calibrator	H19155	30.276670		30.220884	0.07126984			
F5	Ref Calibrator	Bact114	27.558481						
F6	Ref Calibrator	Bact114	27.318616						
F7	Ref Calibrator	Bact114	27.517546		27.4648809	0.12831171			
F8	Target Calibrator	MGMT101	31.478576						
F9	Target Calibrator	MGMT101	31.331270						
F10	Target Calibrator	MGMT101	31.443027		31.4176243	0.0768687			

Appendix IIX ChIP data

Sample data for MGMT in one LC480 ChIP assay

Pos	Cp	Concentration	Standard			Concentration as %	Average	SD	/4
C1	28.91	1.02E-01	0.1			10.20			
C2	28.99	9.68E-02	0.1			9.68			
C3	29.16	8.67E-02	0.1			8.67			
C4	27.27	2.88E-01			Acetyl	28.80	30.33333	0.152194	7.583333
C5	27.19	3.03E-01				30.30			
C6	27.11	3.19E-01				31.90			
D1	32.46	1.07E-02	0.01			1.07			
D2	32.93	7.93E-03	0.01			0.79			
D3	32.29	1.19E-02	0.01			1.19			
D4	28.09	1.71E-01			2 Methyl	17.10	19.23333	0.097756	4.808333
D5	27.74	2.14E-01				21.40			
D6	27.91	1.92E-01				19.20			
E2	37.59	4.11E-04	0.001			0.04			
E3	34.89	2.28E-03	0.001			0.23			
E3	Excluded	ND	0.001						
E4	31.93	1.49E-02			3 Methyl	1.49	1.5	0.007606	0.375
E5	31.76	1.66E-02				1.66			
E6	32.09	1.35E-02				1.35			
E7	Excluded	ND	0.0001						
E8	Excluded	ND	0.0001						
E9	Excluded	ND	0.0001						
F4	32.53	1.02E-02			Beads	1.02	1.12	0.005626	0.279167
F5	32.3	1.18E-02				1.18			
F6	32.34	1.15E-02				1.15			

Note: ÷4 calculation takes into account that input DNA was isolated from 50 µL sonicated chromatin whereas 200 µL were used in each IP

Sample data for β actin in one LC480 ChIP assay

Pos	Cp	Concentration	Standard			Concentration as %	Average	SD	/4
C7	27.98	9.35E-02	0.1			9.35			
C8	27.84	1.02E-01	0.1			10.20			
C9	27.61	1.18E-01	0.1			11.80			
C10	26.83	1.95E-01			Acetyl	19.50	20.8	0.10454	5.2
C11	26.74	2.08E-01				20.80			
C12	26.64	2.21E-01				22.10			
D7	31.58	9.15E-03	0.01			0.92			
D8	31.09	1.25E-02	0.01			1.25			
D9	31.5	9.61E-03	0.01			0.96			
D10	29.08	4.60E-02			2 Methyl	4.60	4.313333	0.022511	1.078333
D11	28.97	4.92E-02				4.92			
D12	29.54	3.42E-02				3.42			
E7	34.98	1.02E-03	0.001			0.10			
E8	34.62	1.29E-03	0.001			0.13			
E9	35.75	6.34E-04	0.001			0.06			
E10	Excluded	ND			3 Methyl		4.85	0.028576	1.2125
E11	28.82	5.42E-02				5.42			
E12	29.19	4.28E-02				4.28			
F8	Excluded	ND							
F9	39.97	1.00E-04	0.0001			0.01			
F10	Excluded	ND	0.0001						
F10	35.09	9.52E-04	0.0001		Beads	0.10	0.146067	0.001014	0.036517
F11	33.8	2.19E-03				0.22			
F12	34.68	1.24E-03				0.12			